Performance Analysis of an Optical CDMA Transmission System Impaired by Four Wave Mixing in a Single Mode Fiber

by

Md. Forkan Uddin

A thesis submitted to the Department of Electrical and Electronic Engineering

of

Bangladesh University of Engineering and Technology

in partial fulfillment of the requirement for the degree of

MASTER OF SCIENCE IN ELCTRICAL AND ELECTRONIC ENGINEERING

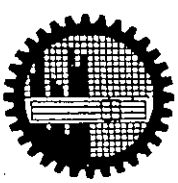

Department of Electrical and Electronic Engineering,

BAGLADESH UNIVERSITY OF ENGINEERING AND TECHNOLOGY

Dhaka-1000, Bangladesh

September, 2005

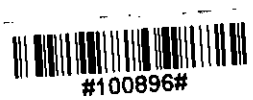

Approval Certificate

The thesis titled "***Performance Analysis of an Optical CDMA Transmission System Impaired by Four Wave Mixing in a Single Mode Fiber***" submitted by Md. Forkan Uddin, Roll No.: 040306239P, Session: April 2003 has been accepted as satisfactory in partial fulfillment of the requirement for the degree of Master of Science in Electrical and Electronic Engineering on 19 September 2005.

BOARD OF EXAMINERS

1. 19/9/05

Dr. Satya Prasad Majumder — Chairman
Professor
Department of Electrical and Electronic Engineering
BUET, Dhaka-1000, Bangladesh.

2.

Dr. S. Shahnawaz Ahmed — Member (Ex-officio)
Professor and Head
Department of Electrical and Electronic Engineering
BUET, Dhaka-1000, Bangladesh.

3.

Dr. A. B. M. Siddique Hossain — Member
Professor
Department of Electrical and Electronic Engineering
BUET, Dhaka-1000, Bangladesh.

4.

Dr. Mohammed Hossam - e - Haider
Member — (External)
Acting Head
Department of EECE
MIST, Mirpur, Dhaka, Bangladesh.

DECLARATION

It is hereby declared that this thesis or any part of it has not been submitted elsewhere for the award of any degree or diploma.

Signature of the candidate

Uddin 26/9/05

(Md. Forkan Uddin)

DEDICATED

To

My beloved parents

Contents:

List of Tables

List of Figures

List of Symbols

L	Fiber length
c	Speed of light
λ	Wavelength
N_{th}	Thermal noise
D	Degeneracy factor
B	Data band width
α	Attenuation constant
$g(t)$	Spreading signal in electrical domain
γ	Fiber chromatic dispersion index
N	Number of chip per bit
B_K	Base band signal of the k-th user
T	Bit period
T_c	Chip period
A_i	Spreading signal of i-th user in optical domain
P_T	Transmitted power per user
P_R	Received optical power
S_{OUT}	Output pulse
U	Mean of signal
σ	Total variance
σ^2_{FWM}	Variance of interference due to four wave mixing
σ^2_{MAI}	Variance of interference due to multiple access interference
N_0	Variance of noise
R_L	Load resistance of the receiver
v_g	Group Velocity
T_m	Receiver temperature
k	Boltzmann constant
K	Number of simultaneous user
n	Fiber refractive index
χ	Fiber nonlinear susceptibility

L_{eff}	Effective length of fiber
D_c	Fiber chromatic dispersion
A_{eff}	Effective core area of fiber
R	Photodetector's responsivity
P_{FWM}	FWM power

List of Abbreviations

SNR	Signal-to-Noise Ratio
BER	Bit Error Rate
BW	Bandwidth
WDM	Wavelength Division Multiplexing
DWDM	Dense Wavelength Division Multiplexing
OTDM	Optical Time Division Multiplexing
FDM	Frequency Division Multiplexing
OFDM	Optical frequency Division Multiplexing
OCDMA	Optical Code Division Multiple Access
DS-CDMA	Direct Sequence Code Division Multiple Access
DS-OCDMA	Direct Sequence Optical Code Division Multiple Access
FH-CDMA	Frequency Hopping Code Division Multiple Access
CSMA	Carrier Sense Multiple Access
FFH	Fast Frequency Hopping
WLAN	Wireless Local Area Networks
SIK	Sequence Inversion Keyed
SRS	Stimulated Raman Scattering
SBS	Stimulated Brillouin Scattering
FWM	Four-Wave Mixing
SPM	Self Phase Modulation
XPM	Cross Phase Modulation
FCD	Fiber Chromatic Dispersion
ASE	Amplifier's Spontaneous Emission
EDFA	Erbium-Doped Fiber Amplifier
LED	Light Emitting Diode
LASER	Light Amplification by Stimulated Emission of Radiation
LD	Laser Diode
APD	Avalanche Photodiode
ISI	Inter Symbol Interference
MAI	Multiple Access Interference

ACI	Adjacent Channel Interference
SMF	Single Mode Fiber
DSF	Dispersion Shifted Fiber
DF	Dispersive Fiber
IM/DD	Intensity Modulation Direct Detection
OOK	On-Off Keying
OCC	Optical Orthogonal Code
PSK	Phase Shift Keying
FSK	Frequency Shift Keying
ASK	Amplitude Shift Keying
MUX	Multiplexer
DeMUX	Demultiplexer
BPSK	Binary Phase Shift Keying
QPSK	Quadrature Phase Shift Keying
OQPSK	Orthogonal Quadrature Phase Shift Keying
CPSK	Continuous Phase Shift Keying
DPFSK	Discontinuous Frequency Shift Keying
PPM	Pulse Position Modulation
OPPM	Overlapping Pulse Position Modulation
ECC	Error-correcting codes
ET	Embedded transmission
TC	Turbo Code
SEC	Symmetric error correcting code
SSFBG	Superstructure Fiber Bragg Grating
SLD	Semiconductor Laser Diode
PN	Pseudo-Noise

Acknowledgements

Firstly, I would like to express my sincerest and profound gratitude to my honorable supervisor Dr. Satya Prasad Majumder, Professor of the Department of Electrical and Electronic Engineering (EEE), Bangladesh University of Engineering and Technology, Dhaka, for his valuable suggestions, continuous guidance and supreme supervision throughout the course of this research work, without which this thesis would never have been into existence.

I would also like to thank Professor M. M. Shahidul Hassan and Head of the Department for providing excellent research facility in Dr. Robert Noyce Simulation Lab.

Special thanks to Muhammad Anisuzzaman Talukder and Mohammad Faisal, Assistant Professors of Department of Electrical and Electronic Engineering (EEE), Bangladesh University of Engineering and Technology, Dhaka, for their continuous encouragement and support to complete this work.

I particularly want to thank my friend Md. Farhad Hossain, Lecturer, Department of Electrical and Electronic Engineering (EEE), Bangladesh University of Engineering and Technology, Dhaka, for all his help and good advice.

I am obliged to Md. Shafayetur Rahman, Electronic Assistant, Dr. Robert Noyce Simulation Lab, Department of EEE, BUET, for his co-operation in laboratory throughout the work.

Finally, I am grateful to Almighty Allah for giving me the strength and courage to complete this thesis.

Abstract

Optical CDMA is one of the most important research topics to the experts on optical communication for its several attractive features such as asynchronous access, privacy and security. Four wave mixing (FWM) is one of the most dominating nonlinear effects in optical communications. But all of the research works on optical CDMA system, performance analyses are carried out without considering the effect of FWM. In this thesis, an asynchronous direct-sequence optical CDMA (DS-OCDMA) system, with intensity modulation and direct detection (IM/DD) transmission link using sequence inversion keyed (SIK) switched correlator receiver, is considered. Firstly, the system is theoretically analyzed in present of FWM in single mode dispersion shifted fiber (DSF) and mathematical expressions of FWM noise, multiple access interference (MAI) and bit error rate (BER) are obtained using necessary assumptions. The BER performances of 100 Mb/s optical CDMA system using DSF are evaluated using analytical expressions. Further, to verify the analytical expressions, FWM noise, MAI and BER performance are evaluated by computer simulation with random data sequences and different m-sequences as well as Gold sequence of each user. It is investigated that simulation results and analytical results are similar in all cases for optical CDMA system using DSF. The BER performance is found to be degraded due to FWM effect if the transmitted power, transmission distance and number of simultaneous users are increased. It is seen that the BER performance can be improved by increasing the number of chips per bit. It is investigated that transmitted power per user, transmission distance and number of simultaneous users are limited due to FWM effect. Maximum allowable transmitted power per user, transmission distance and number of simultaneous users are evaluated at a BER of 10^{-9} to design an effective optical CDMA system using DSF. Also, the value of transmitted power per user is evaluated to obtain minimum BER performance for different values of transmission distance at different chips per bit encoding for different number of simultaneous users.

Further, the analytical approach is modified to evaluate the BER performance of the optical CDMA system using normal dispersive fiber. The BER performance is

evaluated for the DS-OCDMA system using normal fiber with 63 chip m-sequence as well as Gold sequence and compared with the results obtained using DSF. It is found that BER performance using DSF is better than the BER performance using normal dispersive fiber. The BER performance of the optical CDMA system using normal dispersive fiber found to be degraded significantly if the transmission distance is increased.

Chapter 1

Introduction

1.1 Communication System

Communication is the process of transfer of any information like voice, text, data, picture, video etc. from one point to another. Any communication system is composed of the following basic components:

(1) Transmitter: It manipulates the information from the message source and couples it into a transmission channel in the form of a signal, which matches the transfer properties of the channel.

(2) Channel: It bridges the distance between the transmitter and the receiver. As the signal propagates through the channel, it gets attenuated due to transmission loss and distorted due to various nonlinear effects and interference.

(3) Receiver: It extracts the weakened and distorted signal from the channel, amplifies it and restores it to its original form and then passes it into the message destination.

1.2 History of Optical Communication

The use of visible light for communication purposes has been common for thousands of years. Ancient people used signal fires, reflecting mirrors etc. for the purpose of communication. However, the history of modern optical communication is relatively short. Some efforts were made from time to time to utilize the visible light as a carrier of information but it was limited to short distance and low capacity links only. The reason behind this was the lack of suitable light source and the fact that transmission of light is seriously affected by snow, rain, fog and other environmental factors. Lower frequency electromagnetic waves (radar and microwaves) show much

smaller attenuation and hence were preferred as the means of communication in the earlier days.

Attempts to guide the light appear to have been as early as in 1854 by producing reflections in a curved stream of water coming out of a hole in the side of a pail. In 1880, Alexander Graham Bell reported the transmission of speech using a light beam. The photophone proposed by Bell, just four years after the invention of the telephone, modulated the sunlight with a diaphragm giving speech transmission over a distance of 200 m. But all these attempts were limited to low capacity short distance communication. Also it was possible for anyone to intercept the signal. A better light wave communication system would certainly need a light guided to help preserve the signal and so increase the reliability, security and distance of transmission. Then in 1910, a solid cylinder was envisaged to guide a wide range of electromagnetic waves including the upper limits of visible light. Another light guide was developed consisting of a hollow tube with a highly reflective metal coating on its inner surface. However, these devices had high signal loss.

Experiments on glass fibers were carried out in 1930s for use as light guide. Optical fibers were used for other purposes also, such as light conduits for card readers, in material endoscopes, in photography etc. The possibility of fiber optic communication was stimulated in the early 1960s with the invention of the laser. The proposal of optical communication via dielectric waveguides or optical fibers was made by Kao, Hockham and Werts in 1966. However at that time the idea that a block of glass may be used for long haul communication seemed somewhat ludicrous because of the large attenuation of normal glass. The early fibers were extremely lossy (typical loss~1000 dB/km). However, the situation changed drastically around the seventies. Nippon Glass Company of Japan first developed graded index fibers in 1968. Corning Glass Works of US produced fibers in 1970 with sufficient purity for use in telecommunication industry, having a loss of less than 20 dB/km. This level of attenuation seemed to be the absolute minimum to make optical fiber communication economically feasible. Since 1970, tremendous improvement has been made leading to silica-based fiber having very low attenuation. Progress in the fabrication technology resulted by 1979 in a loss of about 0.2 dB/km near the 1.55 μm

wavelength [Miya, 1979], a loss level limited mainly by the fundamental processses like Rayleigh scattering. By 1980s, these activities have led to the development and worldwide installation of practical and commercially feasible optical fiber communication systems that can carry telephone, cable television, voice, data and other telecommunication traffics.

The increasing demand of utilizing higher frequencies led to the rapid development of optical communication in the last two decades. Because the optical frequencies are of the order of 10^{14} Hz, so optical communication has a theoretical information capacity exceeding that of microwave communication by a factor of 10^5.

Rapid progress has been made in both lowering the attenuation loss in fiber and increasing the wavelength it can handle. Early interest in the fiber was in the 800-900 nm wavelength regions, here fibers exhibited a local attenuation minimum. Later interests extended over a wider range of wavelengths up to 1300 nm, the second low attenuation window in optical fiber (The first window near 850 nm was used almost exclusively for multimode fiber applications). In order to optimize the fiber's performance in the 1310 nm window, the fiber dispersion was designed to be very close to zero near that wavelength. That gave the fiber very low dispersion and consequently very high potential bandwidth. As optical fibers became more widespread and the need arose for more bandwidth and distance, the third window near 1550 nm was exploited to provide for single mode fiber operation. The 1550 nm region offers much lower attenuation (0.2 dB/km at 1550 nm vs. 0.5 dB/km at 1310 nm), but it has quite a bit of dispersion (17 ps/nm-km), which seriously limited bandwidth. This could be overcome by using lasers with narrower linewidth. The advancement in laser technology made such narrow linewidth high power lasers readily available. Now-a-days almost all WDM systems operate in the 1550 nm wavelength region employing single mode fiber for operation.

The last two decades were a period of revolutionary development for optical fiber technology. The introduction of fiber amplifiers, especially erbium doped fiber amplifier was the first major steps toward making long-haul wavelength division multiplexed system economically possible. This with the combination of modern laser source and the development of coherent detection scheme, has made the optical

fiber based communication system the major competitor of microwave and satellite communication systems in present world.

The present is such that in the near future optical fiber communications will be the heart of information and communication technology all over the world. The explosive growth of internet traffic provides strong incentives to exploit the huge bandwidth of fiber optic networks. Such requirements are presently met by synchronous network technology/synchronous digital hierarchy (SONET/SDH) and in near future are most likely to be met by ideally suited WDM and its improved version, dense wavelength-division multiplexing (DWDM) technology. And after one or two decade when the total silica based fiber will be replaced by fiber made up with photonic band gap material or even better technology, the communication system will overcome its limitation imposed by today's fiber properties.

1.3 Background of this Study

In the last three decades, the explosive growth of bandwidth requirement, demands on both the capacity and functionality of optical communication system and networks. As a result, recently optical code division multiple access (OCDMA) systems have experienced research interest. There are two main types of techniques used to spectrally code and spread a data signal such as direct-sequence (DS) CDMA and frequency-hopping (FH) CDMA. However, combination of the two techniques can be used to spread the data.

Several types of modulation can be used on a CDMA Optical system but most of the research on optical CDMA has concentrated on the intensity modulation and direct detection signaling for example On-Off-Keying (OOK), Pulse-Position-Modulation (PPM) and Overlapping PPM (OPPM). PPM and OPPM have been described extensively on [1-8], where system bit error rate (BER) performance, achievable throughput and other relevant system parameters can be found - usually the BER is better than for OOK systems because the pulse position multiplicity reduces the effect of multiple access interference (MAI) in addition to good power efficiency of PPM against OOK. However the prime disadvantages of using PPM in optical

CDMA is the decrease in transmission rate relative to the speeds available in the laser and it worsens as the signature sequence length becomes long. The literature for OOK-CDMA is more extensive and we just point out the most relevant, like [9-13].

In OCDMA systems with incoherent signal processing we are obliged to use signature sequences composed of only zeros and ones. Bi-polar codes used currently on radio networks are infeasible so we need to devise a new kind of codes which satisfy this requirement and the cross and auto-correlation conditions. In [14-15] the study of these Optical Orthogonal Codes is given in great detail using an analogy of disk patterns to obtain the codes and its properties. A number of optical orthogonal codes (OOC) have been proposed [16-18] for various OCDMA technologies. Another family of OOC with nearly ideal correlations can be found in [19-20] with the description of quadratic and extended quadratic congruence codes. Novel classes OOCs are required to support independent data rate and data-format as well as time transparent transmission in multimedia applications. Conventional OOC families are designed to support constant bit rate applications [16],[21-23] but their predetermined cross-correlation valid under fixed weight and code length in case of variable-bit-rate or multiple bit rate multimedia applications. To avoid such situations, several novel classes of OOCs were recently proposed [24-25]. These are suitable for spectral amplitude coding, fast frequency hopping and time spreading encoding in multimedia environment [26]. At the same time we can focus our attention on prime sequences (PC) [27-29] and extended prime sequences (EPC) and their performance improvements against OOC.

A unipolar-bipolar correlation allows conventional bipolar signature sequences to be used in a sequence inversion keyed (SIK) direct sequence (DS) code division multiple access (CDMA)[30]. The conventional bipolar signature sequences exhibit larger set sizes thereby supporting more simultaneous users and lower (MAI) than either prime codes [31] or optical orthogonal codes [32] for the same bandwidth expansion factor. All-optical parallel delay line unipolar-bipolar correlator has been reported in [33]. The bit error rate (BER) performance of a direct sequence optical

code division multiple access (DS-OCDMA) system with intensity modulation and direct detection (IM/DD) transmission link using sequence inversion keyed (SIK) switched correlator receiver has been demonstrated [34].

Phase encoded OCDMA has attracted the attention of experts on optical communication where the carrier is phase modulated by the digital data sequence and the code sequence. Several phase encoded OCDMA systems have been reported [35-36]. The channel BER performance can be improved using error-correcting codes (ECCs) [37], [38]. The channel coding involves either decreasing the symbol duration or decreasing the information rate. The embedded modulation scheme is needed [39], [16] to apply ECCs into the optical CDMA effectively. A modified version of the embedded transmission (ET) scheme has been described in [16]. The effectiveness of ET transmission with symmetric error correcting code (SEC) scheme has been applied in [40] using PPM signaling. Another level of complexity and performance improvement can be achieved Turbo Codes (TC) because it offers its substantial gain over uncoded systems and its reasonable decoding complexity as shown in [41]. The performance evaluation using Turbo Codes (TC) on OCDMA systems can be found at [42-45].

A number of DS-CDMA systems based upon fiber Bragg grating encoding–decoding devices has been reported [46]. It is investigated that superstructure fiber Bragg grating (SSFBG) technology is suitable for the generation, recognition, and recoding of phase-encoded optical code sequences containing as many as 63 chips at chip rates as high as 160 Gchip/s. Longer code sequences reduce the multiple access effect (MAI) effect and higher chip rate is necessary for higher bit rate of transmission. The SSFBG is a fiber grating with a rapidly varying refractive index modulation of uniform amplitude and pitch, onto which a slowly varying refractive index modulation has been applied along its length. Thus, SSFBGs can be designed and fabricated with a wide range of complex tailored impulse-response functions with precise amplitude and phase characteristics. Such SSFBGs can be applied for optical-pulse processing systems [47], [48] such as DS-OCDMA code generation and

recognition devices, and for which precise control of the amplitude and phase of the temporal pulse profile is essential.

Fiber dispersion causes spreading of an optical pulse, which in turn degrade system performance due to increased intersymbol interference and reduced received optical peak power [49]. Recently the performance of an asynchronous phase encoding OCDMA considering fiber chromatic dispersion has been reported in [49]. Bit error rate analysis of this system has been performed in the case of both ordinary single mode optical fiber and dispersion shifted fiber. The numerical results demonstrate that even though the system performance improves due the smaller width of initial Gaussian optical pulse, the effect from dispersion is higher. The BER performance as well as power penalty of a direct sequence optical CDMA transmission link using intensity modulated direct detection (IM/DD) sequence inverse keyed (SIK) switched correlator receiver has been reported in 2004 [50].

During the last thirty years or so the study of nonlinear effects in the optical fibers has led to the advent of a new branch of nonlinear optics, referred to as nonlinear fiber optics. A large number of research projects and developments have been carried out over the years in this field. Four-wave mixing (FWM) is a nonlinear process in optical fibers in which beating of three wavelengths generating a fourth wavelength. As a consequence, FWM results in cross-talk and degrades the system BER performance [51-54]. Parametric FWM was studied about thirty years ago [Stolen 1974, 1975].The first detailed study of FWM effect in optical fiber was published by K.O.Hill et al in 1978 [55]. However at that time high capacity optical fiber system was not available and the FWM effect was only a topic of academic interest. Situation changed quickly when the long-haul optical systems for which FWM effect is a major limiting factor began to be installed throughout the world. With the increase of use of optical fiber extensive research took place about the influence of FWM effect over WDM systems. The effect of FWM in WDM system with DSF has been reported [56]. Equations have been developed describing the performance of WDM systems in presence of FWM [57]. The mathematical expression of FWM power for multistage WDM system is developed [53].

In DS-OCDMA, multi-wavelengths generate when the optical carrier is modulated by spreaded signal. In all of the research works on OCDMA systems, mentioned above, performance analyses are carried out without considering the effect of four wave mixing considering the FWM noise power is negligible as compared to signal power. But the FWM noise power increases with increasing transmitted optical power. The OCDMA systems with higher number of simultaneous users transmit high power, thus, FWM effect can not be neglected in that case.

1.4 Objective of this Study

The main objectives of this thesis work are:

(1) To perform a theoretical analysis for the evaluation of the effect FWM in a DS-OCDMA system with IM/DD using SIK switched correlator receiver.

(2) To evaluate the BER performance as a function of transmitted power per user, number of simultaneous users, transmission distance and number of chips per bit for a given data rate at a chip rate of 10-50 Gchip/s.

(3) To find out the eye-closer penalty for different values of transmission distance with normal dispersive fiber at a bit rate of 100 Mb/s.

(4) To determine the limitations imposed due to FWM such as maximum allowable transmitted power per user, maximum allowable transmission distance and maximum allowable number of simultaneous users at a BER of 10^{-9}.

(5) Finally, to determine the value of transmitted power per user to obtain minimum BER performance for particular number of simultaneous users.

1.5 Organization of the Thesis

The thesis consists of nine chapters.

In chapter 1, a brief introduction and historical background of optical communication systems are discussed. A review of recent works in the related field is also presented.

In chapter 2, optical communication systems are examined in a greater detail. The receiver configuration, modulation schemes and multichannel optical systems are discussed.

In chapter 3, various nonlinear optical phenomenons are discussed.

In chapter 4, a brief description of FWM generation is presented. Also, a mathematical expression of FWM power is derived for a multi-span optical system.

In chapter 5, an introduction to spread spectrum techniques and properties of different code sequences is presented. Further, DS-OCDMA system, with IM/DD transmission link using SIK switched correlator receiver, is described briefly. Also, a theoretical analysis is presented to evaluate the effect of FWM on BER performance of the DS-OCDMA system.

In chapter 6, the performance results are evaluated for a DS-OCDMA transmission link using SIK correlator receiver. The effects of different system parameters like fiber length, number of simultaneous users, transmitted power, and number of chips per bit on system performances are also discussed and optimum system design parameters are evaluated.

A brief conclusion and suggestions for future work are presented in chapter 7.

Chapter 2

Optical Fiber Communications

2.1 Introduction

Since long bandwidth (BW) has been a problem in modern telecommunication systems with the introduction of modulation-demodulation techniques. Since optical communication provides a very large BW, it has become the most modern means of communication. Optical fiber communication is similar to a general communication system. In both cases the goal is to convey signal from the information source over the transmission medium to the destination. The communication system therefore consists of a transmitter or modulator linked to the information source, the transmission medium and a receiver or demodulator at the destination. Electrical signal is the most easy to handle and, as such, used in communication system.

In electrical communications the information source provides an electrical signal, derived from a message signal which is non-electrical, to a transmitter comprising electrical and electronic components which converts the signal into a suitable form for propagation over the transmission medium. This is achieved by modulating a carrier. After traveling the transmission medium the signal is transmitted into receiver where it is again transformed into the original form. Important is that in any transmission medium the signal is attenuated, suffers loss, and subject to degradation due to contamination by random signals and noise, as well as possible distortions imposed by mechanisms within the medium itself. Therefore, in all such systems, there is necessity of installation of repeaters or line amplifiers at intervals, both to remove signal distortion and to increase level before transmission is continued down the link.

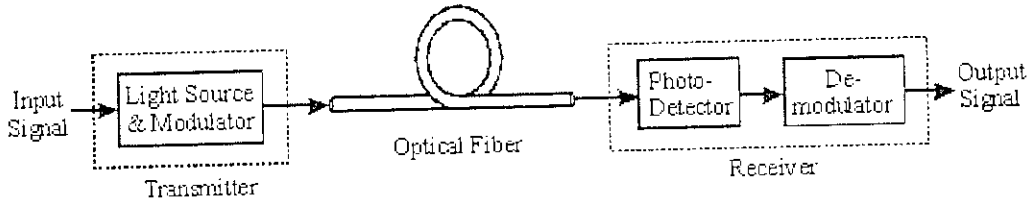

Fig. 2.1 Optical Communication Network

In optical fiber communications the system is to be considered in greater detail. Here the electrical signal as well as the carrier is used in forms of light, which is itself an electro-magnetic wave. Here the information source provides an electrical signal to a transmitter comprising an electrical stage which drives a optical source to give modulation of the light wave carrier. The optical source which provides the electrical – optical conversion may be either a semiconductor laser or light emitting diode (LED). The transmission medium consists of an optical fiber cable and the receiver consists of an optical detector which drives a further electrical stage and hence provides demodulation of the optical carrier. Photodiodes and, in some instances, phototransistors and photoconductors are utilized for the detection of the optical signal and the opto-electrical conversion. Thus there is a requirement for electrical interfacing at either end of the optical link and at present the signal processing is usually performed electrically.

The electrical carrier may be modulated using either an analog or digital information signal. In such a system analog modulation involves the variation of the light emitted from the optical source in a continuous manner. With digital modulation, however, discrete changes in the light intensity are obtained. Although often simpler to implement, analog modulation with an optical fiber communication system is less efficient, requiring a far higher signal to noise ratio at the receiver end than that of digital modulation. Also, the linearity needed for analog modulation is not always provided by semiconductor optical sources, especially at high modulation frequencies. For these reasons, analog optical fiber communication links are generally limited to shorter distances and of lower bandwidths than that of digital links.

Initially the input digital signal from the information source is suitably encoded for optical transmission. The laser drive circuit directly modulates the intensity of the semiconductor laser with the encoded digital signal. Hence a digital optical signal is launched into the optical fiber cable. The avalanche photodiode detectors followed by a front-end amplifier and equalizer or filter to provide gain as well as linear signal processing and noise bandwidth reduction. Finally the signal obtained is decoded to give the original digital information.

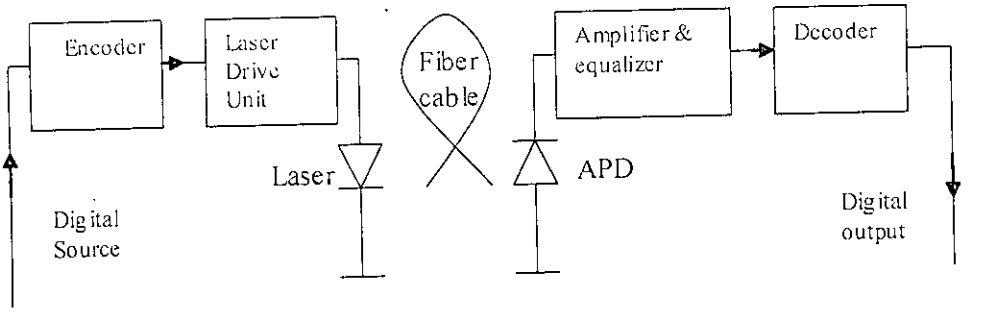

Fig. 2.2 Typical Arrangement for Optical Communication System

2.2 The features of optical fiber communication

The extremely attractive features of optical fibers communication are as follows:

I. enormous potential Band Width
II. Small size an weight
III. Electrical isolation
IV. Immunity to interference and crosstalk
V. Signal security
VI. Low transmission loss
VII. Ruggedness and flexibility
VIII. System reliability and ease of maintenance &
IX. Potential low cost
X. No hazards of short circuits as in metal wires
XI. No problems when used in explosive environments

XII. Immunity to adverse temperature and moisture conditions

Because of these advantages fiber optic communication is being currently utilized in telephone such as loops, trunks, terminals and exchanges, etc., computers, cable television, space vehicles, avionics, ships, submarine cable and security and dark systems, electronic instrumentation systems, medical systems, satellite ground stations and industrial automation and process control. The coming development of integrated optic technology is hoped to play a bigger part in influencing further departures from existing concepts of electronic systems for communication, control and instrumentation.

2.3 Components of Optical Communication System

As is clear from the above discussion an optical communication system consists of the following main components:

1. Optical source
2. Optical modulator
3. Optical fiber as transmission wave guide
4. Optical detector
5. Demodulator

In addition, some other components like fiber amplifiers are also used in modern optical communication systems. In the following section some of these components are discussed briefly.

2.3.1 Optical Source

In an optical communication system electrical signals are first converted into optical signals by modulating an optical source such as light emitting diode (LED) or laser diode (LD).

The advantages of LED are as follows:

(i) Less sensitive to retro reflection

(ii) Possess no interference problem

(iii) Less sensitive to temperature variation

(iv) High reliability

(v) Simple electronic excitation

(vi) Less costly.

But the main disadvantages are:

(i) Low coupling efficiency between an LED and a fiber

(ii) Low modulation bandwidth, typically limited to 100 MHz to 200 MHz

(iii) Wide spectral width of about 50-100 MHz around 1550 nm.

The advantages of LD are:

(i) High conservation gain i.e. with small bias current relatively high power output

(ii) Low numerical aperture and as a result high coupling efficiency.

(iii) High modulation bandwidth

(iv) Narrow spectral width (10-50 MHz).

The main disadvantages are:

(i) Highly sensitive to temperature variation

(ii) Produce supplementary to return reflected power

(iii) Less reliable

(iv) More costly.

In summary, for short links (<10 km) LED is suitable, but for medium and long links LD is to be used.

2.3.2 Optical Fiber

The most important part of an optical communication system is the optical fiber. Optical fiber is essentially a thin filament of glass that acts as a waveguide. A waveguide is a physical medium or path that allows the propagation of electromagnetic waves such as light. The concepts of reflection and refraction can be interpreted most easily by considering the behavior of light rays associated with plane waves traveling in a dielectric material. When a light ray encounters a boundary separating two different media, part of the ray is reflected back into the first medium and the remainder is bent or refracted as it enters the second medium. The bending or refraction of light ray at the interface is a result of the difference in

the speed of light in two materials having different refractive indices. The relationship at the interface is governed by the Snell's law, as stated below.

$$n_1 \sin \theta_1 = n_2 \sin \theta_2$$

or,

$$n_1 \cos \theta_1 = n_2 \cos \theta_2 \qquad (2.1)$$

n_1 and n_2 are the refractive index of the two materials and $n_2<n_1$. The angles θ_1 and θ_2 are the angles of incidence and refraction respectively. So if a light travels from an optically denser material to a loss dense material, the angle of refraction becomes greater than the angle of incidence. If the angle of incidence reaches a particular value θ_c, the refraction angle becomes 90° and the refracted ray emerges parallel to the interface between the dielectrics. This angle is called the critical angle, which can be found as follows.

$$n_1 \sin \theta_c = n_2 \sin 90°$$

i.e.

$$\theta_c = \sin^{-1} (n_2/n_1) \qquad (2.2)$$

Now if the angle of incidence is greater than the critical angle, all of the incident ray will be reflected back and no refraction will occur. This phenomenon is referred to as the *total internal reflection*. Thus the total internal reflection occurs at the interface between two dielectrics when a light is incident on the dielectric of lower index from the dielectric of higher index and the angle of incidence of the ray exceeds the critical angle as shown in Fig. 2.3. This is the mechanism by which light at a sufficiently shallow angle (less than $90°- \theta_c$) may be considered to propagate down an optical fiber with low loss. The fiber consists of a core completely surrounded by a cladding,(both of which consists of glass of different refractive indices. The refractive index of the core is greater than that of the cladding, so the light travels via a series of total internal refractions at the interface of core and cladding as shown in Fig. 2.4. The light ray is known as a meridional ray as it passes through the axis of the fiber core. However, the above description is an ideal one. In practice, there is always some tunneling of optical energy through the interface. Also there may exist

loss of light into the cladding through refraction, rather than total internal reflection, due to any discontinuities or imperfections at the core-cladding interface.

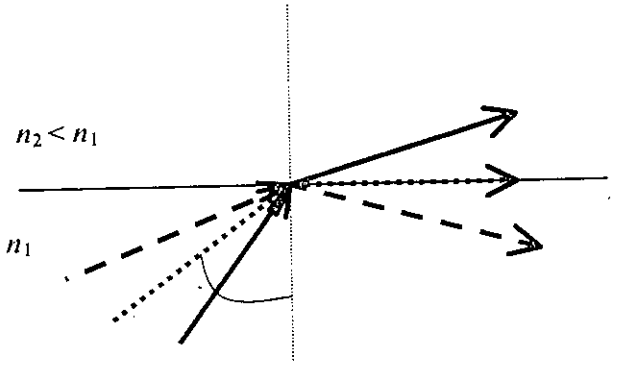

Fig. 2.3 Total internal reflection

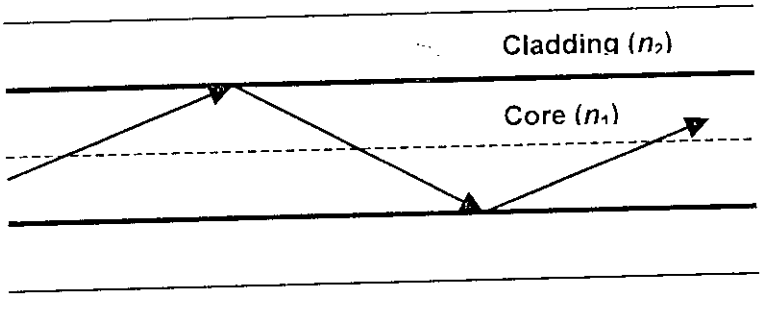

Fig. 2.4 Light propagation through fiber

Two major types of fibers are currently in use. They are stated below:

Single Mode fibers:

This fiber allows the transmission of only one mode of light through it. The core radius of such a fiber is typically from 2 to 10 μm. They are free from intermodal dispersion. They are suitable for transmission with a large bandwidth and chiefly used for long haul systems like undersea cables.

Multimode fibers:

This type of fiber allows more than one mode to propagate through it. It has larger core areas compared to single mode fibers. It supports smaller bandwidth and chiefly limited to applications where transmission distance is small.

2.3.3 Optical Detectors

After optical signal has been launched into the fiber, it becomes progressively attenuated and distorted with the increasing distance because of scattering, absorption, and dispersion in the fiber. At the receiver the attenuated and distorted optical power is detected by the photodiode. The figure of merit for a fiber is the attenuation and distortion which should be minimum and for a receiver there is a minimum optical power necessary at the desired data rate to attain either a given error probability for a digital system or a specified signal to noise ratio (SNR) for an analog system.

In optical communication systems, two important detection techniques are normally employed. These are as follows:

1. Intensity modulation direct detection (IM/DD)
2. Coherent detection

Intensity modulation direct detection (IM/DD):

In direct detection, a photodetector only responds to changes in the power level (the intensity) of an optical signal, and not to its frequency and phase content. So this is known as intensity modulation (IM). At the receiving end, one then uses direct detection (DD) to convert the optical signal into an electrical signal. The IM/DD systems are simple and less costly but the suffer from limited sensitivity and do not take full advantage of the tremendous bandwidth capabilities of optical fiber due to relatively low optical power output of semiconductor laser diode (SLD). Direct detection optical communication systems have been found very promising for future deep space applications, inter-satellite links and terrestrial line of sight communications. To increase the data rate throughput of all semiconductor free space optical channels, extensive research for bandwidth, power efficient coding and modulation schemes were carried out in the last decade.

Coherent detection:

In coherent detection the received optical signal is combined with the light output from a local oscillator (LO) laser and the mixed optical signal is converted to an intermediate frequency (heterodyne) or directly to baseband by homodyne. Two major advantages that coherent systems offer are as follows:

(i) Improved receiver sensitivity (up to 20 dB) relative to direct detection so that either the bit rate or the repeater spacing can be greatly increased.

(ii) A high degree of frequency selectivity on optical wavelength division multiplexing (WDM) system.

In this system information can be impressed on he optical carrier in three ways such as phase shift keying (PSK), frequency shift Keying (FSK) and Amplitude shift keying (ASK). These include binary PSK (BPSK), quadrature PSK (QPSK), orthogonal QPSK (OQPSK), continuous phase (CPSK), discontinuous phase FSK (DPFSK), Pulse position modulation (PPM), etc.

2.3.4 Modulation

In order to transmit optical signal via an optical fiber it is necessary to modulate a property of the light with the information signal. This property may be intensity, frequency, phase or polarization with either digital or analog signal. In analog modulation schemes the variation of light takes place in a continuous manner but in case of digital modulation discrete change in light wave is obtained. Although simpler to implement analog communication is less efficient, requiring a far greater signal to noise ratio than digital modulation. Also the linearity needed in analog modulation is not always provided by semiconductor optical sources. For these reasons analog optical fiber systems are generally limited to shorter distance and lower bandwidth than digital links.

In coherent communication system, information can be impressed on the optical carrier in one of the three ways as mentioned below:

i. Phase shift keying (PSK)
ii. Frequency shift keying (FSK)
iii. Amplitude shift keying (ASK)

Depending on the specific application, various modulation and demodulation formats, similar to those of traditional radio frequency communications, are also employed in coherent light wave transmission. These include binary PSK (BPSK), quadrature PSK (QPSK), orthogonal QPSK (OQPSK), continuous phase FSK (CPFSK), discontinuous phase FSK (DPFSK), binary pulse position modulation (BPPM) etc. Each of the modulation schemes and combinations thereof, with homodyne, heterodyne or diversity receivers has its own merits and demerits and none has emerged as an absolutely preferable.

Actually, the huge transmission capacity of single mode fibers can be exploited efficiently by accessing the fiber bandwidth in the wavelength domain rather than in the time domain. Among WDM systems, DWDM, in which the channel spacing is a few times the bit rate, allows the possibility of transmitting many channels simultaneously, increasing the transmission capacity. A sharp cutoff filter and a modulation scheme with compact spectrum are necessary to construct densely spaced multiplexing system using direct detection scheme.

2.3.5 Optical Amplifiers

Optical fibers attenuate light during propagation like any other material during propagation. In the case of silica fibers the attenuation constant is quite small particularly in the wavelength range 1.0-1.6μm where it is less than 1 dB/km with the minimum value of about 0.2dB/km occurring at 1.55 μm. For applications like local area networks the effect of attenuation can be neglected. But now-a-days optical fibers are heavily used as the transmission medium in long haul communication, which may have length more than several thousand kilometers. In practice the loss limitations are overcome by periodic boosting up of the power level by repeaters. There are two types of repeaters in use now-a-days. The first method is to use regenerators, which convert the optical signal into electrical signal and then, after amplification in the electrical domain, convert it back to optical signal by a transmitter. Much more benefit can be obtained if the electric repeaters are replaced by much simpler and potentially less expensive optical amplifiers, which amplify the optical signal directly.

Several kinds of optical amplifiers were studied and developed in the last two decades. A short description of them is given below.

1) Semiconductor laser amplifiers:

Semiconductor laser amplifiers utilize stimulated emission from injected carriers. Several kinds of laser amplifiers have been used in different applications. The most commonly used are Fabry-Perot amplifier which is an oscillator biased below oscillation threshold, the traveling wave (TW) and the near traveling wave (NTW) amplifiers, which are effectively single pass devices and the injection locked laser, which is a laser oscillator designed to oscillate at the incident signal frequency. Such devices are capable of providing high gain (15 to 35 dB) with low power consumption and their single mode waveguide structure make them particularly suitable for use with single mode fibers.

2) Fiber Amplifiers:

These amplifiers provide gain from excited dopants or by nonlinear effect like stimulated Raman scattering or stimulated Brillouin scattering. A schematic diagram of a general fiber amplifier system is shown in Fig. 2.5. The gain medium normally comprises of a single mode fiber connected to a dichroic coupler, which provides low insertion loss at both signal and pump wavelengths. Excitation occurs through pumping from a high power laser source, which is combined with the optical input signal within the coupler. The amplified optical signal is therefore emitted from other end of the active medium.

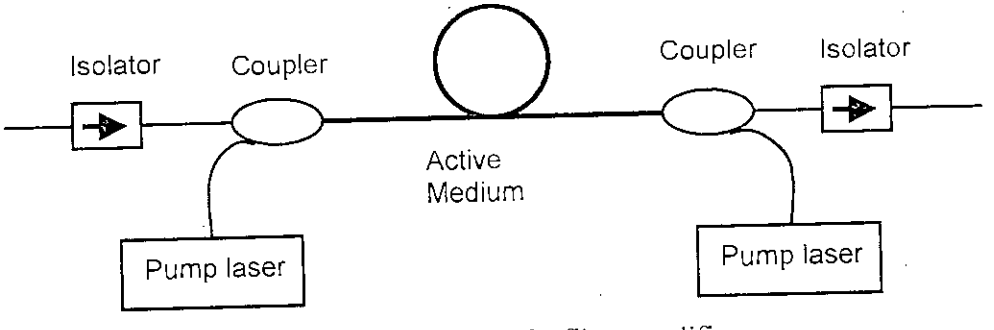

Fig. 2.5 Block diagram of a fiber amplifier

Three common types of fiber amplifiers are listed below.

1) Fiber Raman amplifiers:

It requires high pump powers (0.5 W-1W) that are not readily available from semiconductor lasers.

2) Fiber Brillouin amplifiers:

It can operate at low power levels but have too small bandwidth to be useful as in-line amplifiers in lightwave systems.

3) Erbium Doped Fiber Amplifier:

A new kind of fiber based on silica fibers doped with rare earth ions were developed in the late 1980s and turned out to be the most suitable for lightwave system applications. Of these fibers the most important one is the erbium doped fiber amplifier (EDFA), which has revolutionized the field of fiber optic communication. By making it possible to boost up the power level of the large number of signals that a multichannel optical system has to carry the erbium doped fiber amplifier (EDFA) has been a key enabling technology in popularizing the WDM systems. Erbium is a

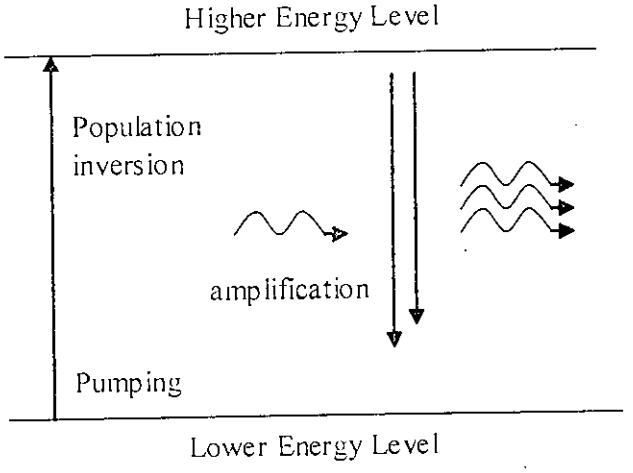

Fig. 2.6 Principle of operation of EDFA

rare earth element that, when excited, emits light around 1.54 μm. A weak signal enters the erbium doped fiber, into which 980 nm or 1480 nm is injected using a pump laser. This injected light stimulates the erbium atoms to release their stored energy as additional 1550 nm light. As this process continues down the fiber, the signal grows stronger. The key performance parameters of EDFA are gain, gain flatness, noise level and output power. EDFAs are typically capable of gains of 30 dB or more and output power of +17 dB or more. In practice, signals can travel for up to 120 km between amplifiers.

Like all optical amplifiers EDFA also amplify the incident light by stimulated emission, the same mechanism used by lasers. In fact optical amplifier is just a laser without feedback. Fig. 2.6 shows a typical optical amplifier. Here the dopants are excited to a higher energy state through absorption of pump photons and then relax rapidly to a lower energy excited state.

4) Regenerative Repeater:

These were used in optical communication system quite a period ago. Here at first at the end of some spans of an optical link the modulated optical signal was detected first and then again modulated to be transferred in further optical link transmission mediums. The name is self explanatory. Here the main objective is to repeat the optical system and to do so the optical signal was at first converted to an electrical signal. The schematic diagram is shown below for that kind of detectors:

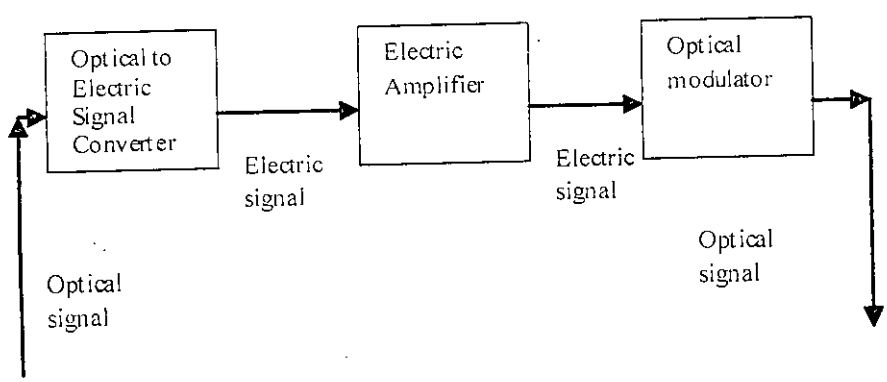

Fig. 2.7 Regenerative Repeater

2.4 Multiplexing in Optical communication System

Huge information can be transmitted through a single fiber by using multiplexing schemes. The different multiplexing techniques employed with IM/DD optical fiber system are wavelength division multiplexing (WDM), optical frequency division multiplexing (OFDM), optical time division multiplexing (OTDM) or a hybrid approach to achieve tera bit per second channel capacity. Wireless CDMA has been successfully implemented, now a day, research interest is beginning with optical code division multiple access (OCDMA) that can further enhance the functionality of optical networks.

2.4.1 Wavelength Division Multiplexing (WDM)

Transmitting many different wavelengths of laser light down the same optical fiber at the same time, in order to increase the amount of information that can be transferred is called wavelength division multiplexing (WDM). There are different types of WDM setups. Two types such as unidirectional and bidirectional setups are discussed below:

Unidirectional WDM:

Unidirectional WDM device is used to combine different signal carrier wavelengths onto a single fiber at one end and separate them onto their corresponding detectors at the other end as shown in Fig. 2.8.

Bidirectional WDM:

In Bidirectional WDM two or more waves are transmitted simultaneously over the same fiber. It involves sending information in one direction at a wavelength λ_1 and simultaneously transmitting data in the opposite direction at a wavelength λ_2 as shown in Fig. 2.9.

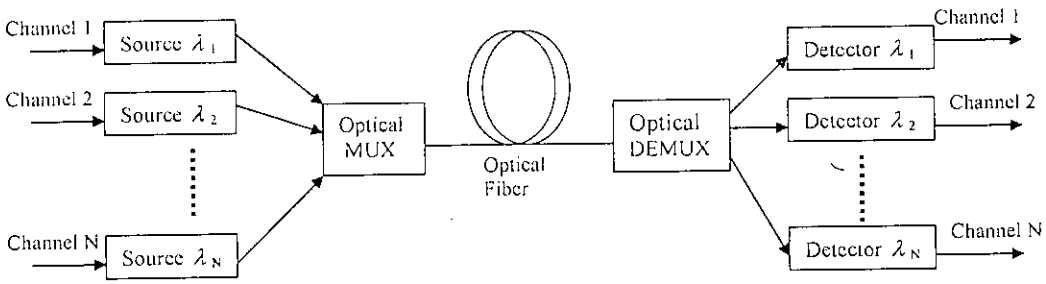

Fig. 2.8 Unidirectional WDM System

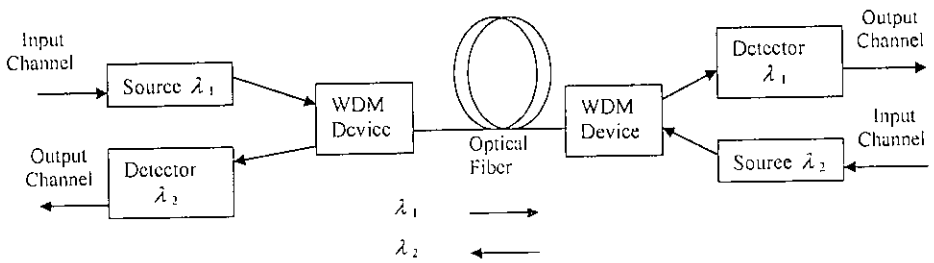

Fig. 2.9 Bi-directional WDM System

2.4.2 Frequency Division Multiplexing (FDM)

In FDM the optical channel bandwidth is divided into a number of nonoverlapping frequency bands and each signal is assigned one of these bands of frequencies. The schematic block diagram of FDM system is shown in Fig. 2.10. The individual signal can be extracted from the combined signal by appropriate electrical filtering in the receive terminal. Hence FDM is usually done electrically at the transmit terminal prior to intensity modulation of a single optical source.

2.4.3 Optical Time Division multiplexing (OTDM)

The principle of OTDM technique is to extend time division multiplexing by optically combining a number of lower speed electronic baseband digital channels as shown in Fig. 2.11.

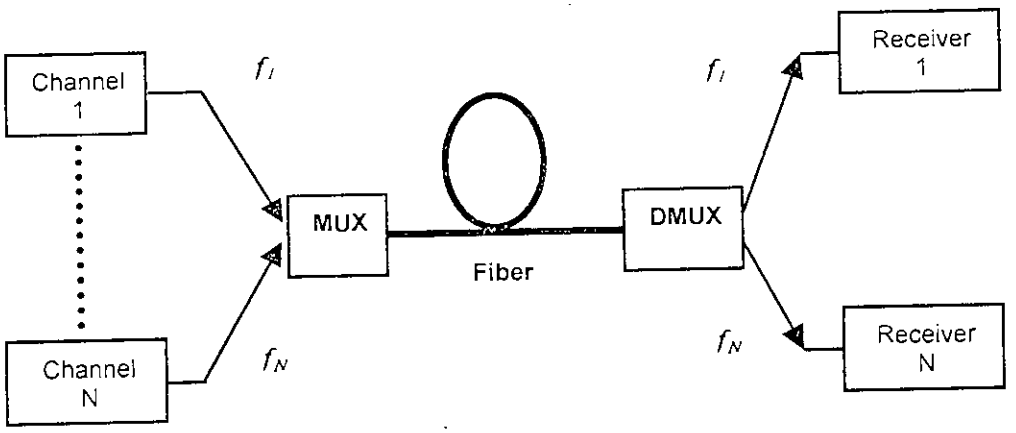

Fig. 2.10 Typical Arrangement for FDM System

2.4.4 Optical Code Division Multiple Access (OCDMA)

In the last decade, OCDMA systems have attention to the researchers on optical communication because they offer several attractive features such as asynchronous access, privacy and security in transmission, ability to support variable bit rate and busy traffic and scalability of the network.

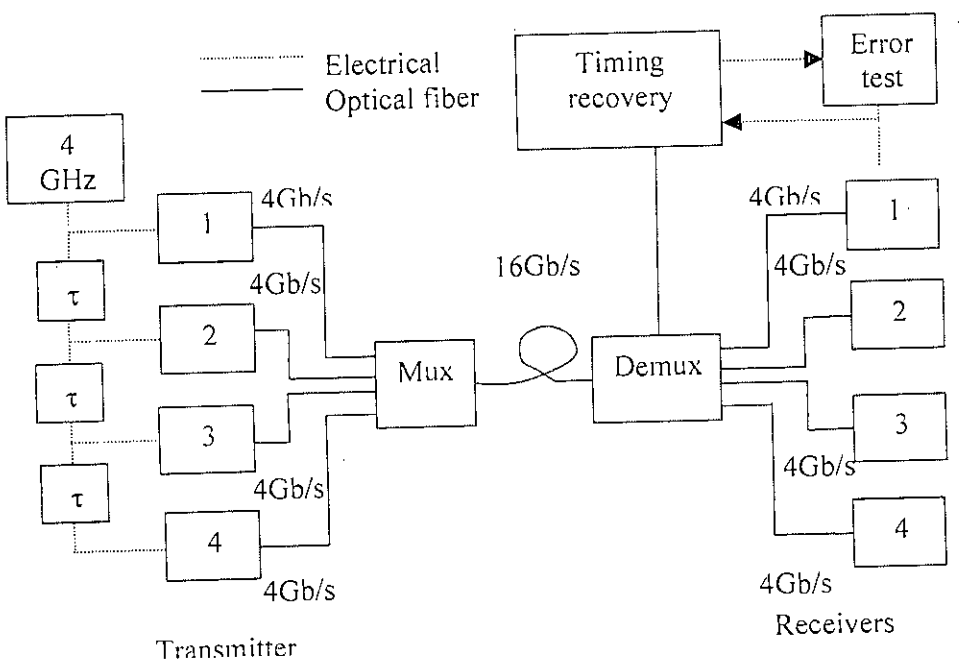

Fig. 2.11 Four channel OTDM fiber system

The broad bandwidth of optical fiber can be utilized in OCDMA system for very high speed communication. In OCDMA system, a large number of separate users share the same extended transmission optical bandwidth but they are separated by individual specific address code signature sequence with good correlation properties. The addressing of the users can be performed either in the time domain [direct sequence (DS-CDMA)] or frequency domain [frequency hopping (FH-CDMA)].

Chapter 3

Limitations of Optical Communications

3.1 Introduction

Although optical communication system is more advantageous there are some limitations of optical fiber communication systems such as

(i) Fiber Chromatic Dispersion (FCD)

(ii) Optical Fiber Nonlinearities

(iii) Laser Phase Noise

(iv) Optical Amplifier's spontaneous emission (ASE) noise

Fiber chromatic dispersion and nonlinearities are described below in brief.

3.2 Fiber Chromatic Dispersion

Dispersion is a phenomenon in optical fiber light transmission which causes distortion to both digital and analog transmission along the fiber. In digital communication the dispersion mechanisms within the fiber cause broadening of the transmitted light pulse as they travel along the channel. We know that all the frequency components must have proportional velocities in the fiber to maintain their in-between relative phase relationship to be added in the receiving end in proper phase to successfully reconstruct the signal. But velocity of propagation of light is influenced by interaction of the waves with the atoms of the material, where the interaction is a function of frequency. This dependence is expressed by the following equation

$$v_g = \frac{c}{n - \lambda \frac{dn}{d\lambda}} \tag{3.1}$$

where v_g is the group velocity, n is the refractive index, λ is the wavelength of the light, c is the velocity of light in vacuum. The refraction index of silica is dependent

upon the signal wavelength. Thus the velocity of propagation becomes a function of wavelength and so different frequency components will travel at different velocities. The time delay between different spectral components causes spectral broadening of the optical signal and overlapping of adjacent pulses. After certain overlap, the adjacent pulses can no longer be individually distinguishable as shown in Fig. 3.1. This is known as intersymbol interference (ISI) [51], [58-59]. Chromatic dispersion can severely limit information capacity of an optical fiber transmission system. Dispersion effect becomes significant in single mode fibers for bit rates higher than 4 GHz.

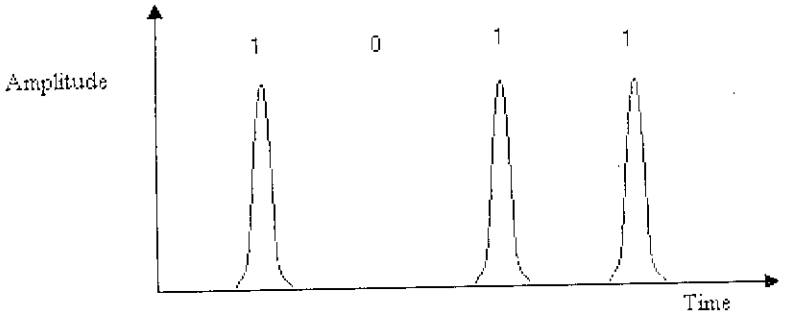

(a) Input pulses

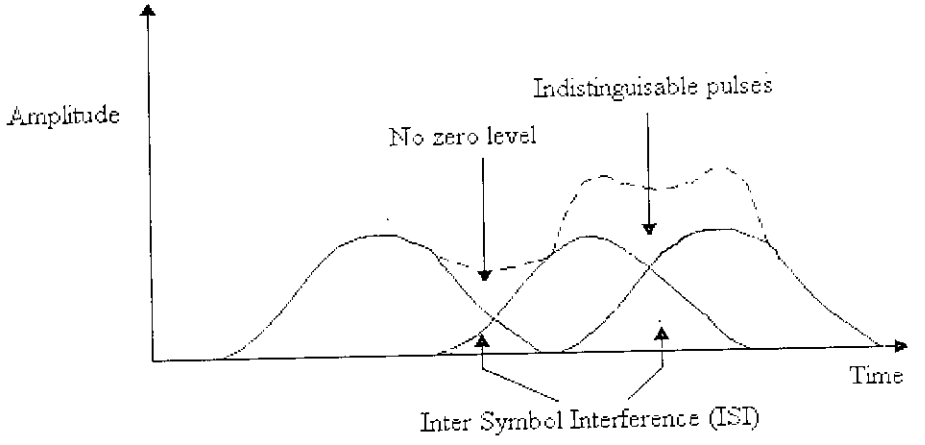

(b) Output pulses

Fig. 3.1 Effect of dispersion

There are basically two types of dispersion:

1) ***Intermodal dispersion:*** In a multimode transmission system, as each mode has a different group velocity at a single frequency, this sort of dispersion results. In a purely single mode fiber this type of dispersion is absent.
2) ***Intramodal dispersion:*** Within a single mode, because of group velocity being a function of wavelength this type of dispersion takes place. This is commonly known as the chromatic dispersion.

Chromatic dispersion again can be separated into three parts:

1) ***Material dispersion (D_M):*** It arises from the variation of the refractive index of the core material as a function of the wavelength. It occurs when the phase velocity of a plane wave propagating in the fiber varies nonlinearly with the wavelength. It is the principal factor causing dispersion.
2) ***Waveguide dispersion (D_W):*** It results from the variation in group velocity with wavelength for a particular mode. Multimode fibers where the majority of modes propagate far from cut off are almost free from waveguide dispersion. However in single mode fibers this kind of dispersion can be quite significant.
3) ***Profile dispersion:*** It originates from the refractive index profile of the fiber. Its contribution is usually quite insignificant and usually neglected in practice.

Total dispersion of the fiber can be obtained by adding material dispersion and waveguide dispersion as shown in Fig. 3.2. Intra-modal or chromatic dispersion may occur in all type of fibers and results from the finite spectral line width of the optical source. Since optical sources do not emit just a single frequency but a band of frequencies (for LASER corresponds to only a fraction of a per cent of the center frequency, whereas LED corresponds a significant percentage), then there will be propagation delay due to variance in velocity between the different spectral components of the transmitted signal. This causes broadening of each transmitted mode and hence intra-modal dispersion. The delay differences may be caused by the dispersive properties of the waveguide material (material dispersion) and also guidance effects within the fiber structure (waveguide dispersion).

A wide variety of single-mode fiber refractive index profiles are capable of modification in order to tune the zero dispersion wavelength point to a specific

wavelength within a region adjacent to the zero-material dispersion point. It is evident that it is appreciable to make the central frequency reside at zero dispersion wavelengths. Now total dispersion is the algebric summation of the dispersion due to material and due to waveguide structure. A general SiO_2 fiber have its zero dispersion wavelength at about 1.375 μm but this wavelength is not preferable in optical fiber because this wavelength is not generally associated with preferable light wavelength range and generally available LASER and LEDs. In the simplest case the step index profile gives a shift to longer wavelength by reducing the core diameter and increasing fractional index difference.

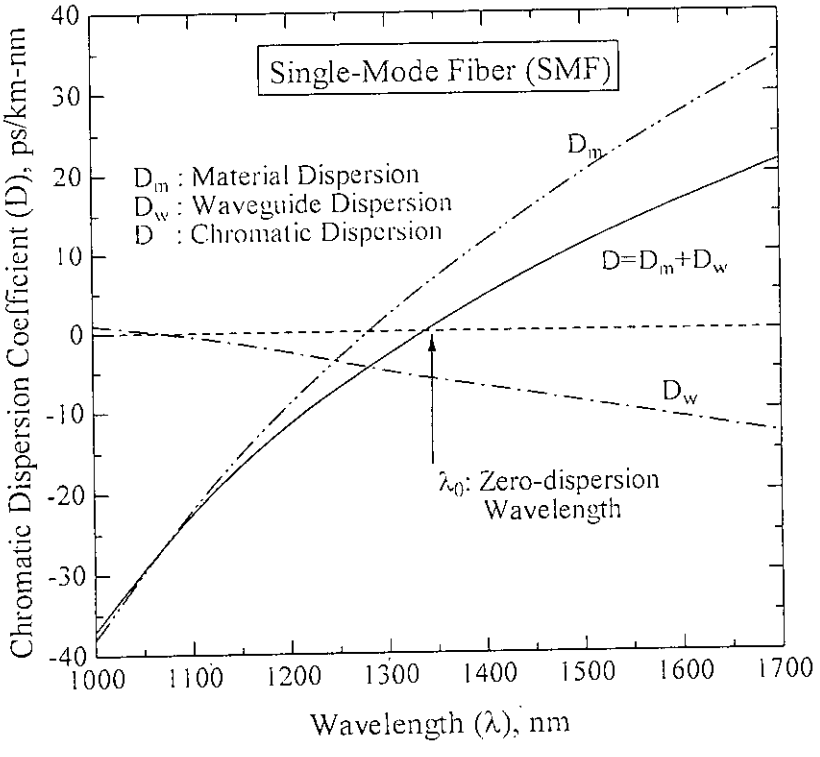

Fig. 3.2 Chromatic dispersion characteristics of standard SMF [58]

We want zero dispersion wavelengths at a wavelength of 1.55 μm because attenuation at this wavelength is minimum. We have no hand on the dispersion due to material but we may slightly alternate the dispersion characteristics due to

waveguide structure by modifying the waveguide structure. As such, we shall alter the dispersion characteristics due to the waveguide structure so that the total dispersion characteristics i.e. the summation of dispersion due to material and due to waveguide have a zero dispersion wavelength at 1.55 μm as shown in Fig. 3.3. This type of optical fiber is known as dispersion shifted fiber. Further it is evident that as the material dispersion characteristics curve has a positive slope, the waveguide dispersion characteristics curve should be negative and preferably have negative slope. Now for higher performance in the optical fiber communication the dispersion should be as little as possible so that the all frequency components maintain their phase relationships. As such, we may alter the waveguide structure to get the best dispersion characteristics.

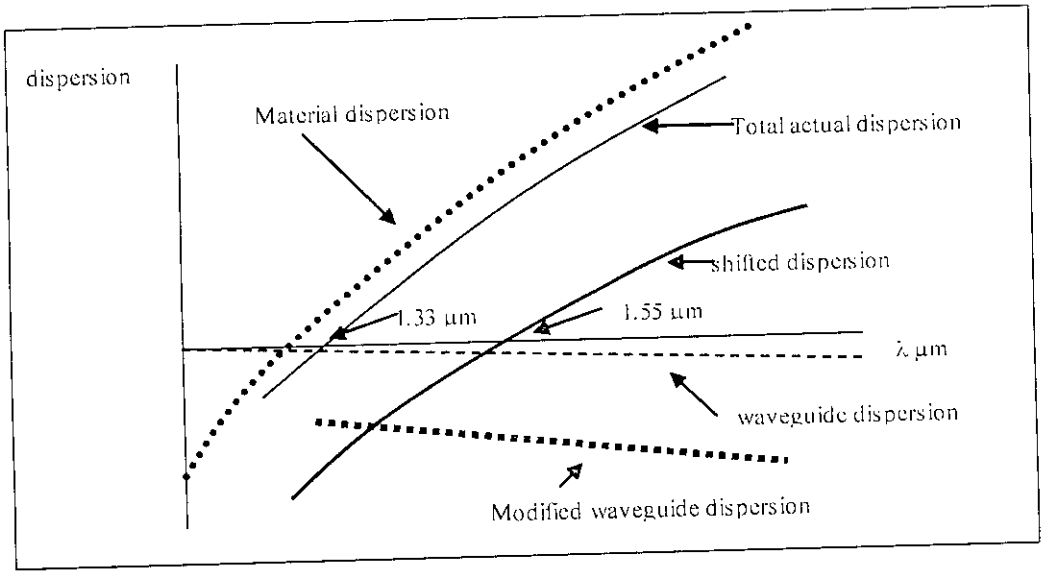

Fig. 3.3 Optical Fiber Dispersions

3.3 Fiber Nonlinearities

Fiber nonlinearities arise from two basic mechanisms. The first, and most serious, is the fact that the refractive index of glass is dependent on the optical power going

through the material. The general equation for the refractive index of the core in an optical fiber is:

$$n = n_0 + n_2 P / A_{eff} \tag{3.2}$$

where n_0 is the refractive index of the fiber core at low optical power levels, N_2 is the nonlinear refractive index coefficient. It is equal to 2.35×10^{-20} m^2/W for silica, P is the optical power in watts. A_{eff} is the effective area of the fiber core in square meters. It can be seen that the magnitude of the change in refractive index is relatively small. It becomes important since the interaction length in a real fiber optic system can be hundreds of kilometers. The power-dependent refractive index of silica gives rise to the SPM, XPM and FWM nonlinearities.

The second mechanism for generating nonlinearities in fiber is scattering phenomena. These mechanisms give rise to SBS and SRS effects.
Fiber nonlinearities that now must be considered in designing state-of-the-art fiber optic systems include stimulated Brillouin scattering (SBS), stimulated Raman scattering (SRS), four wave mixing FWM), self-phase modulation (SPM) and cross phase modulation (XPM). Different types of fiber nonlinearities are discussed shortly here:

3.3.1 Stimualated Brillouin Scattering (SBS)

Stimulated Brillouin scattering (SBS) is a fiber nonlinearity that imposes an upper limit on the amount of optical power that can be usefully launched into an optical fiber. The SBS effect has a threshold optical power. When the SBS threshold is exceeded, a significant fraction of the transmitted light is redirected back toward the transmitter. This results in a saturation of optical power that reaches the receiver, as well as problems associated with optical signals being reflected back into the laser. The SBS process also introduces significant noise into the system, resulting in degraded BER performance [60-61]. As a result, controlling SBS is particularly important in high speed transmission systems employing external modulators and continuous wave laser sources. It is also of vital importance to the transmission of

1550 nm-based CATV transmission, since these transmitters often have the very characteristics that trigger the SBS effect levels that can be carried over the fiber.

3.3.2 Stimulated Raman Scattering (SRS):

Stimulated Raman Scattering occurs when a large pump wave is co-injected at a lower wavelength than the signal to be amplified. In SRS incident light is scattered at a down shifted (stoke shifted) frequency [52], [63]. This process is strongly dependent on the power of the incident beam, called the pimp. As the pump power increases the scattering increases until the scattered power reaches a threshold level. If the pump power is increased beyond this limit the scattering becomes stimulated and the pump rapidly losses its power to the Stoke-shifted beam. The pump is thus depleted due to SRS.

3.3.3 Self Phase Modulation (SPM):

SPM is a phenomenon that is due to the power dependency of the refractive index of the fiber core [51]. It interacts with the chromatic dispersion in the fiber to change the rate at which the pulse broadens as it travels down the fiber. Whereas increasing the fiber dispersion will reduce the impact of FWM, it will increase the impact of SPM. As an optical pulse travels down the fiber, the leading edge of the pulse causes the refractive index of the fiber to rise causing a blue shift. The falling edge of the pulse decreases the refractive index of the fiber causing a red shift. These red and blue shifts introduce a frequency chirp on each edge which interacts with the fiber's dispersion to broaden the pulse.

3.3.4 Cross Phase Modulation (XPM):

Cross phase modulation is very similar to SPM except that it involves two pulses of light, whereas SPM needs only one pulse. In XPM, two pulses travel down the fiber, each changing the refractive index as the optical power varies. If these two pulses happen to overlap, they will introduce distortion into the other pulses through XPM. Unlike, SPM, fiber dispersion has little impact on XPM [63]. Increasing the fiber effective area will improve XPM and all other fiber nonlinearities.

3.3.5 Four Wave Mixing:

When three intelligence lights passes through an optical transmission system a fourth light frequency is produced by the interactions among those three intelligence lights [52-57]. The newly produced light is known as FWM light and the phenomenon is known as FWM. A light frequency f_F of an FWM light which is generated by third order non-linear effect is related to three signal light frequencies f_1, f_2 and f_3 as follows.

$$f_F = f_{ijk} = f_i + f_j - f_k, \qquad i, j \neq k \tag{3.3}$$

Four wave mixing will be discussed in details in the next chapter.

Chapter 4

Four Wave Mixing

4.1 Introduction

Four-wave mixing (FWM) is a nonlinear process in optical fibers in which generally three signal frequencies combine and produce several mixing products. It originates from the weak dependence of the fiber refractive index on the intensity of the optical wave propagating along the fiber through the third order non linear susceptibility. If three signal waves with frequencies f_p , f_q, f_r are incident at the fiber input, new waves are generated whose frequencies are

$$f_{pqr}=f_p+f_q-f_r \quad (p, q, r = 1, 2, 3) \tag{4.1}$$

Here we exclude f_{pqr} with $p=r$ or $q=r$ where interruptions from other channels to signal do not happen. As a result, we will examine FWM lights with the frequency of $f_{321}, f_{312}, f_{213}, f_{332}, f_{331}, f_{223}, f_{221}, f_{113}$, and f_{112} which are shown in Fig. 4.1.

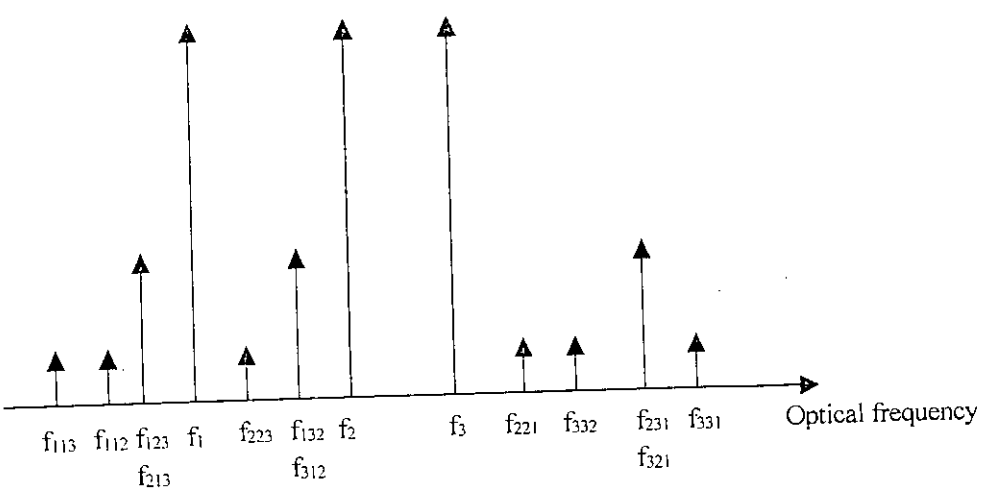

Fig. 4.1 Generated waves through fiber four wave mixing

Note that the number of the FWM lights is enhanced drastically with an increase in the number of frequency components in transmitted signal. This is called "four wave mixing" since three waves interfere to provide a fourth wave. Again it is sometimes called "four photon mixing".

4.2 Effect of FWM

The first effect is that signal power is reduced in order to produce the mixing products. This is known as power depletion. In multi-wavelength optical system FWM products can destructively interfere with the signal, causing major signal effects. And hence deteriorate the system performance. Let's say we take three frequencies named as $p=1$, $q=2$, $r=3$. As a result the three co-propagating waves will give rise by FWM to nine new optical waves with the frequencies of f_{321}, f_{312}, f_{213}, f_{332}, f_{331}, f_{223}, f_{221}, f_{113}, *and* f_{112}. It reveals that from the above that from every three wavelengths there would be nine FWM lights produced i.e. ${}^{3}C_{3} \times 9 = 9$. So if we take four channels it may appear that the resulting FWM lights would be ${}^{4}C_{3} \times 9 = 36$. But actually the case is not like that. There will be some repetitions in the FWM light calculation formula which must be eliminated.

Let four frequencies f_a, f_b, f_c and f_d. The detailed explanation of FWM lights produced is as follows:

TABLE 4.1: The FWM frequency combinations

Row No.	*i=a, j=b, k=c*	*i=b, j=c, k=d*	*i=c, j=d, k=a*	*i=a, j=b, k=d*
1	$f_{abc}=f_a+f-f_c$	$f_{bcd}=f_b+f_c-f_d$	$f_{cda}=f_c+f_d-f_a$	$f_{abd}=f_a+f_b-f_d$
2	$f_{bca}=f_b+f_c-f_a$	$f_{cdb}=f_c+f_d-f_b$	$f_{dac}=f_d+f_a-f_c$	$f_{bda}=f_b+f_d-f_a$
3	$f_{acb}=f_a+f_c-f_b$	$f_{bdc}=f_b+f_d-f_c$	$f_{cad}=f_c+f_a-f_d$	$f_{adb}=f_a+f_d-f_b$
4	$f_{aab}=f_a+f_a-f_b$	$f_{bbc}=f_b+f_b-f_c$	$f_{cca}=f_c+f_c-f_a$	$f_{aab}=f_a+f_a-f_b$
5	$f_{aac}=f_a+f_a-f_c$	$f_{bbd}=f_b+f_b-f_d$	$f_{ccd}=f_c+f_c-f_d$	$f_{aad}=f_a+f_a-f_d$
6	$f_{bbc}=f_b+f_b-f_c$	$f_{ccb}=f_c+f_c-f_b$	$f_{dda}=f_d+f_d-f_a$	$f_{bbd}=f_b+f_b-f_d$
7	$f_{bba}=f_b+f_b-f_a$	$f_{ccd}=f_c+f_c-f_d$	$f_{ddc}=f_d+f_d-f_c$	$f_{bba}=f_b+f_b-f_a$
8	$f_{cca}=f_c+f_c-f_a$	$f_{ddb}=f_d+f_d-f_b$	$f_{aac}=f_a+f_a-f_c$	$f_{dda}=f_d+f_d-f_a$
9	$f_{ccb}=f_c+f_c-f_b$	$f_{ddc}=f_d+f_d-f_c$	$f_{aad}=f_a+f_a-f_d$	$f_{ddb}=f_d+f_d-f_b$

If F is the total number of wavelengths in a transmitted signal then total number of generated FWM lights is given by [63]

$$N_F = (F^3 - F^2)/2 \tag{4.2}$$

The number of FWM products increase sharply with the increase of wavelengths as shown in Fig. 4.2.

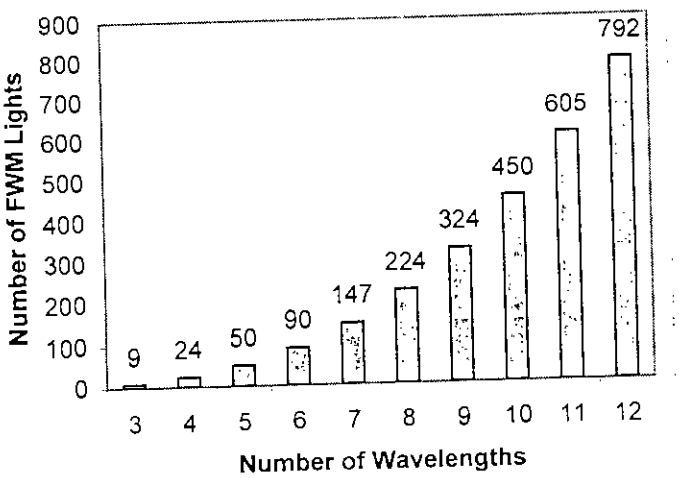

Fig. 4.2 Number of FWM Lights with increasing number of wavelengths

4.3 Mathematical Analysis of FWM

In multi-wavelengths optical communication networks FWM degrades the performance by causing crosstalk and imposing restrictions on the input power. When light propagates in optical channel of uniform chromatic dispersion with wavelengths centered around the zero dispersion wavelength the phase matching criteria is matched and, as such, FWM is generated efficiently. When amplifiers are used in a regular interval of optical fiber span the generated FWM power is amplified and accumulated throughout the optical medium while transmitting. In actual

terrestrial transmission lines the each repeater span is a composition of a number of short length fibers with different and varied zero dispersion wavelengths independent of each other. And, as such, the efficiency of FWM will be different in each of those short length fibers of non-uniform chromatic dispersion. Here we shall analytically analyze FWM expression and evaluate channel crosstalk with randomly chosen dispersive fibers and probability of input powers.

4.3.1 Calculation of FWM Power

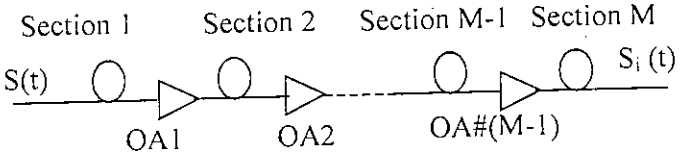

Fig. 4.3 Typical optical transmission line, OA: Optical amplifier

Here the analytical analysis for fiber FWM in multi-amplifier systems with uniform chromatic dispersion starts. Let's consider a model – the total transmission line consists of M section, as such, requiring a number of (M-1) amplifiers with equal repeater span throughout the system. Each repeater has an amplifier to compensate the power loss of the section just before the amplifier. As such, the power input at the beginning of each section is essentially equal. The length of each fiber is also equal. There are some assumptions before we proceed:

I. The polarization states of each optical frequency sources-lights are matched throughout the transmission system.

II. The dispersion characteristic throughout each fiber length is uniform.

III. The amplifiers are tuned to compensate the power loss in each section before, to have a constant input power at the beginning of each section.

IV. For simplicity polarization mode dispersion will be ignored

For every three light frequency components the fourth wave light will be evaluated by the frequency

$$f_F = f_p + f_q - f_r \tag{4.2}$$

where f_F is the fourth wave light frequency and f_p,f_q and f_r are the three light frequencies of transmitted signal.

Let α is attenuation constant co-efficient of fiber, $\beta_p^{(m)}$ is propagation constant for f_p light in the m-th section, $\beta_q^{(m)}$ is propagation constant for f_q light in the m-th section, $\beta_r^{(m)}$ is propagation constant for f_r light in the m-th section, $\beta_F^{(m)}$ is propagation constant for FWM light in the m-th section, k_f is FWM efficiency co-efficient, M is the number of sections L is length of each fiber, $E_p^{(m)}$ is the intensity of electric field of f_p light in the beginning of m-th fiber section, $E_q^{(m)}$ is the intensity of electric field of f_q light in the beginning of m-th fiber section, $E_r^{(m)}$ is Intensity of electric field of f_r light in the beginning of m-th fiber section, $E_F^{(m)}$ is Intensity of electric field FWM generated in nth fiber in mth section and $f_o^{(m)}$ is zero dispersion frequency of m-th fiber section c is the light velocity, n is the refractive index, λ is the guide wavelength and D_c is the fiber chromatic dispersion.

Phase difference for DSF can be written as,

$$\Delta\beta_F^{(m)} = \beta_p^{(m)} + \beta_q^{(m)} - \beta_r^{(m)} - \beta_F^{(m)} =$$

$$-\frac{\pi}{c^2}\frac{dD_c}{d\lambda}\left\{\left(f_p - f_o^{(m)}\right)+\left(f_q - f_o^{(m)}\right)\right\}\left(f_p - f_r\right)\left(f_q - f_r\right) \qquad (4.3)$$

To simplify the calculations another assumption is as follows

FWM light at the end of the transmission line is composed of FWM lights generated in each fiber and linearly propagated through the remaining part of the system.

As such, we are to calculate the FWM light in each fiber in each sections an then after linear propagation, sum them at the end of the transmission line.

Firstly we shall derive a general formula for the FWM light at the end of m-th fiber section then we get by integrated mathematics. FWM electric field at the end of the m-th fiber is given as

$$E_F^{(m)} = k_f E_p^{(m)} E_q^{(m)} E_r^{(m)^*} \exp\left[\left(-\frac{\alpha}{2} + i\beta_F^{(m)}\right)L\right] \frac{1-\exp\left[\left(-\alpha + i\Delta\beta_F^{(m)}\right)L\right]}{\alpha - i\Delta\beta_F^{(m)}} \tag{4.5}$$

where $k_f = \frac{i(2\pi)}{n\lambda} D\chi$, c is light velocity, D is degeneracy factor and χ is third order non-linear susceptibility. The each light field at the m-th fiber section is given by

$$E_p^{(m)} = E_p^1 \exp\left[\sum_{j=1}^{m-1} \left(i\beta_p^{(j)}\right)L\right] \tag{4.6a}$$

$$E_q^{(m)} = E_q^1 \exp\left[\sum_{j=1}^{m-1} \left(i\beta_q^{(j)}\right)L\right] \tag{4.6b}$$

$$E_r^{(m)} = E_r^1 \exp\left[\sum_{j=1}^{m-1} \left(i\beta_r^{(j)}\right)L\right] \tag{4.6c}$$

where E^1 is the field at the beginning of the first fiber section for the corresponding light.

Substituting (4.6) in (4.5) we get

$$\begin{aligned}
E_F^{(m)} &= k_f E_p^1 E_q^1 E_r^{1^*} \exp\left[\sum_{j=1}^{m-1} i\left(\beta_p^{(j)} + \beta_q^{(j)} - \beta_r^{(j)}\right)L\right] \exp\left[\left(-\frac{\alpha}{2} + i\beta_F^{(m)}\right)L\right] \\
&\times \frac{1-\exp\left[\left(-\alpha + i\Delta\beta_F^{(m)}\right)L\right]}{\alpha - i\Delta\beta_F^{(m)}} \\
&= k_f E_p^1 E_q^1 E_r^{1^*} \exp\left[\left(-\frac{\alpha}{2} + i\beta_F^{(m)}\right)L\right] \exp\left[\sum_{j=1}^{m-1} \left(i\left(\beta_p^{(j)} + \beta_q^{(j)} - \beta_r^{(j)} - \beta_F^{(j)}\right) + i\beta_F^{(j)}\right)L\right] \\
&\frac{1-\exp\left[\left(-\alpha + i\Delta\beta_F^{(m)}\right)L\right]}{\alpha - i\Delta\beta_F^{(m)}} \\
&= k_f E_p^1 E_q^1 E_r^{1^*} \exp\left[\left(-\frac{\alpha}{2} + i\beta_F^{(m)}\right)L\right] \exp\left[\sum_{j=1}^{m-1} \left(i\Delta\beta_F^{(j)} + i\beta_F^{(j)}\right)L\right] \frac{1-\exp\left[\left(-\alpha + i\Delta\beta_F^{(m)}\right)L\right]}{\alpha - i\Delta\beta_F^{(m)}}
\end{aligned} \tag{4.7}$$

The above equation gives the expression of the FWM produced in the m-th fiber section and this FWM light linearly propagate to the end to be summed with the FWM lights produced in the other fibers section. If $E_F^{(m)}$ be the FWM produced at the m-th fiber section, at the end of the whole transmission line

$$E_F^{(m)}\big|_{m=M} = E_F^{(m)} \exp\left[i \sum_{k=m+1}^{M} \beta_F^{(k)} \right] \tag{4.8}$$

From (4.7) and (4.8)

$$E_F^{(m)}\big|_{m=M} = k_f E_p^1 E_q^1 E_r^{1\,*} \exp\left[\left(-\frac{\alpha}{2} + i\beta_F^{(m)}\right)L\right] \exp\left[\sum_{j=1}^{m-1}\left(i\Delta\beta_F^{(m)} + i\beta_F^{(m)}\right)L\right]$$

$$\frac{1-\exp\left[\left(-\alpha + i\Delta\beta_F^{(m)}\right)L\right]}{\alpha - i\Delta\beta_F^{(m)}} \exp\left[i \sum_{k=m+1}^{M} \beta_F^{(k)}\right]$$

$$= k_f E_p^1 E_q^1 E_r^{1\,*} \exp\left(-\frac{\alpha L}{2}\right) \exp\left[\sum_{j=1}^{m-1} i\Delta\beta_F^{(j)} L\right] \frac{1-\exp\left[\left(-\alpha + i\Delta\beta_F^{(m)}\right)L\right]}{\alpha - i\Delta\beta_F^{(m)}}$$

$$\exp\left[i \sum_{k=1}^{M} \beta_F^{(k)}\right] \tag{4.9}$$

At the end of the transmission line the total FWM light will be got by the following summation.

$$E_F\big|_{total} = \sum_{m=1}^{M} E_F^{(m)}\big|_{m=M}$$

$$= \sum_{m=1}^{M} k_f E_p^1 E_q^1 E_r^{1\,*} \exp\left(-\frac{\alpha L}{2}\right) \exp\left[\sum_{j=1}^{m-1} i\Delta\beta_F^{(j)} L\right]$$

$$\frac{1-\exp\left[\left(-\alpha+i\Delta\beta_F^{(m)}\right)L\right]}{\alpha-i\Delta\beta_F^{(m)}}\exp\left[i\sum_{k=1}^{M}\beta_F^{(k)}\right] \tag{4.10}$$

The above equation corresponds to intensity. The following equation will give power

$$P_{FWM}=\frac{1024\pi^6}{n^4\lambda^2c^2}(D\chi)^2\frac{P_pP_qP_r}{A_{eff}^2}\exp(-\alpha L)$$
$$\cdot\left|\sum_{m=1}^{M}\exp\left[i\sum_{j=1}^{m-1}\Delta\beta_F^{(j)}L\right]\frac{1-\exp\left[\left(-\alpha+i\Delta\beta_F^{(m)}\right)L\right]}{\alpha-i\Delta\beta_F^{(m)}}\exp\left[i\sum_{k=1}^{M}\beta_F^{(k)}\right]\right|^2 \tag{4.11}$$

where A_{eff} is effective mode area, P_p is input power of f_p light, P_q is input power of f_q light and P_r is input power of f_r light.

Chapter 5

Analysis of Optical Code Division Multiple Access (OCDMA) Transmission System

5.1 The Principle of Spread Spectrum

In spread spectrum techniques, a modulated signal is further modulated (spreaded) by a noise-like code of much higher bit rate in such a way as to generate an extended bandwidth signal that does not significantly interfere with other signals and resembles white noise. Bandwidth expansion is achieved by a second modulation means. The receiver can only detect the signal and extract it from noisy signal if it knows the spreading code (signature sequence) that has been used to spread the signal.

The term spread spectrum has been used in a wide variety of military and commercial communication system. In spread spectrum systems each information signal requires significantly more radio frequency (RF) bandwidth than a conventional modulated signal would require. The benefits of using spread spectrum techniques are:

- Improved interference rejection
- Code division multiplexing for code division multiple access (CDMA) application.
- Low density power spectra for signal hiding
- High resolution ranging
- Secured communication
- Lower cost of implementation readily available IC (Integrated Circuit) components.

5.2 Radio Frequency Communications Spread Spectrum Techniques

The most commonly employed spread spectrum modulation techniques in electrical domains are:

- Direst sequence spread spectrum (DS-SS), including CDMA
- Frequency hopped (FH) spread spectrum, including slow frequency hopping (SFH) and fast frequency hopping (FFH) system.
- Carrier sense multiple access (CSMA) spread spectrum
- Time hopping
- Hybrid Spread Spectrum Method

In mobile radio systems and wireless local area networks (WLAN), direct sequence, frequency-hopped CDMA, ands CSMA methods have been extensively used. Brief description of direct sequence and frequency hopped spread spectrum techniques is given below.

5.2.1 Direst Sequence Spread Spectrum

Direct sequence CDMA is automatically associated to a spread spectrum communication system. The message is first modulated by traditional amplitude, frequency or phase techniques. A pseudo noise signal is then used as a code sequence (PN code) to spread the modulated waveform over a relative wide bandwidth. The signal message may be also coded by the code sequences and after that, modulated by a BPSK (for example) waveform. A schematic block diagram of direct-sequence spread spectrum system is given in figure 5.1 (a) and 5.2 (b). The digital binary base-band information, $d(t)$, also known as nonreturn to zero(NRZ) data, having a source bit rate of $R_b=1/T_b$, modulated by BPSK (for example) in the first modulator. $d(t)$ is an unfiltered binary signal having two states +1 or-1. The direct sequence spread spectrum may be obtained by multiplying the modulated signal signal $S(t)$ by a pseudorandom noise signal $g(t)$ having a chip rate of $R_c = 1/T_c$. Transmitted signal can be written as

$$S_{tx}(t) = S(t).g(t) \tag{5.1}$$

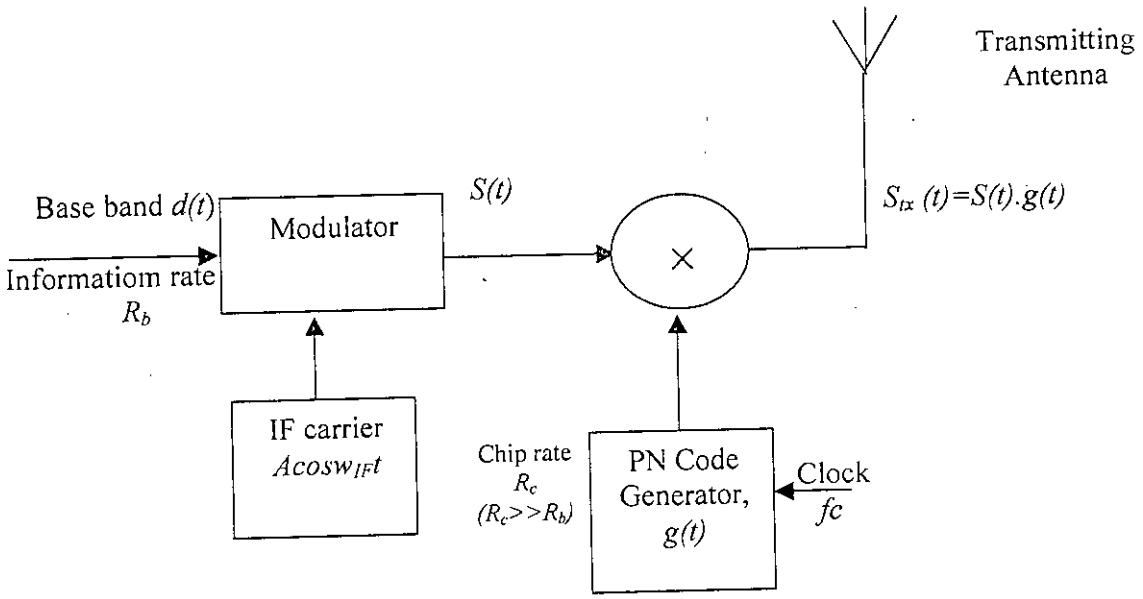

Fig 5.1(a) Direct Sequence Spread Spectrum Block Diagram (Transmitter)

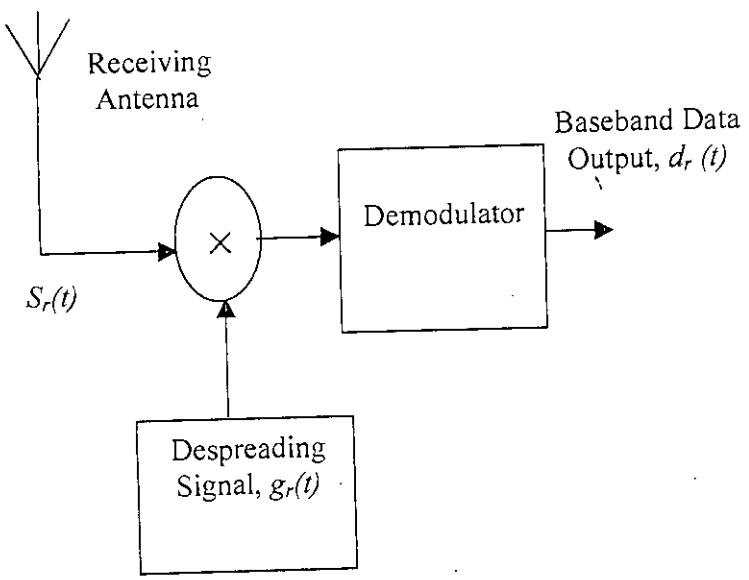

Fig 5.1 (b) Direct Sequence Spread Spectrum Block Diagram (Receiver)

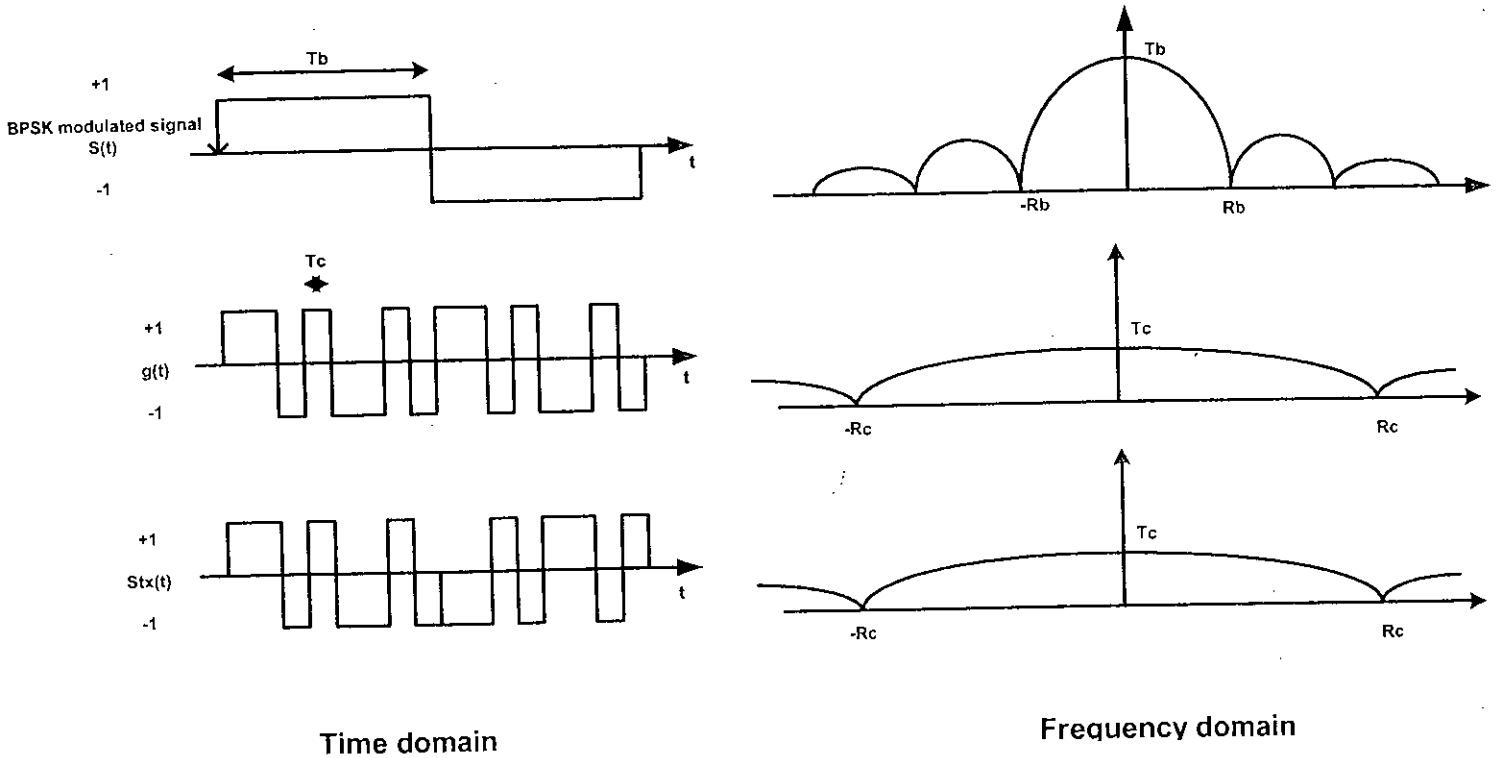

Fig. 5.2 Spread spectrum modulation in time domain and frequency domain

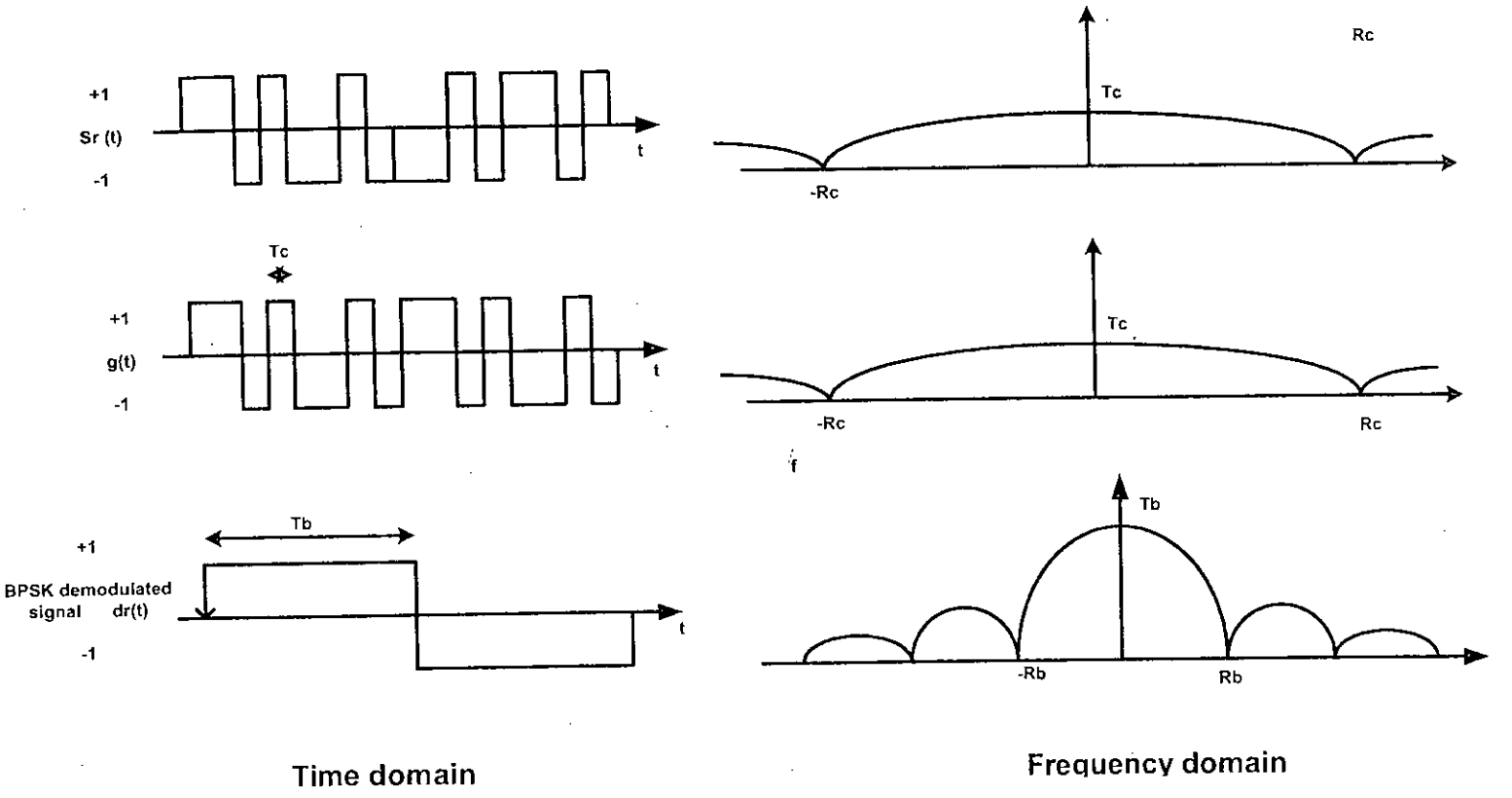

Fig. 5.3 Spread spectrum demodulation in time domain and frequency domain

Fig. 5.2 gives an example of this modulation in time domain as well as frequency domain. The effect of multiplication of BPSK modulated signal with PN sequence $g(t)$ is to spread the bandwidth R_b of $S(t)$ to a bandwidth of R_c. The spread spectrum signal can not be detected by a conventional narrow band receiver.

In the receiver, the received signal $S_r(t)$ is multiplied with the PN signal $g_r(t)$. If $g_r(t) = g(t)$ and synchronized to the PN sequence in the received data, than the recovered binary data is produced on $d_r(t)$. The spread spectrum demodulation is shown in Figure 5.3 in time domain as well as frequency domain. The effect of multiplication of the spread spectrum signal $Sr(t)$ with the PN sequence $g(t)$ used in the transmitter is to despread the bandwidth of $Sr(t)$ to R_b. If $g_r(t) \neq g(t)$, then there is no dispreading action. The signal $d_r(t)$ is spread spectrum, thus, a receiver not knowing the PN sequence of transmitter can not reproduce the transmitted data.

5.2.2 Frequency Hopped Spread Spectrum

In frequency hopping spread spectrum, the chips, that compose the code sequence assigned to a given user, are modulated in frequency. Each of the N chips corresponds to a sinusoidal waveform whose frequency is chosen pseudo-randomly from a given set of frequencies. In addition to the appropriate codewords choices, the frequency hopping model may be reduce the multi access interferences created by the users messages. Frequency hopping model is considered as slow when several data bits are transmitted at the same frequency. In opposite, frequency hopping model is considered as fast when the chips, in one bit, are transmitted at different frequencies. Fig. 5.4 shows how slow frequency hopping CDMA operate.

5.3 Spread Spectrum as a Multiple Access Techniques

There are a number of spread spectrum techniques, depending on the domain in which the signal space is shared among the remote users:

- FDMA – frequency division multiple access
- CDMA - code division multiple access
- TDMA - time division multiple access

- SDMA - space division multiple access
- PDMA - polarization division multiple access

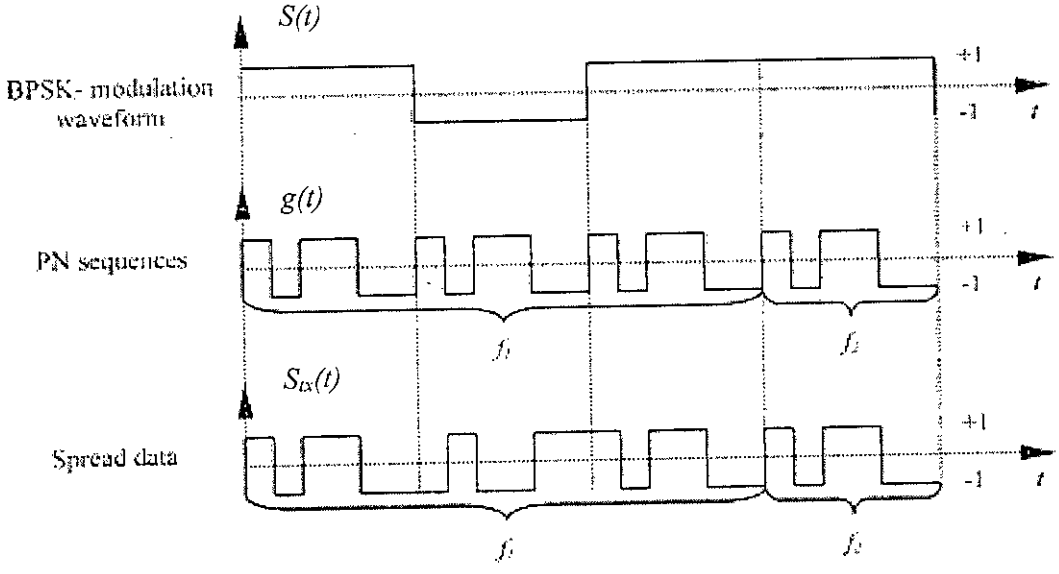

Fig. 5.4 Frequency hopped spread spectrum

In FDMA each user gets allocated a frequency channel for its sole use, in TDMA it is a time slot in time frame. In CDMA all users transmit in the same frequency band for all time, but they are separated by the codes allocated to them. The last two multiple access techniques are never used on their own, but combination with the first three to enhance the system capacity.

The advantage of CDMA for personal communication services is its ability to accommodate many users on the same frequency at the same time. As we mentioned earlier, a specific code is assigned to each user and only that code can demodulate the transmitted signal. Multiple accesses in CDMA can be two ways:

- Orthogonal Multiple Access
- Non-orthogonal Multiple Access or Asynchronous CDMA

5.3.1 Orthogonal Multiple Access

Orthogonal multiple access is used in synchronous CDMA in which each user is assigned one or many orthogonal waveform derived from an orthogonal code. Since

the waveforms are orthogonal, users with different codes do not interfere with each other.

***Orthogonal Codes*:**

Walsh set is one of the most important set of orthogonal code. Walsh functions are generated using an iterative process of constructing a Hadamard matrix starting with $H_1 = [0]$. The Hadamard matrix is built by:

$$H_{2n} = \begin{pmatrix} H_n & H_n \\ H_n & \overline{H_n} \end{pmatrix}$$

Walsh-Hadamard codes of length 2 and 4 are given below.

$$H_2 = \begin{pmatrix} 0 & 0 \\ 0 & 1 \end{pmatrix}$$

$$H_4 = \begin{pmatrix} 0 & 0 & 0 & 0 \\ 0 & 1 & 0 & 1 \\ 0 & 0 & 1 & 1 \\ 0 & 1 & 1 & 0 \end{pmatrix}$$

From the corresponding matrix, the Walsh-Hadamard codewords are given by the rows. Polar form can be achieved from the binary data of Walsh-Hadamard codewords mapping 0's to 1's and 1's to -1.

Walsh-Hadamard codes are orthogonal codes with different spreading factors. This property becomes useful when we want signals with different spreading factors to share the same frequency channel. However, the auto-correlation cahracteristics of Walsh-Hadamard codewords is not good one because it can have more than one peak. Thus, it is not possible for the receiver to detect the beginning of the codeword without an external synchronization scheme. Power spectral density of Walsh-Hadamard codes is concentrated in a small number of discrete frequencies and cross-correlation can also be non zero for a number of time shifts. Thus, Walsh-Hadamard codes do not have the best spreading behavior and un-synchronized users can interfere with each other. This is why Walsh-Hadamard codes can not be used in asynchronous CDMA.

5.3.2 Non-Orthogonal Multiple Access

Non-orthogonal multiple access is used in asynchronous CDMA. The code sequences which have good spreading behavior, balance property, higher number of independent sequence, autocorrelation and cross-correlation property is used for asynchronous CDMA. PN sequences are used to spread the spectrum. Gold sequences and m-sequences are in the family of PN sequence but *Gold* sequences is in particular popular for non-orthogonal CDMA

***m-Sequence*:**

Maximal length shift resister sequences are still of importance in digital communications and in spread spectrum and ranging systems. The widely used hardware implementation of a PN sequence generator and corresponding correlator and matched data filter register has been shown in Figure 5.5. The generator contains type D flip flops and is connected so that each data input except D_0 is the Q output of the preceding flip flop. Not all Q flip flop outputs need be connected to the parity generator (indicated by the dashed lines). The number of flip flops n and the selection of which flip flop outputs are connected to the parity generator determine the length and the characteristics of the generated PN sequence.

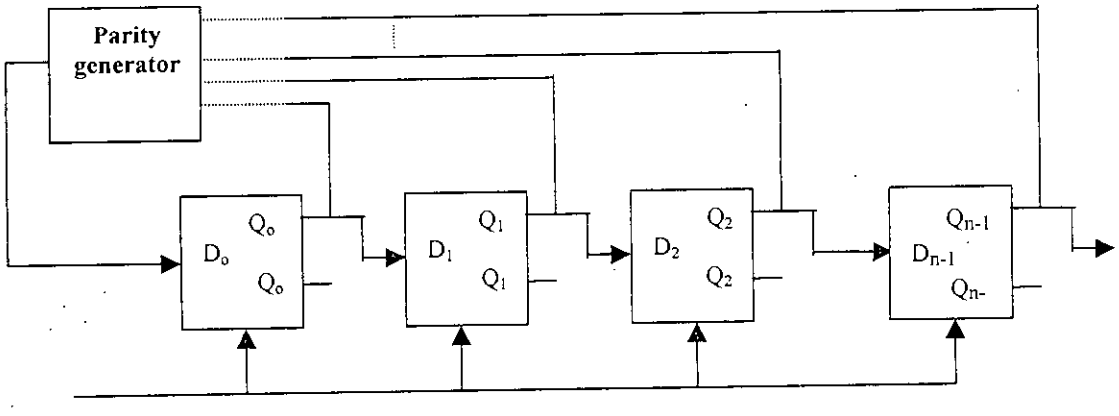

Fig. 5.5 Hardware of a pseudo-noise (PN) generator

The parity generator provides an output logic 0, when an even number of inputs are at logic 0 and generates logic 1 output when an odd number of inputs are at logic 1 state.

Properties of m-sequences:

(1) Balance property

In each period of the sequence, the number of binary ones differs from the number of binary zeros by one digit. In m- sequence number of ones is 2^{n-1} and number of zeros is 2^{n-1}-1 where n is number of flip-flops. For example, 1110010 is a 7 chip m-sequence in which number of ones is 4 and number of zeros is 3.

$$\sum g(t) = \sum 1+1+1-1-1+1-1 = 1$$

when modulating a carrier with a m-sequence, one-zero balance (DC component) can limit the degree of carrier suppression obtainable, because carrier suppression is dependent on the symmetry of the modulating signal.

(2) Sequence length

For maximal length linear codes, it is always possible to find a set of connections from flip-flop outputs to the parity generator that will yield a maximal length sequence of

$$L_m = 2^{n_f} - 1 \qquad (5.2)$$

where n_f is the number of flip-flops. A specific connection diagram of flip flop outputs to the parity generator input illustrated in Table 5.1. The resultant maximal-length PN sequence L_m is between 7 & 32767 bits.

(3) Independent sequence

One possible logic design connection is illustrated in Table5.1. There are many possible connections the parity generator, which has small correlation with one another. The upper bound S of the number of independent sequence is given by

$$S \le \frac{L_m - 1}{n_f} \qquad (5.3)$$

Table 5.1 Numerical values are illustrated in Table

Number of stages n_f	Sequence Length $L_m = 2^{n_f} - 1$	S=Number of m- sequences	D_o for $L_m = 2^{n_f} - 1$ In fig. 5.5
3	7	2	$Q_1 \otimes Q_2$
4	15	2	$Q_2 \otimes Q_3$
5	31	6	$Q_2 \otimes Q_4$
6	63	6	$Q_4 \otimes Q_5$
7	127	18	$Q_5 \otimes Q_6$
8	255	16	$Q_1 \otimes Q_2 \otimes Q_3 \otimes Q_7$
9	511	48	$Q_4 \otimes Q_8$
10	1023	60	$Q_6 \otimes Q_9$
11	2047	176	$Q_8 \otimes Q_{10}$
12	4095	144	$Q_1 \otimes Q_9 \otimes Q_{10} \otimes Q_{11}$
13	8191	630	$Q_0 \otimes Q_{10} \otimes Q_{11} \otimes Q_{12}$
14	16383	756	$Q_1 \otimes Q_{11} \otimes Q_{12} \otimes Q_{13}$
15	32767	1800	$Q_{13} \otimes Q_{14}$

(4) Autocorrelation property

The m-sequences have an interesting cyclic or periodic autocorrelation property. The origin of the name pseudo noise is that it has an autocorrelation function very similar to that of white noise signal. The auto correlation function of m-sequence is – 1 for all values of chip phase shift τ, except for the [-1, +1] chip phase shift area, in which correlation varies linearly from the -1 value to $L_m = 2^{n_f} - 1$(the sequence length). Replacing each 0 by –1and each 1 by +1, then the periodic correlation function is given by

$$R(\tau) = \begin{cases} 2^{n_f} - 1, \tau = 0 \\ -1, \tau \neq 0 \end{cases} \tag{5.4}$$

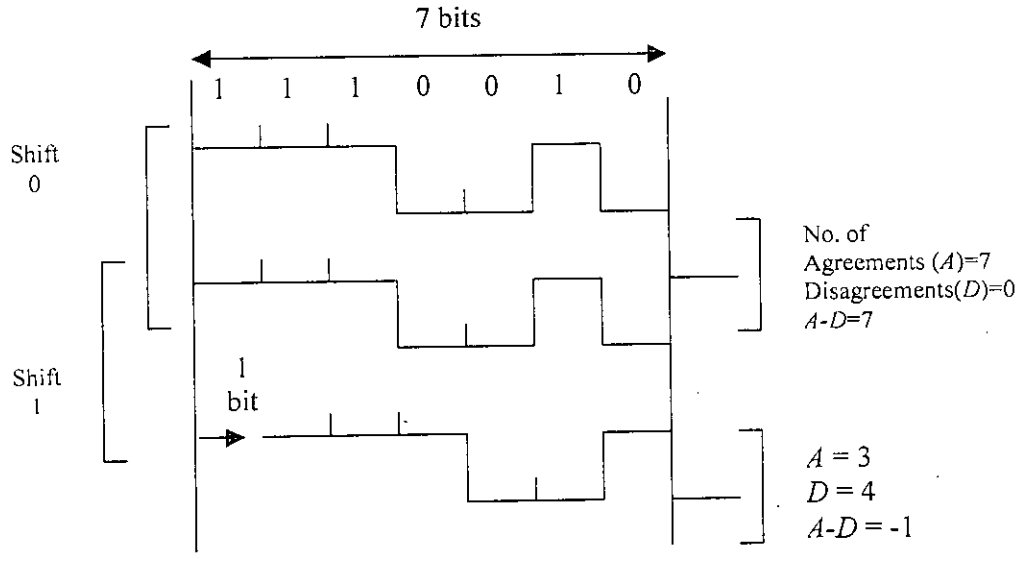

Fig. 5.6 Auto correlation of 7 chip m-sequence with shift 1

Table5.2 Reference Sequence: 1110010

Shift	Sequence	Agreements(A)	Disagreements(D)	A-D
0	1110010	7	0	7
1	0111001	3	4	-1
2	1011100	3	4	-1
3	0101110	3	4	-1
4	0010111	3	4	-1
5	1001011	3	4	-1
6	1100101	3	4	-1

For an $n_f = 3$ stage shift register generator, generating a 7 bit maximal length pseudorandom code, with a chip rate of 10 Mc/s and a 7 bit reference sequence 1110010.

Time domain agreements (A) and disagreements (D) for shift $\tau = 0$ and $\tau = 1$ is given in Fig. 5.6 which shows $A = 7$ and $D = 0$ for $\tau = 0$ but $A = 3$ and $D = 4$ for $\tau = 1$. The table of the number of agreements (A) and disagreements (D) by lining up the

shifted autocorrelation code sequence in one bit increments is given in table 5.2. Auto-correlation function is shown in Fig. 5.7.

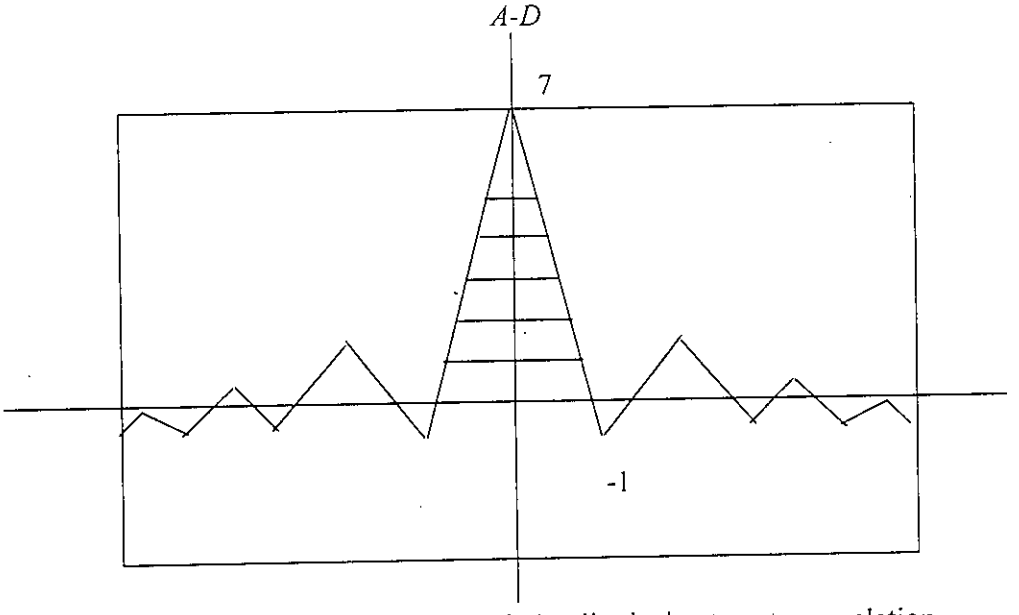

Fig. 5.7 A peak amplitude due to auto-correlation

(5) Cross-correlation property

Cross-correlation is the measure of between two different codes. This property is very important for asynchronous CDMA because multiple access interference (MAI) depends on this property. Unfortunately, cross-correlation is not so well behaved as auto correlation. The cross correlation between two different m-sequences: 1110010 and 1001110 is shown in Figure 5.8. When large numbers of transmitters, using different codes, are to share a common frequency band, the code sequence must be carefully chosen to avoid interference among users.

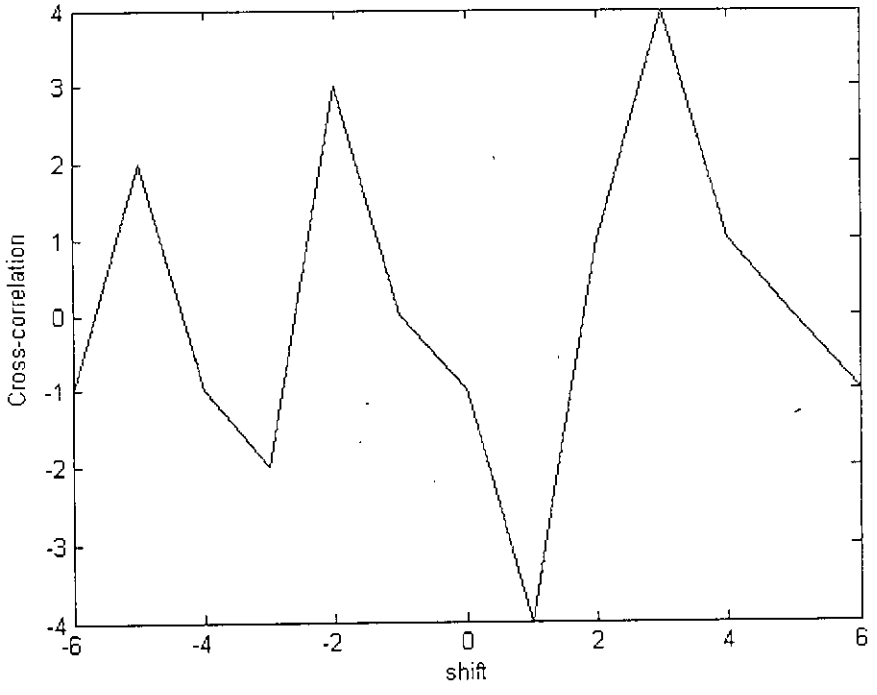

Fig. 5.8 The cross correlation between two different m-sequences of 1110010 and 100110.

Gold sequence:

Gold-sequences are more suitable than *m*-sequence for multiple user CDMA systems. They offer a large number of sequences sets with good cross-correlation properties between the single sequences. Gold sequences have only three cross-correlation peaks, which tend to get less important as the length of the code increases. They also have a single auto-correlation peak at zero, just like ordinary PN sequences.

The gold sequences are generated by modulo-2 addition of two m-sequences of same length clocked by the same chip-clock (Figure 5.9). Since both m-sequences have equal length L_m and use the same clock, the created the gold sequence is of length L_m and use the same clock. If n_f is the number of stages in each m-sequence generator then the length of generated Gold sequence

$$L_m = 2^{n_f} - 1 \tag{5.5}$$

It can be shown that for any shift in the initial conditions between the two m-sequences a new gold sequence is generated. Thus a gold sequence generator combining two different m sequences can create a number of different $L_m = 2^{n/} - 1$ Gold sequences. But all of them have no good cross-correlation property. The m-sequences pair which gives only three cross-correlation peaks is used to generate Gold sequence.

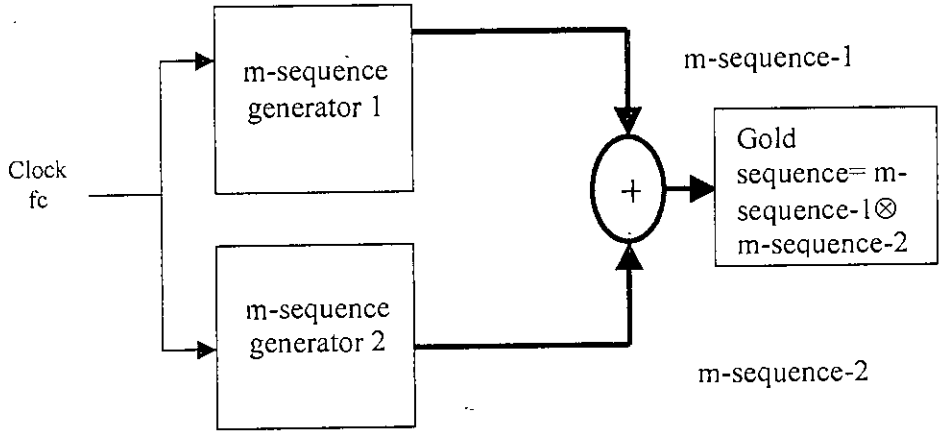

Fig. 5.9 Block diagram of Gold sequence Generator

5.4 Optical CDMA

We have seen very rapid development of the Internet and the information superhighway, all over the world. The growth rate in the bandwidth demand is at a speed faster than Moore's law, which is used to describe the improvement rate of Silicon integrated circuits. In order to meet these needs, Optical communication is an attractive solution. Most optical research work is focused on the use of wavelength division multiplexing (WDM), optical time division multiplexing (OTDM) or a hybrid approach to achieve tera bit per second channel capacity. Recently, there has been a lot of interest in applying the concepts of CDMA to optical fiber communication systems that can further enhance the functionality of optical networks [41], [43].

The aim of Optical Code Division Multiple Access is to take benefit of radio frequency communications CDMA techniques to share the huge optical bandwidth. Specific constraints associate to the optical communication systems have to be taken into account while preserving the advantages brought by this technique, principally:

- improvement of multiplexing capacity
- more flexible bandwidth usage
- higher granularity and scalability within optical network
- improved crosstalk performance
- asynchronous access
- potential for improved system security
- Resource sharing
- Cost reduction of network installation.

OCDMA is the spread spectrum technique in optical domain that permits a large number of separate users to share the same extended transmission optical bandwidth but to be individually addressable through the allocation of specific address code signature sequence with good correlation properties [47]. In radio communication systems, bipolar sequences are used as codes to modulate data streams. These sequences are composed by [1, −1] chips and are strictly orthogonal in the synchronous case. However, this orthogonality may be degraded in asynchronous systems. In optical communications, bipolar sequences cannot be used to code data streams due to square law of optical detection. In optical CDMA, unipolar code sequence is used to encode the data streams.

The encoding can be performed either in the time domain (DS-OCDMA) or frequency domain (FH-OCDMA). In DS-OCDMA each data bit to be transmitted is defined by a code composed of sequence of pulses. The individual pulses comprising the coded bit are commonly referred to as chips. The encoded bits are then broadcast onto the network but are only received by the simple match filtering within the receiver. By contrast, in FH-OCDMA, the carrier frequency of the chip is changed

according to a well defined code sequence that can once again be suitably identified by an appropriate receiver.

There are two categories in Optical CDMA, the first one use coherent detection (heterodyne detection), and the second one use non-coherent detection (direct detection). In the coherent detection orthogonal codes can be used. But it is important to note that it is difficult, in optical communication, to preserve the signal phase during the transmission through the optical channel. Even if some experimental set-ups exist using coherent Optical CDMA, these systems are complex and expensive to be implemented since they need a special set up to manage the phase dispersions of the transmitted CDMA signal. The non-coherent CDMA present a more attractive solution even if strict orthogonal sequence cannot be used. Direct detection is normally used in asynchronous CDMA applications, in which PN sequences (Gold sequence) is used to encode the data streams.

5.5 System Description of the Research Work

In the present research work, asynchronous SIK modulation-demodulation technique is considered for optical fiber CDMA network. The schematic block diagram of an optical CDMA transmitter, transmission line and SIK switched correlator receiver [34] is shown in Fig. 5.10(a), Fig. 5.10(b) and Fig. 5.10(c), respectively.

In the transmitter, a user's data is modulated either by a unipolar signature sequence or by its complement, depending on whether it is a '1' or '0', respectively then a laser is intensity modulated by the encoded data signal. The optical signals of K users is coupled using *K:1* coupler and transmitted through a transmission line with M sections and *(M-1)* in-line optical amplifiers.

In the receiver, a bipolar reference sequence is correlated directly with the channel unipolar signature sequence in order to recover the original data. This unipolar-bipolar correlation can be implemented optically by separating the bipolar reference sequence into two complementary unipolar reference sequences which provide

unipolar switching functions to despread the optical channel signal [34]. The despreaded optical signal is subtracted in a balanced *pin* diode receiver and then integrated over a data bit period prior to zero threshold detection.

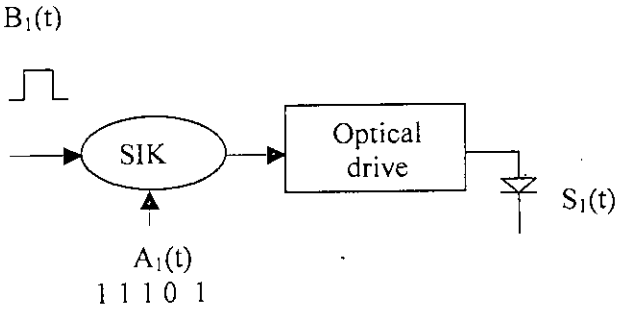

(a)

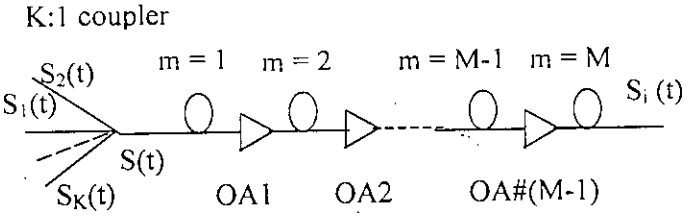

(b)

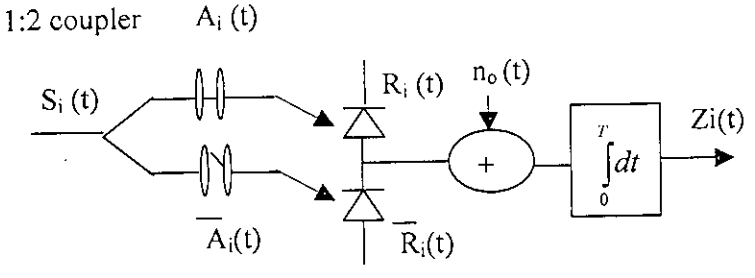

(c)

Fig. 5.10 Schematic block diagram of an optical CDMA transmitter (a), transmission line (b) and receiver with sequence inversion keyed (SIK) optical correlator (c), OA: optical amplifier.

5.6 System Analysis of the Work

5.6.1 Transmitted Signal

In the transmitter, a user's data is modulated either by a unipolar signature sequence or by its complement, depending on whether it is a '1' or '0', respectively. The SIK signal is driven by a suitable optical light source such as a light emitting diode (LED) or Laser diode. The LED or Laser diode output is transmitted through the fiber thus, the total input light signal in optical fiber of the transmission line is given by

$$S(t) = \sum_{k=1}^{K} \sqrt{2P_T}\, B_k(t-\tau_k) \circ A_k(t-\tau_k) \exp[i\omega_0 (t-\tau_k)] \tag{5.6}$$

where for k-th user $2P_T$ is the peak incident chip optical power at the transmitter, $B_k(t)$ and $A_k(t)$ are binary data and signature sequences, respectively, τ_k is the relative time delay, K is the total number of simultaneous users and 'o' is the operator that denotes sequence inversion keying (SIK) modulation such that either the sequence $A_k(t)$ or its complement $\bar{A}_k(t)$ is transmitted for a '1' or '0' data bit, respectively and ω_0 is the light frequency. $B_k(t)$ is a sequence of unit amplitude unipolar rectangular pulses of duration T and $A_k(t)$ is a periodic sequence of N unit amplitude unipolar rectangular pulses of duration T_c such that $T = NT_c$. The average power of the transmitted signal $S(t)$ can be written as

$$P_{avg} = \frac{1}{T} \int_0^T \sum_{k=1}^{K} \left| \sqrt{2P_T}\, B_k(t-\tau_k) \circ A_k(t-\tau_k) \exp[i\omega_0 (t-\tau_k)] \right|^2 dt \tag{5.7}$$

It is assumed that the signature sequence is balanced and P_{avg} can be found as

$$P_{avg} = KP_T \tag{5.8}$$

Thus, transmitted power per channel is P_T. Fourier transform of the total input signal, $S(t)$, shows that number of frequency components in $S(t)$ is infinity. Thus, $S(t)$ can be written as

$$S(t) = \sum_{k=1}^{K} \sqrt{2P_T}\, B_k(t-\tau_k) \circ A_k(t-\tau_k) \exp[i\omega_0(t-\tau_k)]$$

$$= \sqrt{2P_T} \exp[i\omega_0 t] \sum_{j=-\infty}^{\infty} c_j \exp[i(j\omega_d t)] \tag{5.9}$$

where c_j are the coefficients Fourier transform, ω_d is frequency difference in radians with $\omega_d = 2\pi / T_p$. Hence, $T_p \to \infty$. From (5.9), *S(t)* can be written as

$$S(t) = \sqrt{2P_T}\, c_0 \exp[i\omega_0 t] + \sqrt{2P_T} \sum_{\substack{j=1 \\ F\to\infty}}^{F} c_j \exp[i\omega_j t]$$

$$= \sqrt{2P_T}\,|c_0| \exp[i\omega_0(t-\tau_0)] + \sqrt{2P_T} \sum_{\substack{j=1 \\ F\to\infty}}^{F} |c_j| \exp[i\omega_j(t-\tau_j)]$$

$$= \sqrt{P_0} \exp[i\omega_0(t-\tau_0)] + \sqrt{P_j} \sum_{\substack{j=1 \\ F\to\infty}}^{F} \exp[i\omega_j(t-\tau_j)]$$

$$= \sum_{\substack{j=0 \\ F\to\infty}}^{F} E_j(t) \tag{5.10}$$

where $E_j(t)$, P_j and τ_j are the electric field, power and time delay of frequency ω_j, respectively. It should be noted that $|c_0|^2 = K/4$ if the signature sequence is balanced, thus,

$$P_0 = KP_T / 2 \tag{5.11}$$

and

$$\sum_{\substack{j=1 \\ F\to\infty}}^{F} P_j = KP_T / 2 \tag{5.12}$$

$P_0 + \sum_{\substack{j=1 \\ F\to\infty}}^{F} P_j = KP_T$ is the total transmitted light power through the fiber.

5.6.2 Generation of FWM

It is seen that multi-wavelength signal is generated after modulation, thus, FWM occur while the signal propagates through the fiber [51]. According to (4.10), the FWM electric field, $E_F(t)$, generated at the receiver due to FWM is given by

$$E_F(t) = k_f \sum_{\substack{p,q,r=0 \\ p=q\neq r \\ p\neq q\neq r \\ F\to\infty}}^{F} E_p(t)E_q(t)E_r^*(t)\exp(-\frac{\alpha L}{2})\exp[\sum_{m=1}^{M} i\beta_F^{(m)}L]\sum_{m=1}^{M}\exp[i\sum_{j=1}^{m-1}\Delta\beta_F^{(j)}L]$$

$$\frac{1-\exp[(-\alpha+i\Delta\beta_F^{(m)})L]}{\alpha-i\Delta\beta_F^{(m)}} \qquad (5.13)$$

where $k_f = \frac{i(2\pi)}{n\lambda}D\chi$, D is the degeneracy factor, χ is the third order nonlinear susceptibility, n is the refractive index, λ is the wavelength, L is the length of each span so that $ML = L_t$ is the total fiber length, α is the fiber attenuation coefficient, M is the number of fiber span and

$$\Delta\beta_F^{(m)} = \beta_p^{(m)} + \beta_q^{(m)} - \beta_r^{(m)} - \beta_F^{(m)} \qquad (5.14)$$

where $\beta_p^{(m)}$, $\beta_q^{(m)}$, $\beta_r^{(m)}$ and $\beta_F^{(m)}$ are the propagation constant of electric fields $E_p(t)$, $E_q(t)$ $E_r(t)$ and $E_F(t)$ at span m.

5.6.3 Mean Value and Variance of Output Signal for Transmission System with Dispersion Shifted Fiber

The power depletion due to FWM can be neglected, thus, the signal at the switched correlator receiver of each users, $S_i(t)$, can be written as

$$S_i(t) = S(t)\exp(-\frac{\alpha L}{2}) + E_F(t) \tag{5.15}$$

The optical power is equally divided in 1:2 star coupler of the switched correlator receiver, so the electric fields, $R_i(t)$ and $\bar{R}_i(t)$ received by the *pin* diodes of i-th user with $\tau_i = 0$, can be written as follow

$$R_i(t) = \frac{1}{\sqrt{2}} S_i(t)\, A_i(t) \tag{5.16}$$

$$\bar{R}_i(t) = \frac{1}{\sqrt{2}} S_i(t)\, \bar{A}_i(t) \tag{5.17}$$

The output of the correlator, $Z_i(t)$, matched to the i-th user is given by

$$Z_i(t) = R\int_0^T \{|R_i(t)|^2 - |\bar{R}_i(t)|^2\}dt + \int_0^T n_0(t)dt \tag{5.18}$$

where R is the responsibility of each photodiode and $n_o(t)$ is the total channel noise. It should be noted that $E_F(t)^2$ is negligible as compared to others since $E_F(t)^2 \ll E_F(t)$, thus, from (5.6), (5.15), (5.16), (5.17) and (5.18), $Z_i(t)$ can be written as

$$Z_i(t) = \frac{R}{2}\int_0^T \{\sum_{k=1}^{K} (\sqrt{2P_T})^2 B_k{}^2(t-\tau_k) \circ A_k{}^2(t-\tau_k)\exp(-\alpha L)$$

$$+2\sum_{k=1}^{K}\sqrt{2P_T}B_k(t-\tau_k)\circ A_k(t-\tau_k)\exp(-\alpha L/2)\,|\,E_F(t)\,|\}$$

$$.[A_i(t)-\bar{A}i(t)]dt+\int_0^T n_O(t)dt \qquad (5.19)$$

It should be mentioned here that $B_k^2(t-\tau_k)=B_k(t-\tau_k)$ and $A_k^2(t-\tau_k)=A_k(t-\tau_k)$ since binary data and chip sequences are '1' or '0', thus, $Z_i(t)$ can be rewritten as

$$Z_i(t)=\frac{R}{2}\int_0^T\{\sum_{k=1}^{K}2P_T B_k(t-\tau_k)\circ A_k(t-\tau_k)\exp(-\alpha L)$$

$$+2\sum_{k=1}^{K}\sqrt{2P_T}B_k(t-\tau_k)\circ A_k(t-\tau_k)\exp(-\alpha L/2)\,|\,E_F(t)\,|\}$$

$$.[A_i(t)-\bar{A}i(t)]dt+\int_0^T n_O(t)dt \qquad (5.20)$$

Equation (5.20) can be written as

$$Z_i(t)=Z_{is}(t)+Z_{iF}(t)+\int_0^T n_O(t)dt \qquad (5.21)$$

with

$$Z_{is}(t)=R\int_0^T\sum_{k=1}^{K}P_T B_k(t-\tau_k)\circ A_k(t-\tau_k)\exp(-\alpha L)\ \{A_i(t)-\bar{A}i(t)\}dt \qquad (5.22)$$

and

$$Z_{iF}(t)=R\int_0^T\sum_{k=1}^{K}\sqrt{2P_T}B_k(t-\tau_k)\circ A_k(t-\tau_k)\exp(-\alpha L/2)\,|\,E_F(t)\,|\,\{A_i(t)-\bar{A}_i(t)\}dt \qquad (5.23)$$

If $a_k(.)$ and $b_k(.)$ are the bipolar form of $A_k(.)$ and $B_k(.)$ then $a_i(.) = A_i(.) - \bar{A}_i(.)$ and $B_k(.)oA_k(.)=\{1+b_k(.)a_k(.)\}/2$ then $Z_{is}(t)$ can be written as,

$$Z_{is}(t) = RP_R \int_0^T \sum_{k=1}^{K} \frac{1+b_k(t-\tau_k)a_k(t-\tau_k)}{2} a_i(t)dt$$

$$= \frac{RKP_R}{2} \int_0^T a_i(t)dt + \frac{RP_R}{2} \int_0^T \sum_{\substack{k=1 \\ k \neq i}}^{K} b_k(t-\tau_k)a_k(t-\tau_k)\, a_i(t)dt + \frac{RP_R}{2} \int_0^T b_i(t)dt \tag{5.24}$$

where received power

$$P_R=P_T \exp(-\alpha L) \tag{5.25}$$

The first term in (5.24) is the offset effect which is removed by using balanced signature sequence. The second and third term in (5.24) are the multiple access interference (MAI) and in phase autocorrelation peak, respectively. The mean of $Z_{is}(t)$ is given as [34]

$$U=RP_R/2 \tag{5.26}$$

The variance of interference due to MAI, is given by [34]

$$\sigma^2_{MAI} = U^2 \frac{2(K-1)}{3N} \tag{5.27}$$

The variance of interference due to FWM, σ^2_{FWM}, can be obtained from $Z_{iF}(t)$ taking the variance of $Z_{iF}(t)/T$. Thus, σ^2_{FWM} can be written as

$$\sigma^2_{FWM} = 2R^2 P_T \exp(-\alpha L)|E_F(t)|^2$$
$$\cdot \mathrm{var}[\frac{1}{T}\int_0^T \sum_{k=1}^{K} B_k(t-\tau_k) \circ A_k(t-\tau_k)\{A_i(t) - \bar{A}_i(t)\}dt] \quad (5.28)$$

Using bipolar form of $A_k(.)$, $B_k(.)$ and $\{A_i(.) - \bar{A}_i(.)\}$, it can be written that

$$\mathrm{var}[\frac{1}{T}\int_0^T \sum_{k=1}^{K} B_k(t-\tau_k) \circ A_k(t-\tau_k)\{A_i(t) - \bar{A}_i(t)\}dt]$$
$$= \mathrm{var}[\frac{1}{T}\int_0^T \sum_{k=1}^{K} \frac{1 + b_k(t-\tau_k)b_k(t-\tau_k)}{2} a_i(t)dt]$$
$$= \mathrm{var}[\frac{1}{2T}\int_0^T \sum_{k=1}^{K} a_i(t)dt] + \mathrm{var}[\frac{1}{2T}\int_0^T a_i(t)dt] + \mathrm{var}[\frac{1}{2T}\int_0^T \sum_{\substack{k=1 \\ k\neq i}}^{K} b_k(t-\tau_k)b_k(t-\tau_k)a_i(t)dt] \quad (5.29)$$

According to [34]

$$\mathrm{var}[\frac{1}{2T}\int_0^T \sum_{k=1}^{K} a_i(t)dt] = 0 \text{ and } \mathrm{var}[\frac{1}{2T}\int_0^T \sum_{\substack{k=1 \\ k\neq i}}^{K} b_k(t-\tau_k)b_k(t-\tau_k)a_i(t)dt] = \frac{1}{4}\cdot\frac{2(K-1)}{3N}$$

Thus, σ^2_{FWM} can be found as

$$\sigma^2_{FWM} = \frac{R^2 P_T (K-1)}{3N} \exp(-\alpha L)\left|E_F(t)\right|^2 \quad (5.30)$$

In (5.30), $|E_F(t)|^2$ is the power of FWM electric fields P_{FWM} and can be written as [53-54]

$$P_{FWM} = \frac{1024\pi^6}{n_o^4 \lambda^2 c^2}(D\chi)^2 \sum_{\substack{p,q,r=0 \\ p\neq q\neq r \\ p=q\neq r \\ F\to\infty}}^{F} \frac{|E_p|^2 |E_q|^2 |E_r^*|^2}{A_{eff}^2} \exp(-\alpha L)$$

$$\cdot \left| \sum_{m=1}^{M} \exp[i \sum_{j=1}^{m-1} \Delta\beta_F^{(m)} L] \frac{1-\exp[(-\alpha + \Delta i \beta_F^{(m)})L]}{\alpha - i\Delta\beta_F^{(m)}} \right|^2 \qquad (5.31)$$

where A_{eff} is the effective mode area of the fiber, c is the light velocity and

$$\Delta\beta_F{}^{(m)} = -\frac{\pi\lambda^4}{c^2}\frac{dD_c}{d\lambda}\left\{\left(f_p - f_o^{(m)}\right) + \left(f_q - f_o^{(m)}\right)\right\}\left(f_p - f_r\right)\left(f_q - f_r\right) \qquad (5.32)$$

where $f_o^{(m)}$ is zero-dispersion frequency of fiber in m-th section and D_c is the chromatic dispersion coefficient.

It should be mentioned that all the users are using source of same wavelength and wavelength differences among the multi-wavelengths is less. Thus, $\Delta\beta_F^{(m)} \ll \alpha$ for transmission system with DSF and $\left| \sum_{m=1}^{M} \exp[i \sum_{j=1}^{m-1} \Delta\beta_F^{(m)} L] \right|^2 \approx M^2$. Thus, P_{FWM} can be rewritten as

$$P_{FWM} = \frac{1024\pi^6}{n^4 \lambda^2 c^2}(D\chi)^2 \exp(-\alpha L) M^2 \frac{[1-\exp(-\alpha L)]^2}{\alpha^2 A_{eff}^2} \sum_{\substack{p,q,r=0 \\ p=q\neq r \\ p\neq q\neq r \\ F\to\infty}}^{F} P_p P_q P_r$$

$$= \frac{1024\pi^6}{n^4\lambda^2 c^2}\chi^2 \exp(-\alpha L) M^2 \frac{[1-\exp(-\alpha L)]^2}{\alpha^2 A_{eff}^2}$$

$$\{D_1^2 \sum_{\substack{p,q,r=0 \\ p\neq q\neq r \\ F\to\infty}}^{F} P_p P_q P_r + D_2^2 \sum_{\substack{p,q,r=0 \\ p=q\neq r \\ F\to\infty}}^{F} P_p P_q P_r\}$$

$$= \frac{1024\pi^6}{n^4\lambda^2 c^2}\chi^2 \exp(-\alpha L) M^2 \frac{[1-\exp(-\alpha L)]^2}{\alpha^2 A_{eff}^2}[D_1^2 X + D_2^2 Y] \tag{5.33}$$

where D_1=6 and D_2=3 are the degeneracy factor for non-degenerate and degenerate cases of FWM, respectively.

X can be written as follow,

$$\begin{aligned} X = {} & P_0P_1(P_2+P_3+P_4+P_5+....+P_{F'}) \\ & +P_0P_2(P_1+P_3+P_4+P_5+....+P_{F'}) \\ & +P_0P_3(P_1+P_2+P_4+P_5+....+P_{F'}) \\ & +..... \\ & +P_0P_{F'}(P_1+P_2+P_3+P_4+P_5+....) \end{aligned} \quad + \quad \begin{aligned} & +(P_2+P_3+P_4+P_5+....+P_{F'})P_1P_0 \\ & +(P_1+P_3+P_4+P_5+....+P_{F'})P_2P_0 \\ & +(P_1+P_2+P_4+P_5+....+P_{F'})P_3P_0 \\ & +..... \\ & +(P_1+P_2+P_3+P_4+P_5+....)P_{F'}P_0 \end{aligned} \tag{5.34}$$

A_1: P_0 in first position, others changing

A_2: P_0 in third position, others changing

It is obvious that $\sum_{\substack{j=1 \\ F\to\infty}}^{F} P_j - P_z \approx KP_T/2$ because P_z, the power of one frequency components, is very less compare to summation of others. It is seen that A_1 and A_2 are equal in equation (5.34) and can be written as follow

$$\begin{aligned} A_1 = A_2 = {} & P_0P_1KP_{T'}/2 \\ & +P_0P_2KP_{T'}/2 \\ & +P_0P_3KP_{T'}/2 \\ & +..... \\ & +P_0P_{F'}KP_{T'}/2 \end{aligned}$$

$$= P_0 K P_T / 2(P_1 + P_2 + P_3 + P_4 + P_5 + ... + P_F)$$
$$= P_0 K P_T / 2 \times K P_T / 2 = K^3 P_T^3 / 8 \quad (5.35)$$

Thus, X can be written as

$$X = K^3 P_T^3 / 4 \quad (5.36)$$

Further, Y can be written as

$$\begin{aligned} Y &= P_0 P_0 (P_1 + P_2 + P_3 + P_4 + P_5 + ... + P_F) \\ &\quad + P_1 P_1 (P_0 + P_2 + P_3 + P_4 + P_5 + ... + P_F) \\ &\quad + P_2 P_2 (P_0 + P_1 + P_3 + P_4 + P_5 + ... + P_F) \\ &\quad + ... \\ &\quad + P_F P_F (P_0 + P_2 + P_3 + P_4 + P_5 + ...) \\ &= P_0^2 K P_T / 2 + P_1^2 K P_T + P_2^2 K P_T + .. + P_F^2 K P_T \\ &= P_0^2 K P_T / 2 + K P_T (P_1^2 + P_2^2 + P_3^2 + .. + P_F^2) \end{aligned} \quad (5.37)$$

It is obvious that $\sum_{\substack{m=1 \\ F\to\infty}}^{F} P_m^2 \ll (\sum_{\substack{m=1 \\ F\to\infty}}^{F} P_m)^2$. Thus $(P_1^2 + P_2^2 + P_3^2 + .. + P_F^2) \ll P_0^2$

and from (5.37), Y can be written as

$$Y \approx K P_T / 8 \quad (5.38)$$

Using (5.36) and (5.38) in (5.33), P_{FWM} can be written as

$$P_{FWM} = \frac{128\pi^6}{n^4 \lambda^2 c^2} \chi^2 M^2 K^3 P_T^3 \exp(-\alpha L) \frac{[1 - \exp(-\alpha L)]^2}{\alpha^2 A_{eff}^2} (2D_1^2 + D_2^2)$$

$$= \frac{10368\pi^6}{n^4\lambda^2c^2}\chi^2M^2K^3P_T^3\exp(-\alpha L)\frac{[1-\exp(-\alpha L)]^2}{\alpha^2A_{eff}^2} \tag{5.39}$$

Finally, total variance of signal, σ^2, can be expressed as

$$\sigma^2 = \sigma_{MAI}^2 + \sigma_{FWM}^2 \tag{5.40}$$

and the variance of noise n_o *(t)* is given by [34]

$$N_0 = 2B(qRKP_R/2 + 2qI_{dk} + N_{th}) \tag{5.41}$$

where N_{th} is the receiver thermal noise, $B=\frac{1}{2T}$ is the data bandwidth, K is the number of simultaneous users, q is the electron charge and I_{dk} is the dark current. Receiver thermal noise N_{th} can be written as

$$N_{th} = 4kT_mBR_L \tag{5.42}$$

where k is the Boltzmann constant, T_m is the temperature and R_L is the load resistance.

5.6.4 Mean Value and Variance of Output Signal for Transmission System with Single Mode Dispersive Fiber

The optical pulses of the input signal, *S(t)*, undergoes dispersion due to fiber chromatic dispersion during propagation through the fiber [51]. According to [64], the output pulse corresponding to input pulse $s_{in}(t)$ with Fourier transform of $S_{in}(f)$ can be approximated as

$$s_{out}(t) = \frac{1}{T_c\sqrt{\pi|\gamma|}} e^{-j[(1/\gamma)(\frac{t}{Tc})^2-(\pi/4)\mathrm{sgn}\,\gamma]} S_{in}(\frac{-t}{\pi\gamma T_c^2}) \quad \text{for } \gamma(\pi B_c T_c)^2 \gg 1 \tag{5.43}$$

where T_c is duration of pulse, B_c is the band width of pulse and the chromatic dispersion index of the fiber

$$\gamma = \frac{\lambda^2}{\pi c} D_c R_c^{\,2} L_t \tag{5.44}$$

where R_c is the chip rate and L_t is the total fiber length. In case of rectangular pulse, $s_{out}(t)$ can be written as [64]

$$s_{out}(t) = \frac{1}{\sqrt{\pi|\gamma|}} e^{-j[(1/\gamma)(\frac{t}{Tc})^2-(\pi/4)\mathrm{sgn}\,\gamma]} \sin c(\frac{t}{\pi\gamma T_c}) \text{ for } .3 \le \gamma \le 1 \tag{5.45}$$

Again, neglecting power depletion due to FWM, the signal at the switched correlator receiver of each users, $S_i(t)$, can be written as

$$S_i(t) = \sum_{k=1}^{K}\sum_{j=0}^{N-1}\sqrt{2P_T}B_k(t-\tau_k)\circ A_k(t-\tau_k)s_{outk}(t-\tau_k^{/}-jT_c+T_c/2)\exp(\alpha L/2)+E_F(t) \tag{5.46}$$

where $\tau_k^{/}$ is the delay of k-th user first chip which is nearest to $t = 0$. $\tau_k^{/}$ can be found as

$\tau_k^{/}$ = remainder (τ_k / T_c).

From (5.6), (5.16), (5.17), (5.18) and (5.41), $Z_i(t)$ can be written as

$$Z_i(t)=\frac{R}{2}\int_0^T\{\sum_{k=1}^{K}\sum_{j=0}^{N-1}2P_T B_k\ (t-\tau_k)\circ A_k\ (t-\tau_k)s^2_{outk}(t-\tau_k^{/}-jT_C+T_C/2)\exp(-\alpha L)$$

$$+2\sum_{k=1}^{K}\sum_{j=0}^{N-1}\sqrt{2P_T}B_k(t-\tau_k)\circ A_k(t-\tau_k)s_{outk}(t-\tau_k^{/}-jT_C+T_C/2)$$

$$.\exp(-\alpha L/2)|E_F(t)|\}[A_i(t)-\bar{A}i(t)]dt+\int_0^T n_O(t)dt \qquad (5.47)$$

Equation (5.47) can be written as

$$Z_i(t)=Z_{is}(t)+Z_{iF}(t)+\int_0^T n_o(t)dt \qquad (5.48)$$

with

$$Z_{is}(t)=R\int_0^T\sum_{k=1}^{K}\sum_{j=0}^{N-1}P_T B_k\ (t-\tau_k)\circ A_k\ (t-\tau_k)$$

$$.s^2_{outk}(t-\tau_k^{/}-jT_C+T_C/2)\exp(-\alpha L)\{A_i(t)-\bar{A}i(t)\}dt \qquad (5.49)$$

and

$$Z_{iF}(t)=R\int_0^T\sum_{k=1}^{K}\sum_{j=0}^{N-1}\sqrt{2P_T}B_k(t-\tau_k)\circ A_k(t-\tau_k)s_{outk}(t-\tau_k^{/}-jT_C+T_C/2)$$

$$.\exp(-\alpha L/2)|E_{F}(t)|\{A_i(t)-\bar{A}_i(t)\}dt \qquad (5.50)$$

Again, using polar form $Z_{is}(t)$ can be written as

$$Z_{is}(t)=\frac{R}{2}\int_0^T\sum_{k=1}^{K}\sum_{j=0}^{N-1}P_T\exp(-\alpha L)s^2_{outk}(t-\tau_k-jT_C+T_C/2)a_i(t)dt$$

$$+\frac{R}{2}\int_0^T \sum_{\substack{k=1 \\ k\neq i}}^{K} \sum_{j=0}^{N-1} P_T \exp(-\alpha L) b_k(t-\tau_k) a_k(t-\tau_k) s_{outk}^2(t-\tau_k^{/} - jT_c + T_c/2) a_i(t) dt$$

$$+\frac{R}{2}\int_0^T \sum_{j=0}^{N-1} P_T \exp(-\alpha L) s_{outi}^2(t - jT_c - T_c/2) dt \qquad (5.51)$$

The mean of $Z_{is}(t)$, U, is given as

$$U = \frac{RP_T \exp(-\alpha L)}{2} \frac{1}{T} \int_0^T \sum_{j=0}^{N-1} s_{outi}^2(t - jT_c - T_c/2) dt$$

$$= \frac{RP_R}{2} \frac{1}{T} \int_0^T \sum_{j=0}^{N-1} s_{outi}^2(t - jT_c - T_c/2) dt \qquad (5.52)$$

The variance of multiple access interference (MAI), σ_{MAI}^2, can be found as

$$\sigma_{MAI}^2 = \frac{R^2 P_R^2}{4} \mathrm{var}\left[\frac{1}{T}\int_0^T \sum_{\substack{k=1 \\ k\neq i}}^{K} \sum_{j=0}^{N-1} b_k(t-\tau_k) a_k(t-\tau_k) s_{outk}^2(t-\tau_k^{/} - jT_c + T_c/2) a_i(t) dt\right] \qquad (5.53)$$

The variance of interference due to FWM, σ^2_{FWM}, can be obtained from $Z_{iF}(t)$ taking the variance of $Z_{iF}(t)/T$. Thus, σ_{FWM}^2 can be written as

$$\sigma_{FWM}^2 = 2R^2 P_T \exp(-\alpha L) \mid E_F(t) \mid^2$$

$$.\mathrm{var}\left[\frac{1}{T}\int_0^T \sum_{k=1}^{K} \sum_{j=0}^{N-1} B_k(t-\tau_k) \circ A_k(t-\tau_k) s_{outk}(t-\tau_k^{/} - jT_c + T_c/2) a_i(t) dt \right. \qquad (5.54)$$

In (5.54), $|E_F(t)|^2$ is the power of FWM electric fields P_{FWM} and can be found by (5.31) with

$$\Delta\beta^{(m)} = (f_p - f_r)\ (f_q - f_r)\frac{2\lambda^2\pi}{c}\left[D_C - [(f_p - f_r) + (f_q - f_r)]\frac{\lambda^2}{2c}\frac{dD_C}{d\lambda} \right] \tag{5.55}$$

Finally, total variance of signal, σ^2, can be expressed as

$$\sigma^2 = \sigma^2_{MAI} + \sigma^2_{FWM} \tag{5.56}$$

and the variance of noise $n_o\ (t)$ is given by (5.41).

5.6.5 Bit Error Rate Performance of the System

The signal to noise ratio at the correlator output can be obtained as

$$SNR = \frac{U^2}{\sigma^2 + No} \tag{5.57}$$

The BER performance for the OCDMA transmission system is then given by [34]

$$BER = (1/2)erfc\ (\frac{\sqrt{SNR}}{\sqrt{2}}) \tag{5.58}$$

Chapter 6

Results and Discussion

Following the analytical formulation presented in Sec. 5.6, the performances of the OCDMA transmission system are evaluated considering the effect of FWM. The data signal, $B_1(t)$ and transmitted signal, $S_1(t)$ of user-1 with 0.1 mW peak incident chip optical power are shown in Fig. 6.1. Fig. 6.2 represents the data signal and transmitted signal of user-2. Hence, 100 Mb/s data signal is modulated with 63 chips per bit Gold sequence and then light frequency is further modulated by modulated data signal. The figures show that chip sequences for data bit '1' and '0' are compliment. The total transmitted signal and corresponding power spectrum are presented in Fig. 6.3 and Fig. 6.4, respectively. According to analysis, the center frequency power of the total transmitted signal of two simultaneous users is half of the peak incident chip optical power. From Fig. 6.4, it is evident that the power of center frequency is half of peak incident chip optical power.

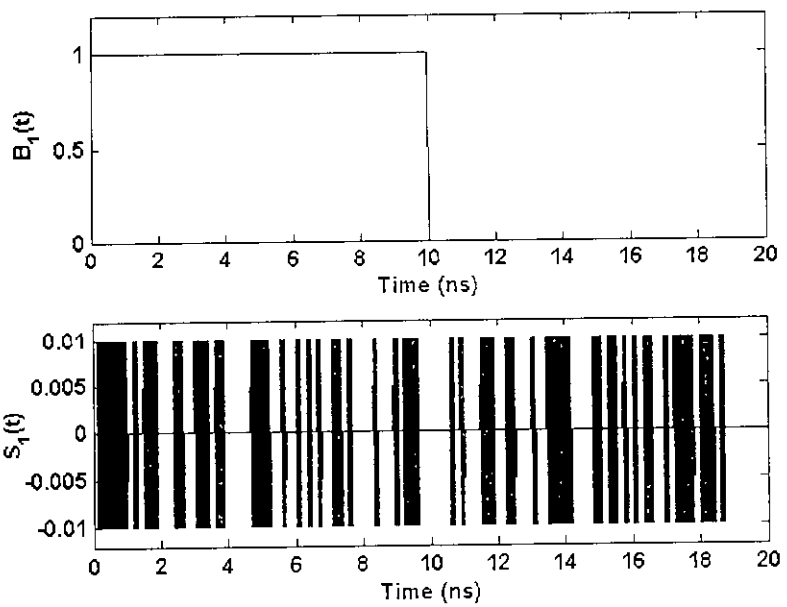

Fig. 6.1 Data signal, $B_1(t)$ and transmitted signal, $S_1(t)$ of user-1 at a bit rate of 100 Mb/s with 0.1 mW peak incident chip optical power and chips per bit, $N = 63$.

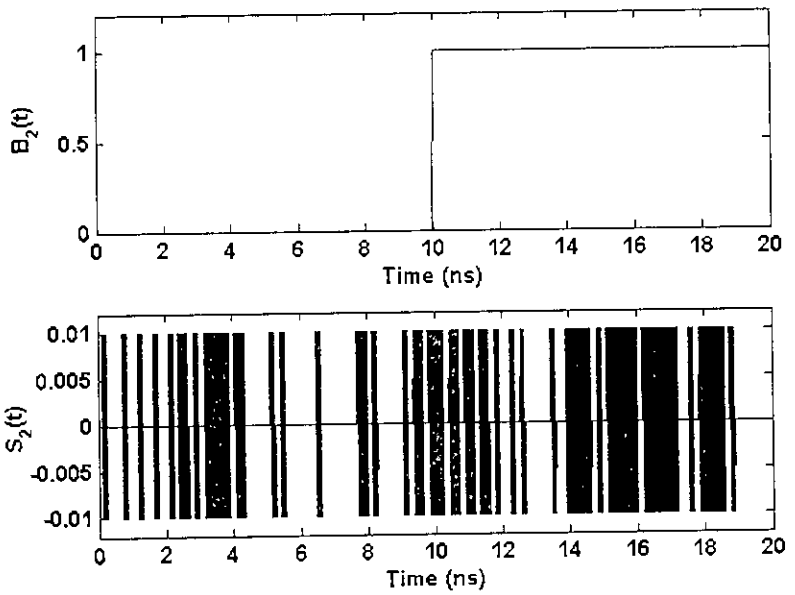

Fig. 6.2 Data signal, $B_2(t)$ and transmitted signal, $S_2(t)$ of user-2 at a bit rate of 100 Mb/s with 0.1 mW peak incident chip optical power and chips per bit, $N = 63$.

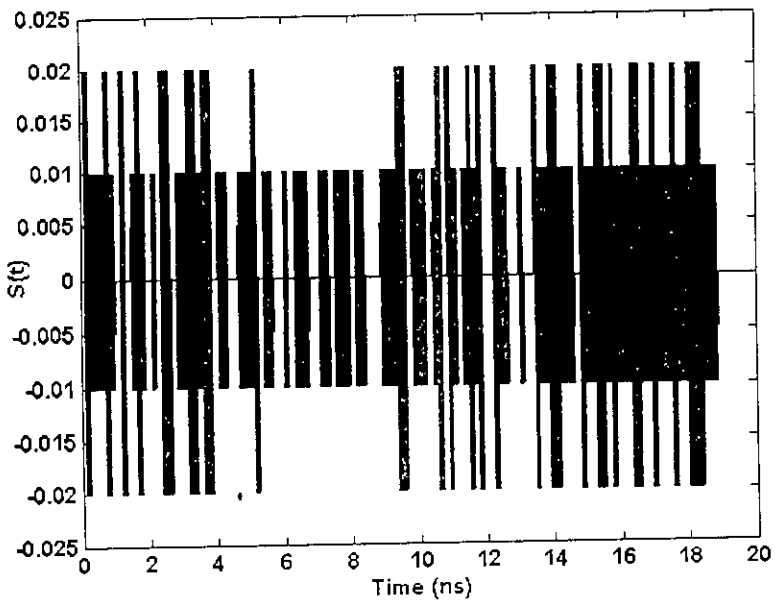

Fig. 6.3 Transmitted signal of 100 Mb/s DS-OCDMA systems. Number of simultaneous users, $K = 2$ with 0.1 mW peak incident chip optical power and chips per bit, $N = 63$.

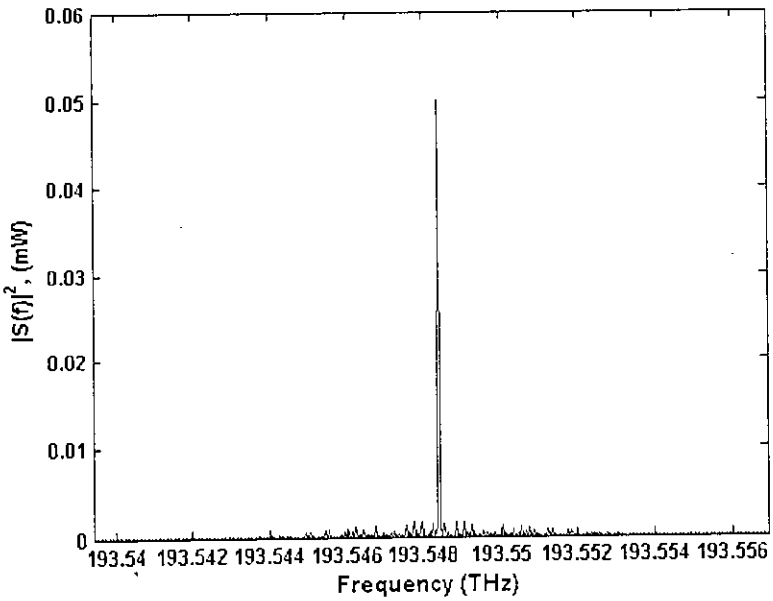

Fig. 6.4 Power spectrum of transmitted signal for 100 Mb/s DS-OCDMA systems. Number of simultaneous users, $K = 2$ with 0.1 mw peak incident chip optical power and chips per bit, $N = 63$.

To evaluate the BER performance of the system with DSF, FWM noise power is simulated from the power spectrum of the transmitted signal and MAI power is obtained by simulation from the output of the correlator. Further, the MAI power, FWM noise power and BER performance is evaluated using analytical expressions and compared with the simulation results. The typical system parameters assumed in computation are n_o=1.43, operating wavelength λ=1.55 mm, *Aeff*=50 μm2, $\chi = 4\times10^{-15}$ esu, α=0.21 dB/km, $dDc/d\lambda$ = 0.07 ps/km-nm^2, fiber span length L=100 km, R=0.85AW^{-1}, I_{dk}=10 nA, thermal current PSD N_{th}=1 pA^{2}Hz^{-1}, data rate $1/T$=100 Mbit/s. The total fiber length of the system is taken to be 1000 km comprising of 10 spans. The MAI power, FWM noise power and BER performance with respect to the number of simultaneous users for different values of transmitted power per user, using 63 chips per bit encoding, are shown in Fig. 6.5, Fig. 6.6 and Fig. 6.7, respectively. It is found that BER performance degrades with increasing number of

simultaneous users and transmitted power per user. The noise power (MAI and FWM) and BER performance with respect to number of users for different values of transmission distance with DSF, using 63 chips per bit encoding, are shown in Fig. 6.8 and Fig. 6.9, respectively. The plots show that FWM noise power and BER increase with increasing the transmission distance but MAI remains constant. The MAI power, FWM noise power and BER performance with respect to the number of users for different number of chips per bit, with -15 dBm transmitted power per user, are shown in Fig. 6.10, Fig. 6.11 and Fig. 6.12, respectively. It is found that BER is improved significantly as the number of chips per bit is increased from 31 to 127. From the Fig. 6.5 to Fig. 6.12, it is investigated that simulation and analytical results are similar in all cases. Thus, the analytical derived expressions can be used to evaluate the performances of OCDMA transmission systems with DSF.

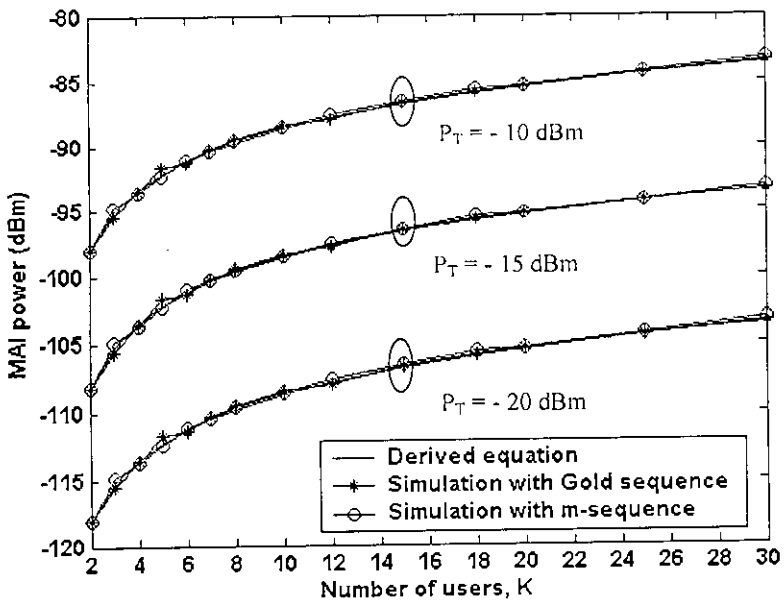

Fig. 6.5 MAI power versus number of simultaneous users for different values of transmitted power per user for a 100 Mb/s, 1000 km OCDMA system with DSF. Number of chips per bit, $N = 63$ in all cases.

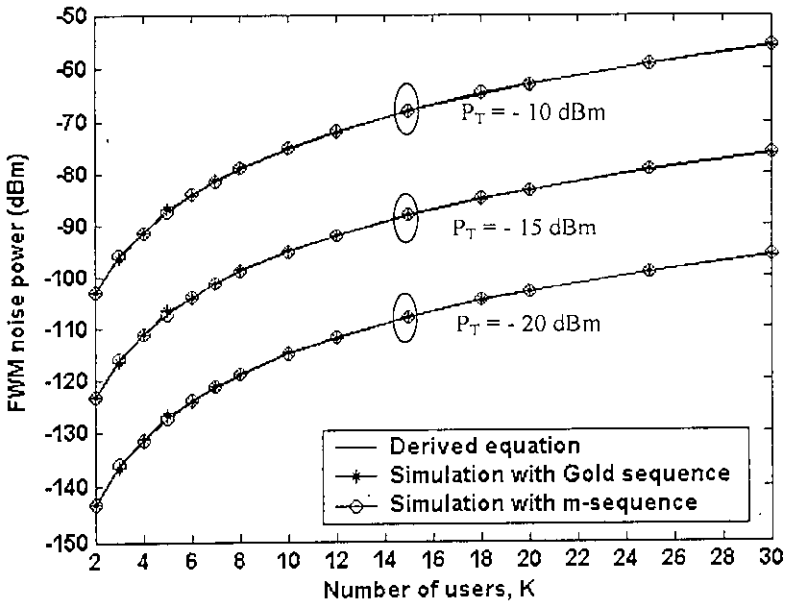

Fig. 6.6 FWM noise power versus number of simultaneous users for different values of transmitted power per user for a 100 Mb/s, 1000 km OCDMA system with DSF. Number of chips per bit, $N = 63$ in all cases.

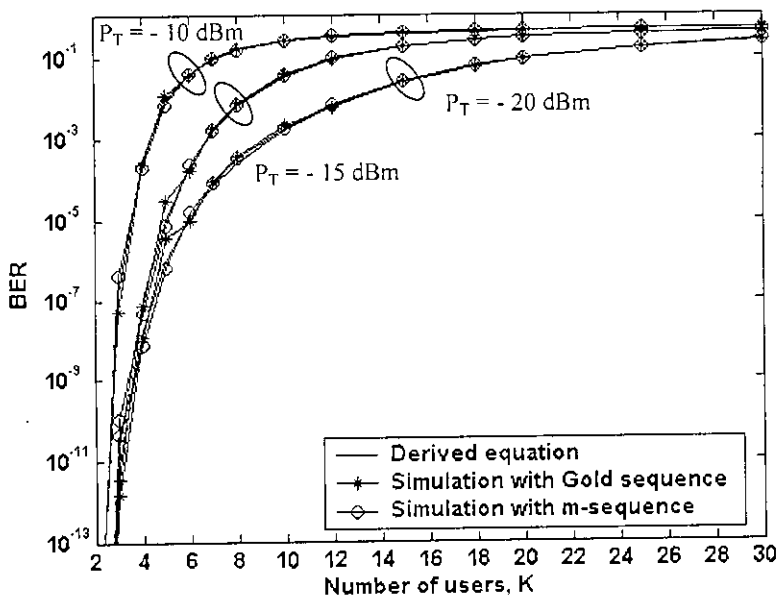

Fig. 6.7 BER versus number of simultaneous users for different values of transmitted power per user for a 100 Mb/s, 1000 km OCDMA system with DSF. Number of chips per bit, $N = 63$ in all cases.

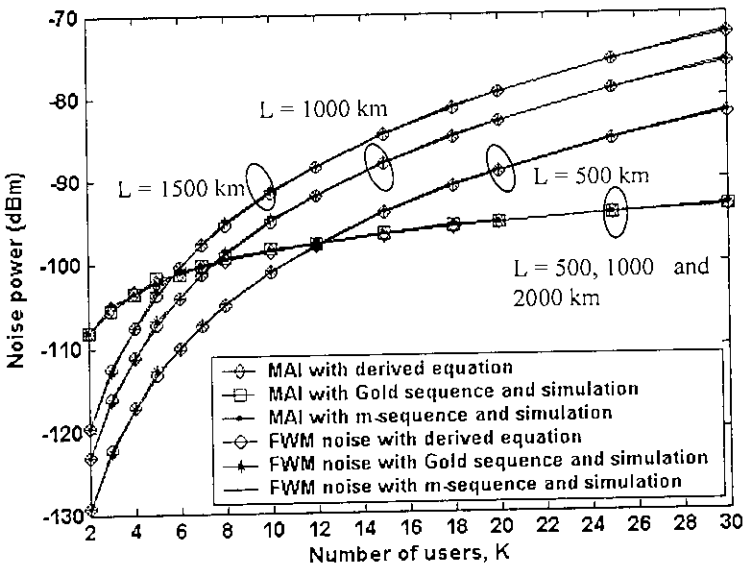

Fig. 6.8 FWM noise power and MAI power with respect to the number of simultaneous users for different values of transmission distance for a 100 Mb/s OCDMA systems with DSF. Number of chips per bit, N = 63 and transmitted power per user, P_T = -15 dBm in all cases.

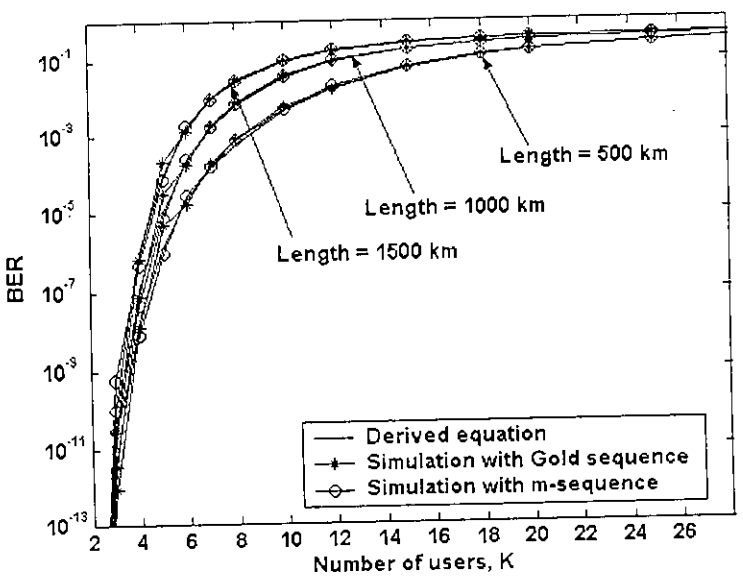

Fig. 6.9 BER versus number of simultaneous users for different values of transmission distance for a 100 Mb/s OCDMA system with DSF. Number of chips per bit, N = 63 and transmitted power per user, P_T = -15 dBm in all cases.

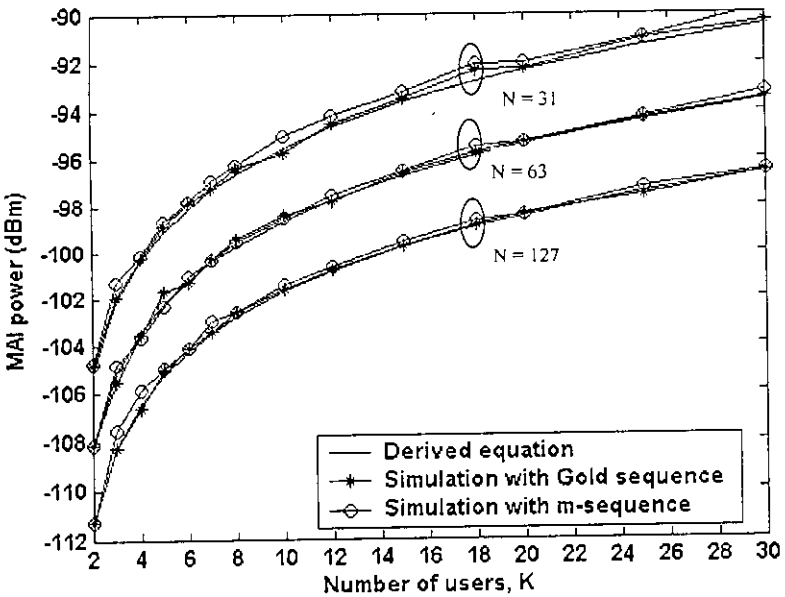

Fig. 6.10 MAI power versus number of simultaneous users for different number of chips per bit encoding for a 100 Mb/s, 1000 km OCDMA systems with DSF. Transmitted power per user, P_T = -15 dBm in all cases.

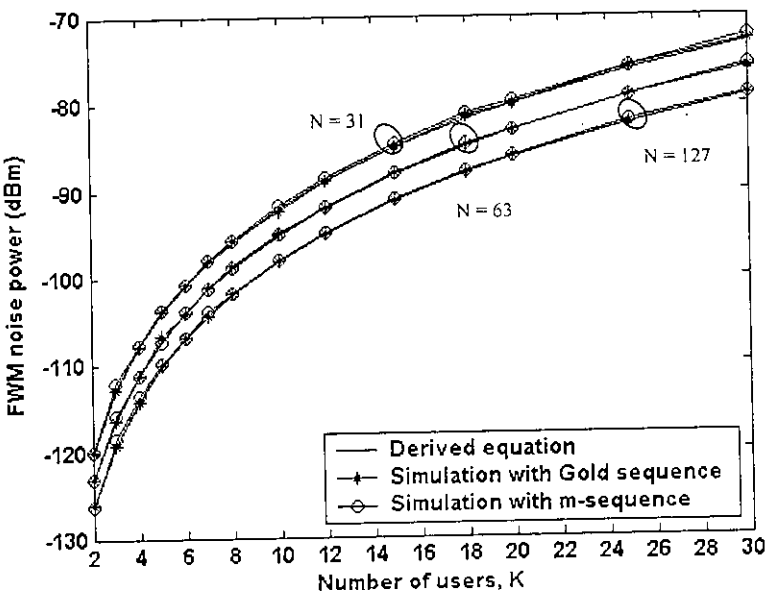

Fig. 6.11 FWM noise power versus number of simultaneous users for different number of chips per bit encoding for a 100 Mb/s, 1000 km OCDMA systems with DSF. Transmitted power per user, P_T = -15 dBm in all cases.

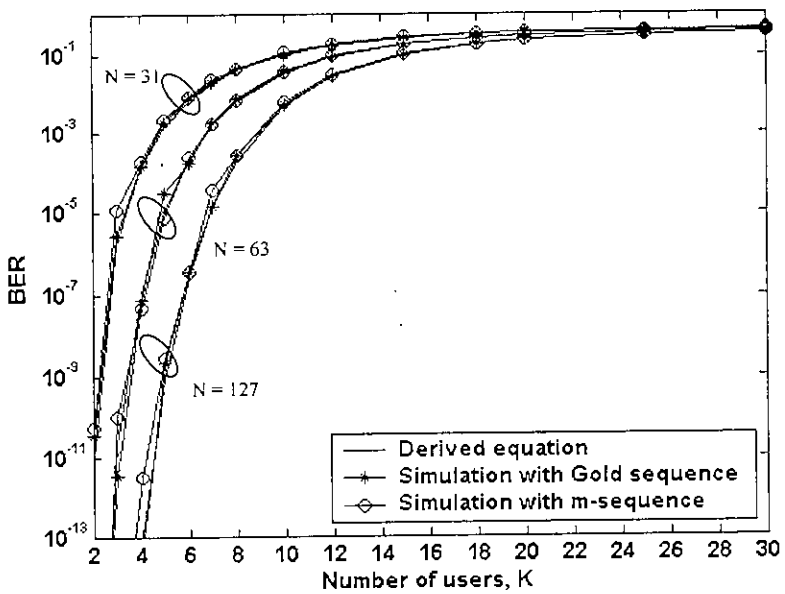

Fig. 6.12 BER versus number of simultaneous users for different number of chips per bit encoding for a 100 Mb/s, 1000 km OCDMA systems with DSF. Transmitted power per user, P_T = -15 dBm in all cases.

The BER performance 10 Mb/s OCDMA system with 1023 chip sequence is evaluated using analytical expressions. Further, BER performances are evaluated excluding the FWM noise and compared with previous results. Fig. 6.13 shows the BER performance versus transmitted power per user for 1000 km OCDMA systems with DSF for different number of simultaneous users. It is found that BER performances including and excluding FWM effect are same at lower transmitted power because FWM power is very less at lower transmitted power. BERs are poor at lower transmitted power, although the FWM power is less since thermal noise and dark noise are comparable with signal power. Signal power increases with increasing transmitted power but thermal noise and dark noise almost remain constant. That's why, SNR as well as BER improve with increasing transmitted power at lower transmitted power region since FWM noise does not effect significantly at lower transmitted power. It is found that BER is minimum at a certain amount of transmitted power. It is investigated that BER starts to degrade with increasing

transmitted power if the transmitted power is higher than the certain amount of transmitted power since FWM noise power significantly increases with increasing transmitted power at higher transmitted power. It is observed that the BER is minimum at higher transmitted power if the FWM effect is not considered. BER performances including and excluding FWM effect differ significantly at higher transmitted power. BER is found to be degraded if the number of simultaneous users is increased since MAI and FWM noise increase with increasing number of simultaneous users. The BER performances versus the transmission distance for different number of simultaneous users is shown in Fig. 6.14. It is found that the BER performance is independent of transmission distance for a number of simultaneous users, if the FWM effect is not considered. The FWM effect degrades the BER performance for higher number of simultaneous and higher values of transmission distance.

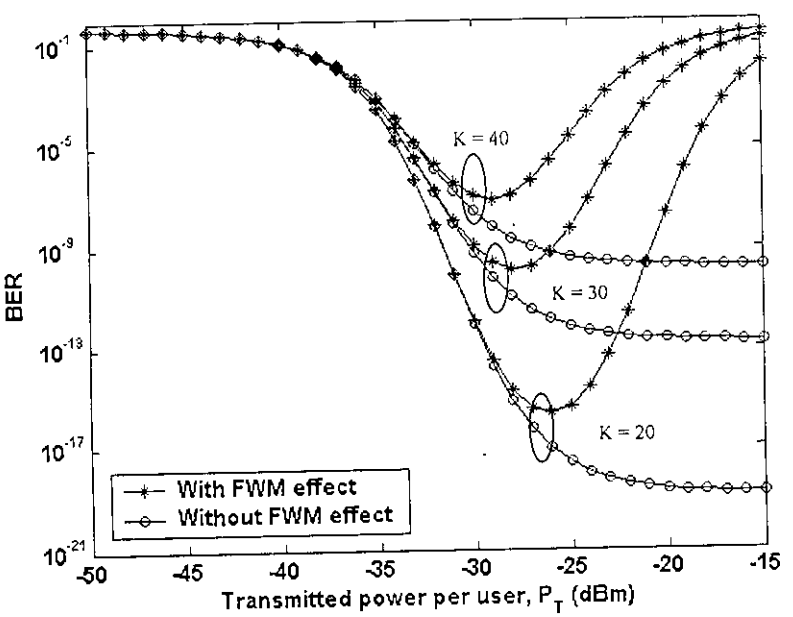

Fig. 6.13 BER versus transmitted power per user for different number of simultaneous users for a 10 Mb/s, 1000 km OCDMA systems with DSF. Number of chips per bit, $N = 1023$ in all cases.

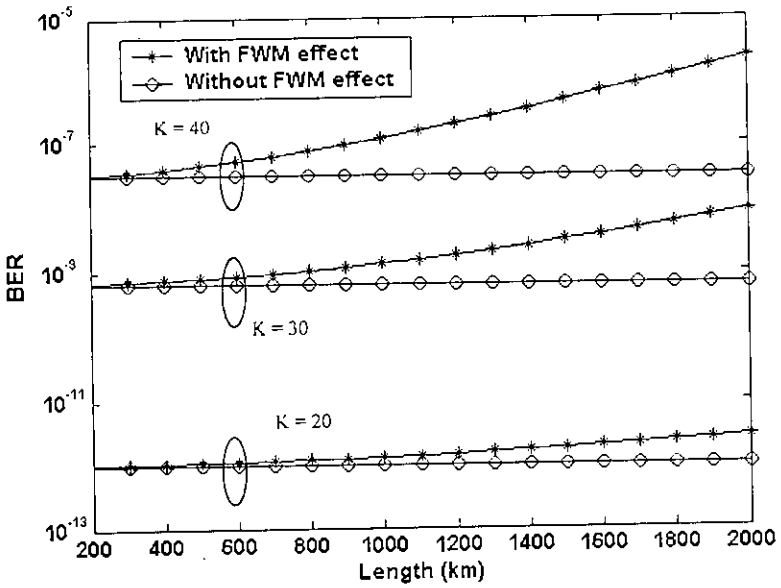

Fig. 6.14 BER versus transmission distance for a 10 Mb/s OCDMA systems with DSF for different number of simultaneous users. Number of chips per bit, N = 1023 and transmitted power per user, P_T = -30 dBm in all cases.

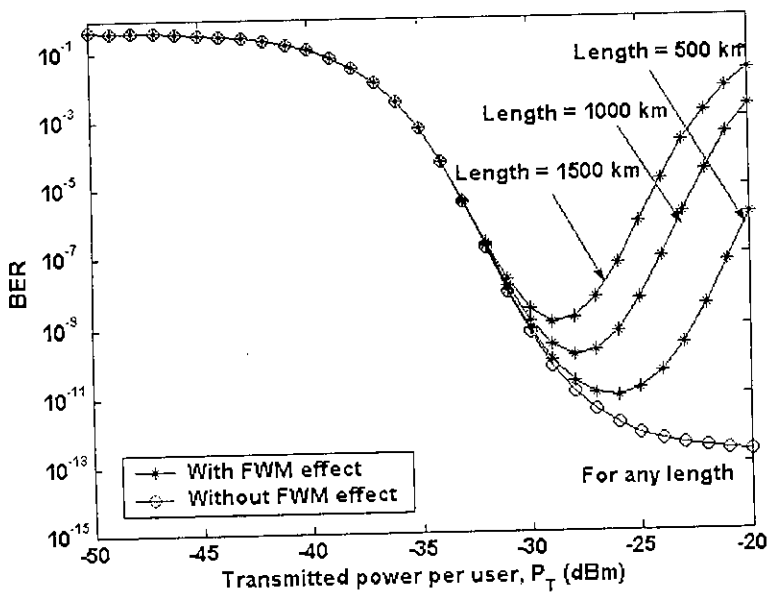

Fig. 6.15 BER versus transmitted power per user for different values of transmission distance for a 10 Mb/s OCDMA systems with DSF. Number of chips per bit, N = 1023 and number of simultaneous users, K = 30 in all cases.

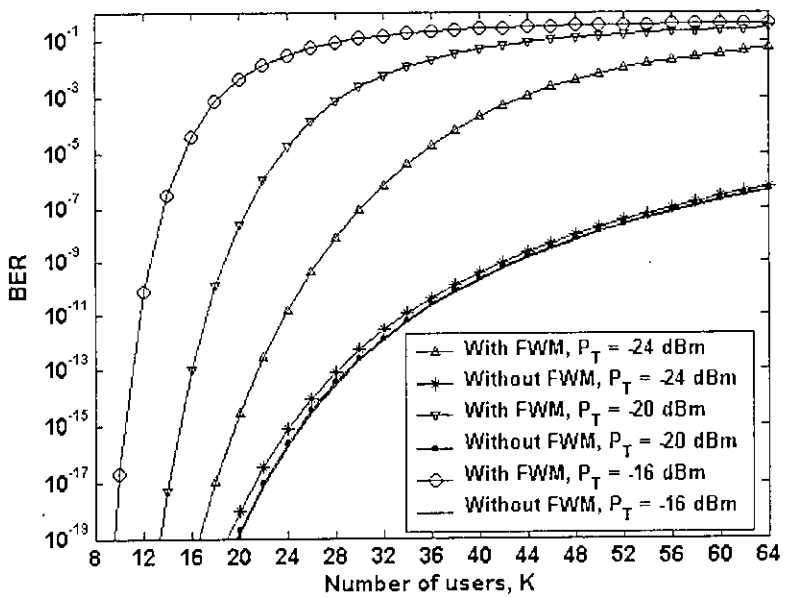

Fig. 6.16 BER performance versus number of simultaneous users for different values of transmitted power per user for a 10 Mb/s, 1000 km OCDMA systems with DSF. Number of chips per bit, N = 1023 in all cases.

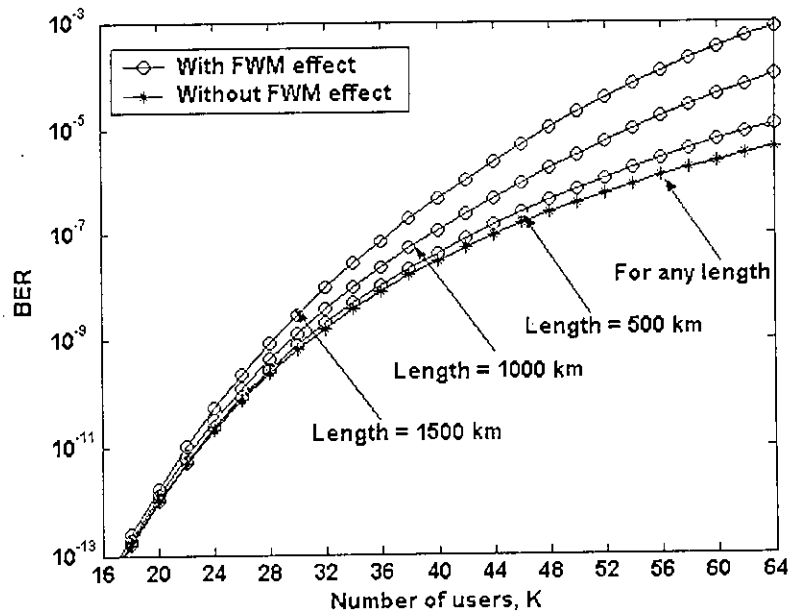

Fig. 6.17 BER versus number of simultaneous users for different values of transmission distance for a 10 Mb/s OCDMA systems with DSF. Number of chips per bit, N = 1023 and transmitted power per user, P_T = -30 dBm in all cases.

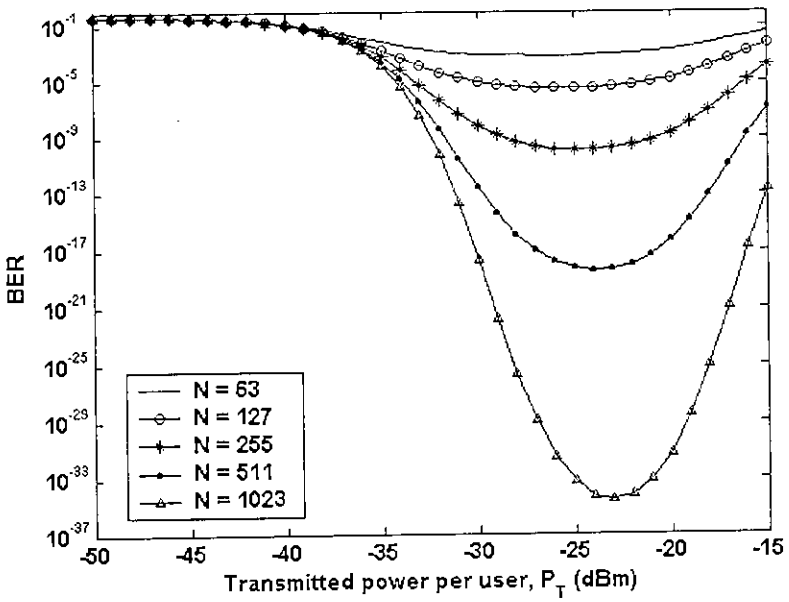

Fig. 6.18 BER versus transmitted power per user for different values chips per bit encoding for a 10 Mb/s, 1000 km OCDMA systems with DSF. Number simultaneous users $K = 10$ in all cases.

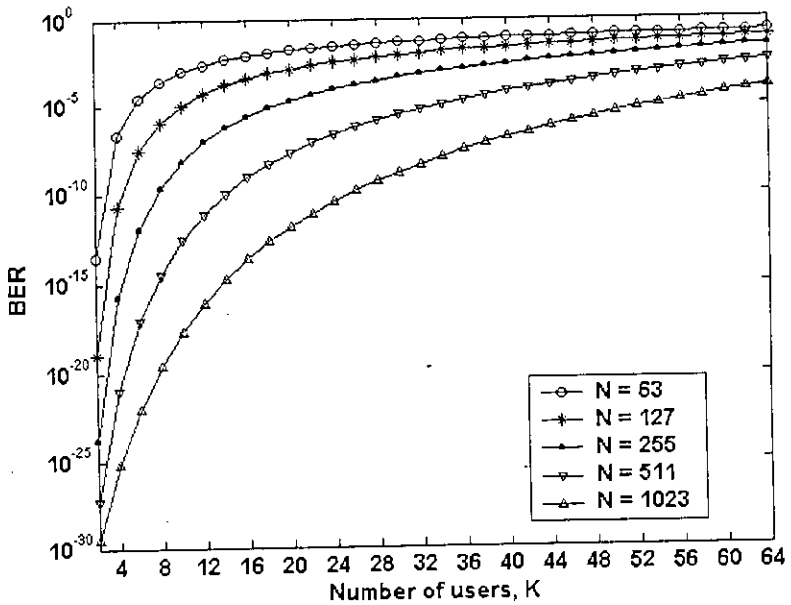

Fig. 6.19 BER versus number of simultaneous users for different values of chips per bit encoding for a 10 Mb/s, 1000 km OCDMA systems with DSF. Transmitted power per user, P_T = -30 dBm in all cases.

BER performance as a function of transmitted power per user for different values of transmission distance and different number of chips per bit encoding are shown in Fig. 6.15 and 6.18, respectively. BER versus number of simultaneous users for different values of transmitted power per user, different values of transmission distance and different number of chips per bit encoding are shown in Fig. 6.16, Fig. 6.17 and Fig. 6.19, respectively. From the Fig. 13 to Fig. 19, it is evident that FWM effect is significant for higher number of simultaneous users, transmission distance and transmitted power. Thus, performance should be evaluated considering the effect of FWM for a long distance OCDMA system with higher number of simultaneous users.

From the figures of BER performance, it is evident that transmitted power per user, number of simultaneous users and transmission distance are limited by FWM for a given BER of the system. Maximum allowable transmitted power per user at a BER of 10^{-9} for 10 Mb/s OCDMA systems with DSF is evaluated. Maximum allowable transmitted power versus transmission distance for 10 simultaneous users OCDMA systems with DSF for different values of chips per bit encoding is shown in Fig. 6.20. It is investigated that maximum allowable transmitted power per user decreases with increasing the transmission distance. Maximum allowable transmitted power can be increased by increasing number of the chips per bit. Fig. 6.21 shows the maximum allowable transmitted power per user versus transmission distance for different number of simultaneous users for 1023 chips per bit encoding in all cases. It is found that maximum allowable transmitted power is -13 dBm for 10 simultaneous users at a distance of 1000 km and it reduced significantly to -26 dBm for 30 simultaneous users. Maximum allowable transmitted power per user versus number of simultaneous users for different values of chips per bit encoding and transmission distance are shown in Fig. 6.22 and Fig. 6.23, respectively. Maximum allowable transmission distance at a BER of 10^{-9} for 10 Mb/s OCDMA systems with DSF for different cases are shown in Fig. 6.24 and Fig. 6.25. It is investigated that maximum allowable transmission distance decreases as the number of users and transmitted power per user are increased. It can be increased by increasing the chips per bit.

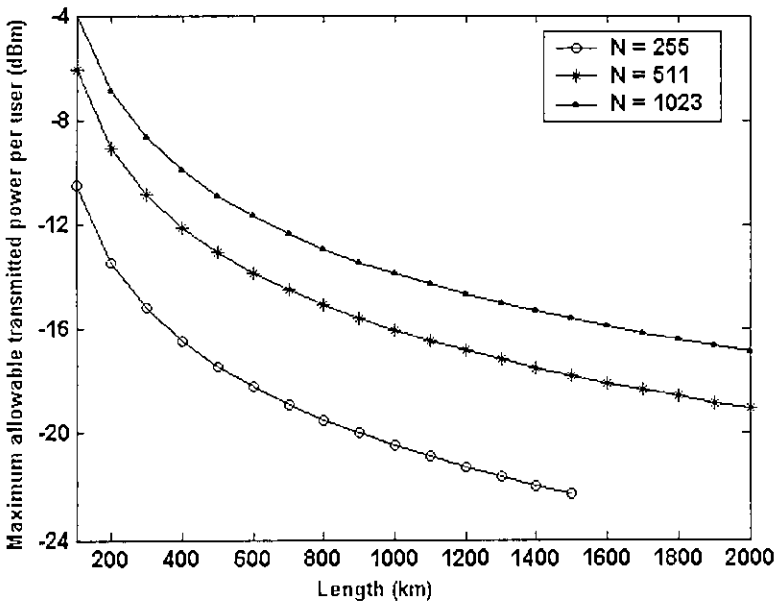

Fig. 6.20 Maximum allowable transmitted power per user versus transmission distance for different values of chips per bit encoding at a BER of 10^{-9} for 10 Mb/s OCDMA systems with DSF. Number of simultaneous users, $K = 10$ in all cases.

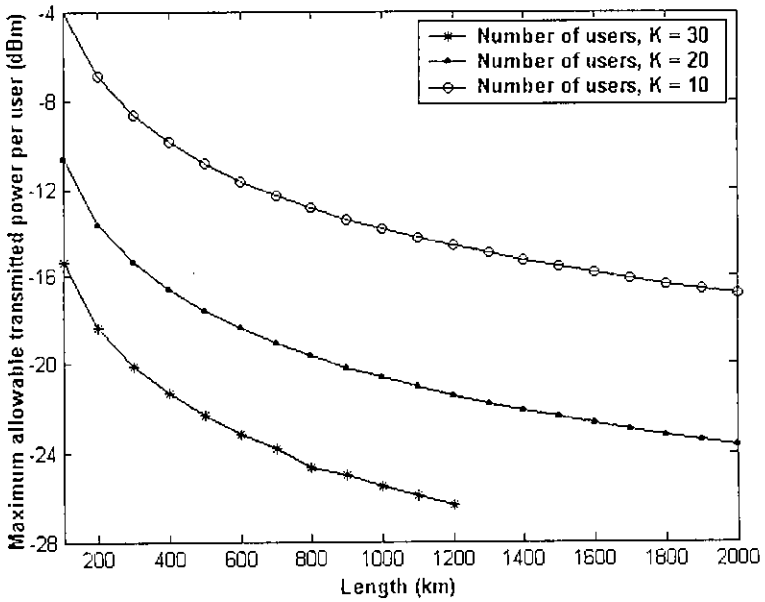

Fig. 6.21 Maximum allowable transmitted power per user versus transmission distance for different number of simultaneous users at a BER of 10^{-9} for 10 Mb/s OCDMA systems with DSF. Chips per bit, $N = 1023$ in all cases.

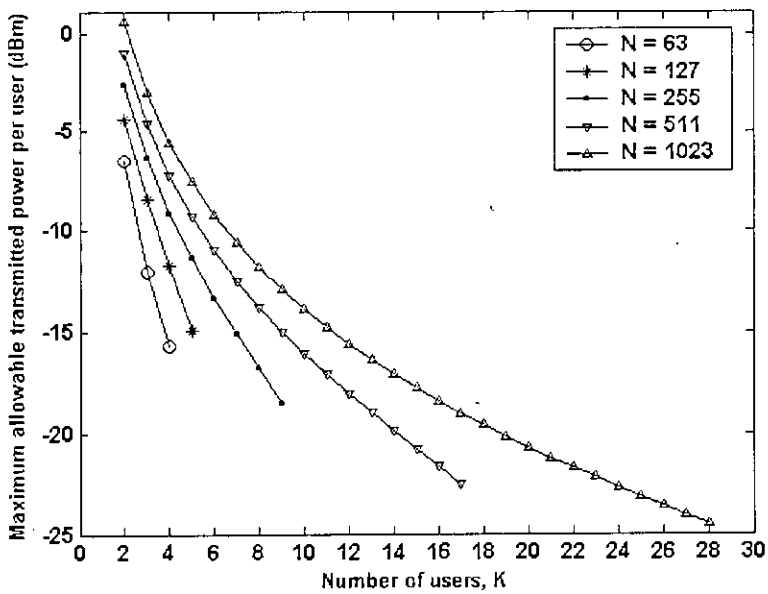

Fig. 6.22 Maximum allowable transmitted power per user versus number of simultaneous users for different values of chips per bit encoding at a BER of 10^{-9} for 10 Mb/s, 100 km OCDMA systems with DSF.

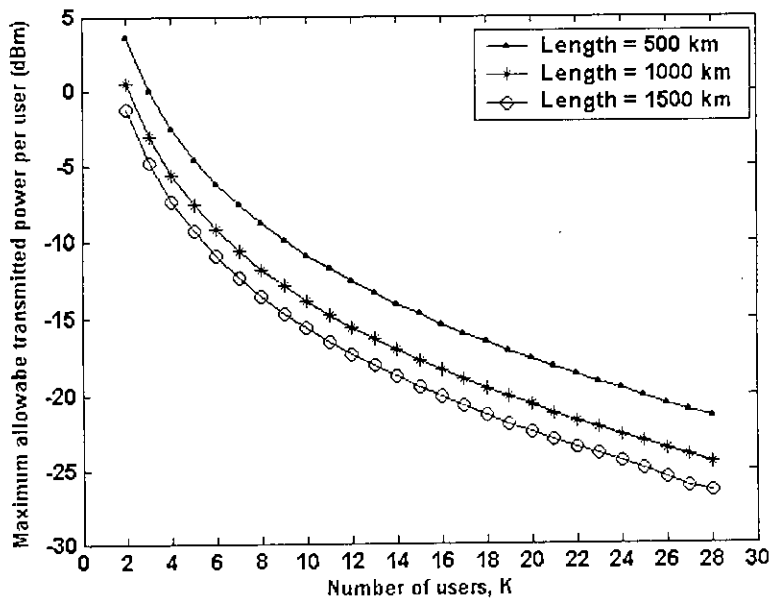

Fig. 6.23 Maximum allowable transmitted power per user versus number of simultaneous users for different values of transmission distance at a BER of 10^{-9} for a 10 Mb/s OCDMA systems with DSF. Number of hips per bit, $N = 1023$ in all cases.

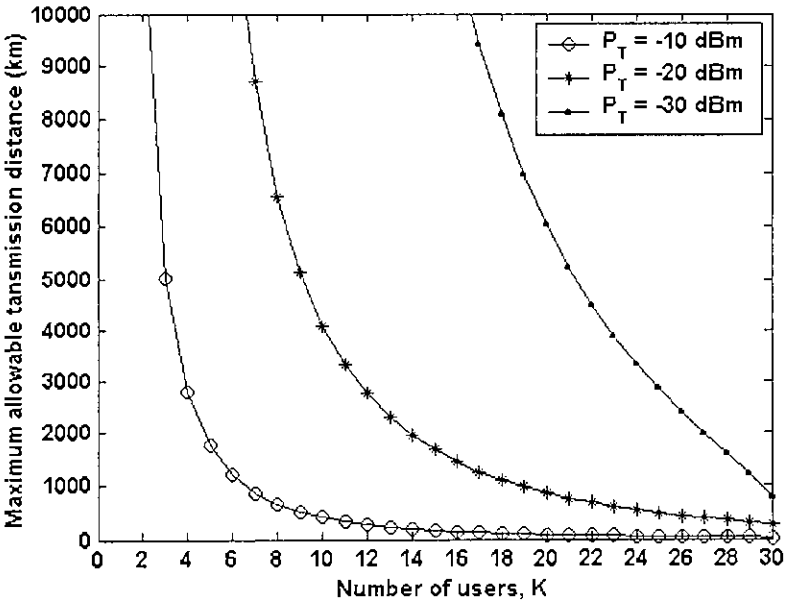

Fig. 6.24 Maximum allowable transmission distance versus number of simultaneous users for different values of transmitted power per user at a BER of 10^{-9} for a 10 Mb/s OCDMA systems with DSF. Number of chips per bit, N = 1023 in all cases.

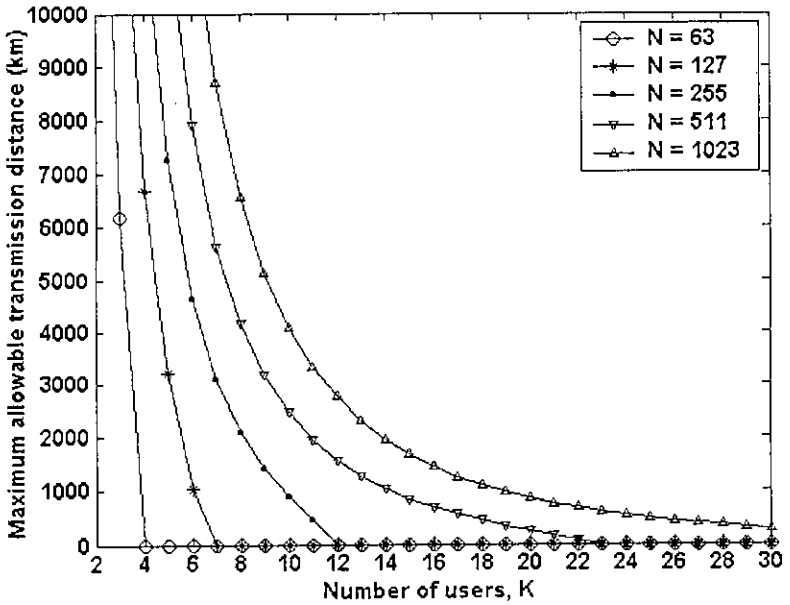

Fig. 6.25 Maximum allowable transmission distance versus number of simultaneous users for different values of chips per bit encoding at a BER of 10^{-9} for 10 Mb/s OCDMA systems with DSF. Transmitted power per user, P_T = -20 dBm in all cases.

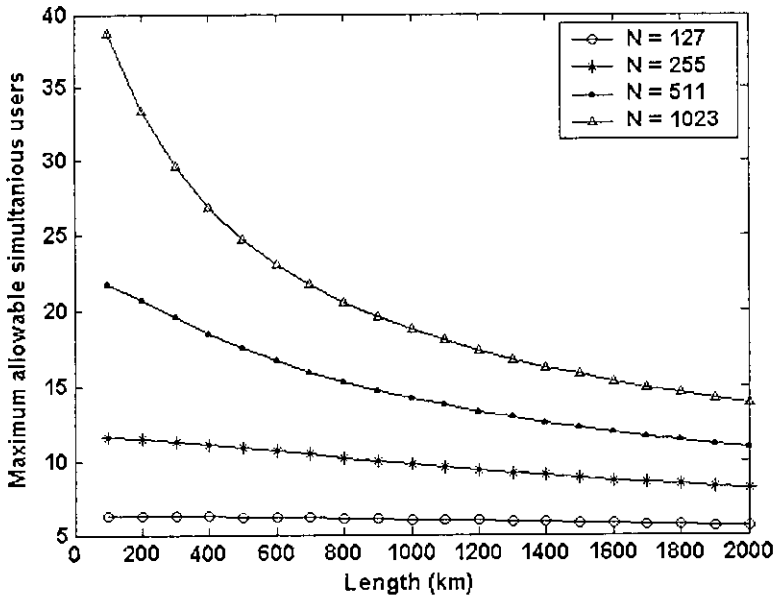

Fig. 6.26 Maximum allowable simultaneous users versus transmission distance for different values of chips per bit encoding at BER of 10^{-9} for 10 Mb/s OCDMA systems with DSF. Transmitted power per user, P_T = - 20 dBm in all cases.

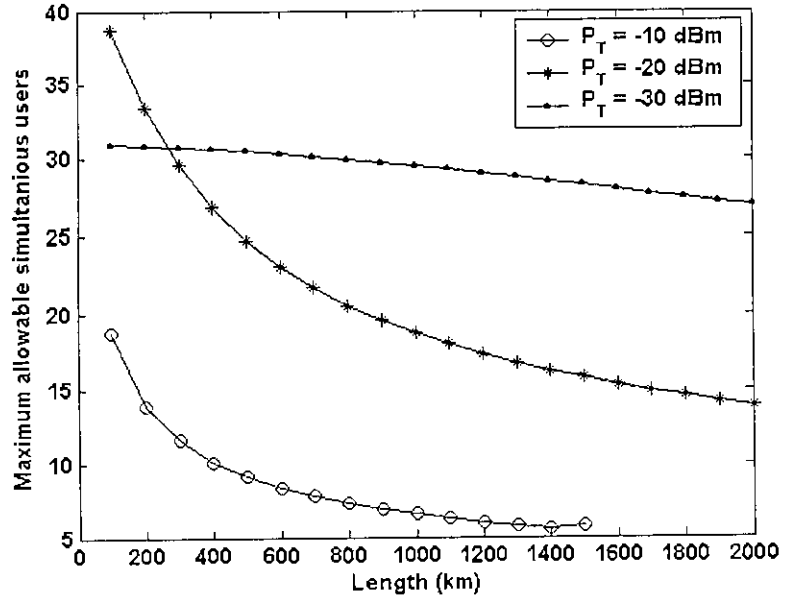

Fig. 6.27 Maximum allowable simultaneous users as a function of transmission distance for different values of transmitted power per user at BER of 10^{-9} for 10 Mb/s OCDMA systems with DSF. The chips per bit, N = 1023 all cases.

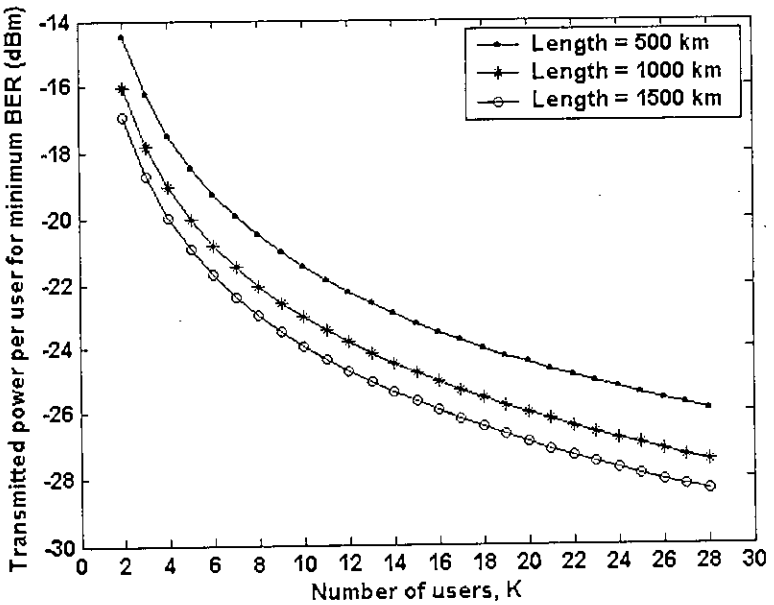

Fig. 6.28 Transmitted power per user versus number of simultaneous users for different values of transmission distance to obtain minimum BER for 10 Mb/s OCDMA systems with DSF. Number of chips per bit, N = 1023 in all cases.

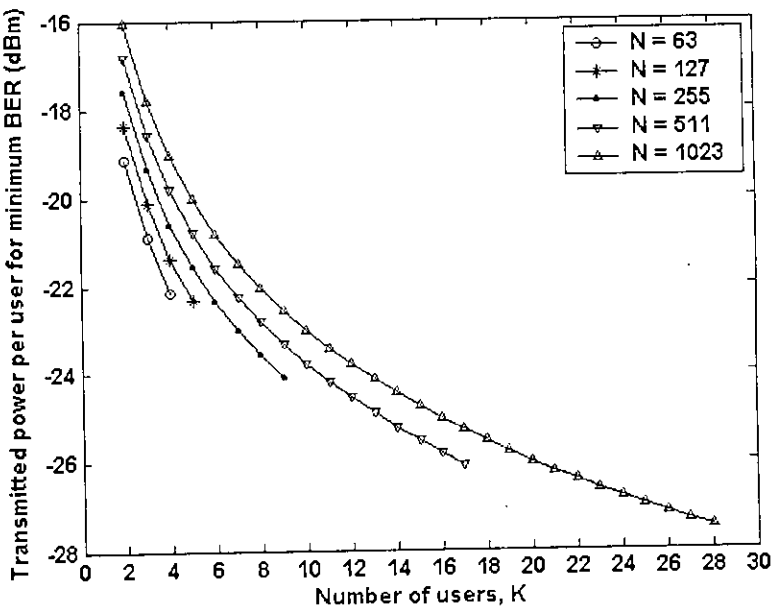

Fig. 6.29 Transmitted power per user as a function of number of number of simultaneous users for different values of chips per bit encoding to obtain minimum BER for 10 Mb/s, 100 km OCDMA systems with DSF receiver.

From Fig. 24, it is found that maximum allowable transmission distance is around 7000 km with -30 dBm transmitted power per user and it reduced significantly to around 1000 km with -20 dBm transmitted power per user for 20 users for 1023 number of chips per bit encoding. From Fig. 25, it is found that maximum allowable transmission distance is around 800 km with 255 chip sequence and it increased to around 4500 km with 1023 chip sequence for 10 users with -20 dBm transmitted power per user.

Maximum allowable simultaneous users at BER of 10^{-9} for 10 Mb/s OCDMA systems with DSF are evaluated for different cases. Fig. 6.26 shows the maximum allowable simultaneous users versus transmission distance for different values of chips per bit encoding with - 20 dBm transmitted power per user. Maximum allowable simultaneous users versus transmission distance for different values of transmitted power per user with 1023 chips per bit encoding is shown in Fig. 6.27. It is investigated that the maximum allowable simultaneous users decreases if the transmission distance and transmitted power per user are increased. It can be increased by increasing the number of chips per bit. From Fig. 6.26, it is found that maximum 6 users can be transmitted simultaneously for 127 chip sequence and 18 users can be transmitted simultaneously for 1023 chip sequence at a 1000 km transmission distance with -20 dBm transmitted power per user.

The required transmitted power per user for minimum BER of a 10 Mb/s OCDMA systems with DSF is determined. Fig. 6.28 shows the required transmitted power per user at a minimum BER varying the number of simultaneous users for different values of transmission distance with 1023 chips per bit in all cases. The required transmitted power per user at a minimum BER versus the number of simultaneous users for different values of chips per bit encoding is shown in Fig. 6.29. It is investigated that required transmitted power per user decreases if the number of simultaneous users as well as transmission distance are increased.

Further, the performance of a 100 Mb/s OCDMA transmission system with single mode dispersive fiber (DF) is evaluated using matlab simulation with m-sequence as well as Gold sequence and compared with the results of system with DSF. Fiber chromatic dispersion is taken to be 16 ps/km-nm. Fig. 6.30 shows the eye diagram of received signal for (a) 200 km (b) 250 km (c) 300 km and (d) 350 km transmission systems with 63 chips per bit encoding and 0.1 mW peak incident chip optical power. It is investigated that eye opening decreases as the transmission distance is increased from 200 km to 350 km due to fiber chromatic dispersion. Eye closer penalty versus transmission distance with 63 chips per bit encoding is shown in Fig. 6.31. The penalty is given by as

$$Penalty(db)=20\log\frac{a}{b} \tag{6.1}$$

where a is the opening of eye without dispersion and b is opening of eye with dispersion.

From Fig. 6.31, it is found that penalty increases sharply as the transmission distance is increased. Signal to MAI ratio, signal to FWM noise ratio and BER performance with respect to the number of simultaneous users for different value of transmitted power for a 300 km OCDMA system with 63 chips per bit encoding are shown in Fig. 6.32, Fig. 6.33 and Fig. 6.34, respectively. It is investigated that signal to MAI ratio is independent of transmitted power but reduces if the number of simultaneous users is increased. Signal to FWM noise ratio and BER increases as the number of simultaneous users and transmitted power are increased. It is found that system with DSF gives better performance than the system with dispersive fiber. Signal to MAI ratio, signal to FWM noise ratio and BER performance as a function of number of simultaneous users for different values of transmission distance for a 300 km system with 63 chips per bit are shown in Fig. 6.35, Fig. 6.36 and Fig. 6.37, respectively. Signal to MAI ratio, signal to FWM noise ratio decrease as the transmission distance is increased, thus, the BER performance degrades for increasing transmission distance.

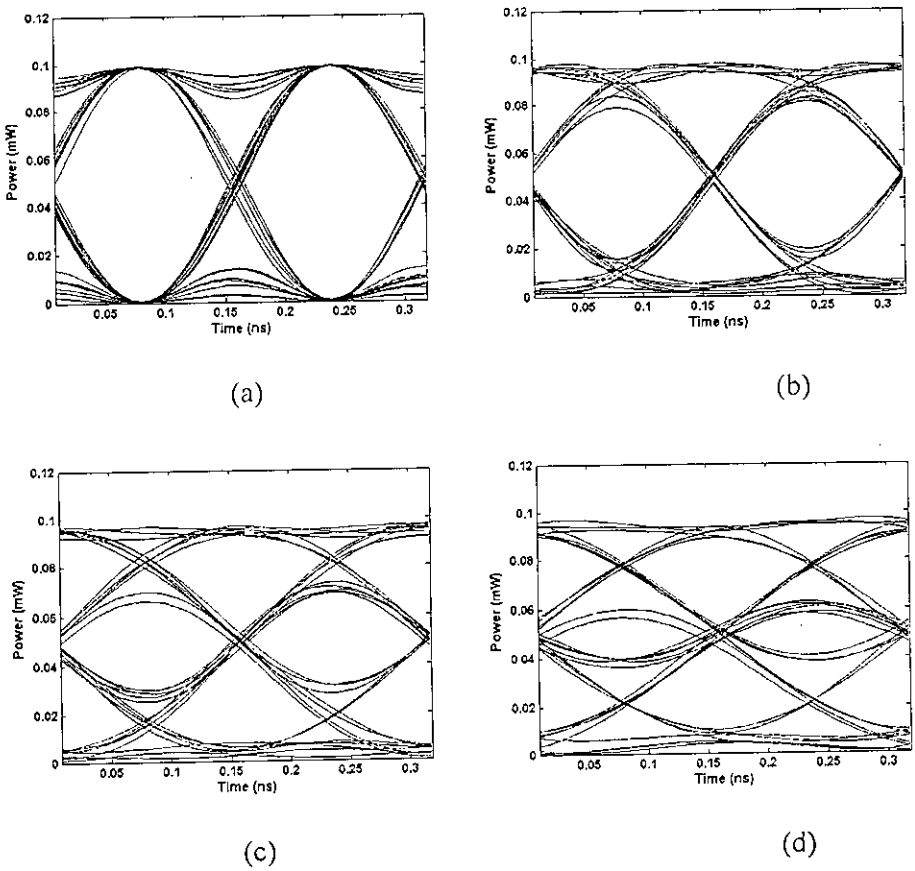

Fig. 6.30 Eye diagram of received signal for (a) 200 km (b) 250 km (c) 300 km and (d) 350 km transmission system. Number of chips per bit is 63 for 100 Mb/s system with 0.1 mW peak incident chip optical power and fiber chromatic dispersion coefficient, D_c = 16 ps/km-nm.

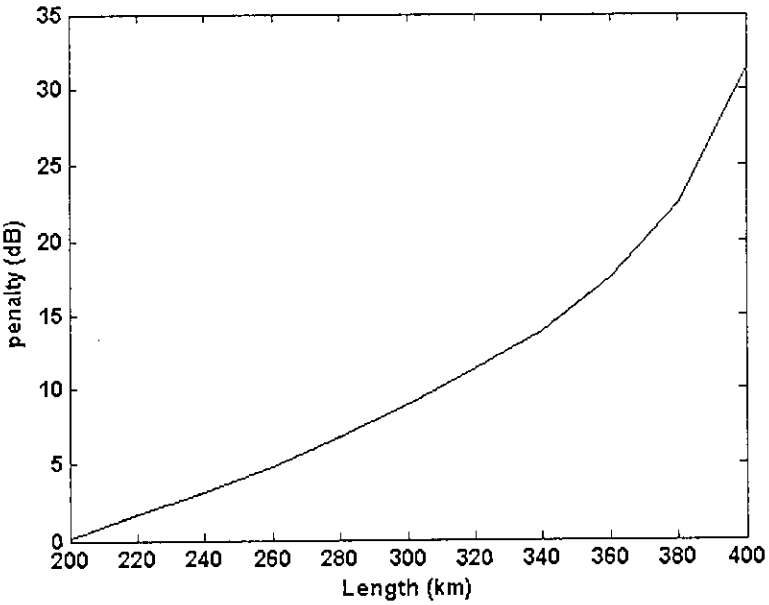

Fig. 6.31 Eye penalty versus transmission distance for a 100 Mb/s OCDMA system. Number of chips per bit is 63 with fiber chromatic dispersion coefficient, D_c = 16 ps/km-nm.

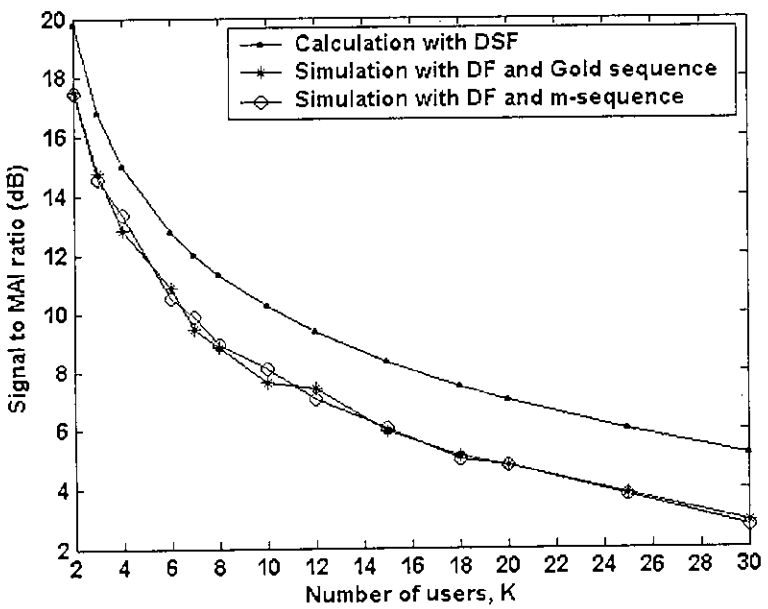

Fig. 6.32 Signal to MAI ratio versus number of simultaneous users for any value of transmitted power for a 100 Mb/s, 300 km OCDMA system. Number of chips per bit is 63 and fiber chromatic dispersion coefficient, D_c = 16 ps/km-nm for dispersive fiber (DF).

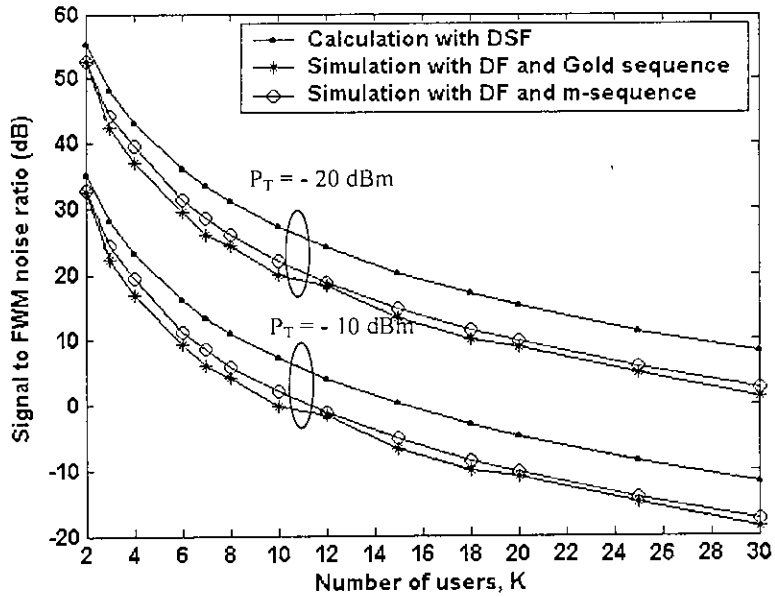

Fig. 6.33 Signal to FWM noise ratio as a function of number of simultaneous users for different values of transmitted power per user for a 100 Mb/s, 300 km OCDMA system. Number of chips per bit is 63 and fiber chromatic dispersion coefficient, D_c = 16 ps/km-nm for DF.

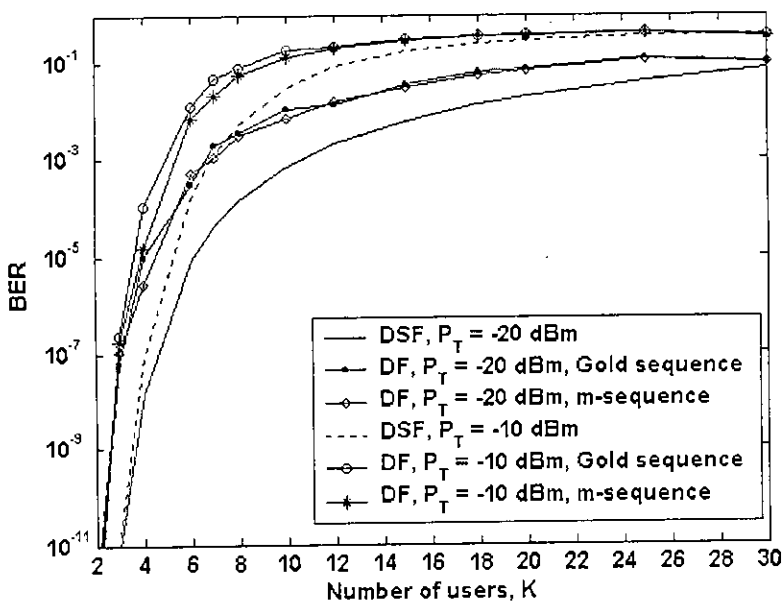

Fig. 6.34 BER versus number of simultaneous users for different value of transmitted power per user for a 100 Mb/s, 300 km OCDMA system. Number of chips per bit is 63 and fiber chromatic dispersion coefficient, D_c = 16 ps/km-nm for DF.

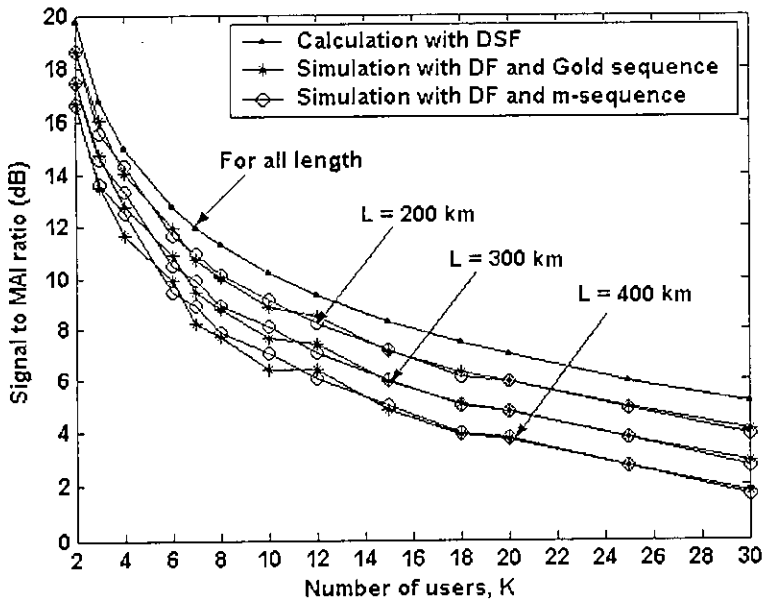

Fig. 6.35 Signal to MAI ratio versus number of simultaneous users for different values of transmission distance at any value of transmitted power per user for a 100 Mb/s OCDMA system. Number of chips per bit is 63 and fiber chromatic dispersion coefficient, D_c = 16 ps/km-nm for DF.

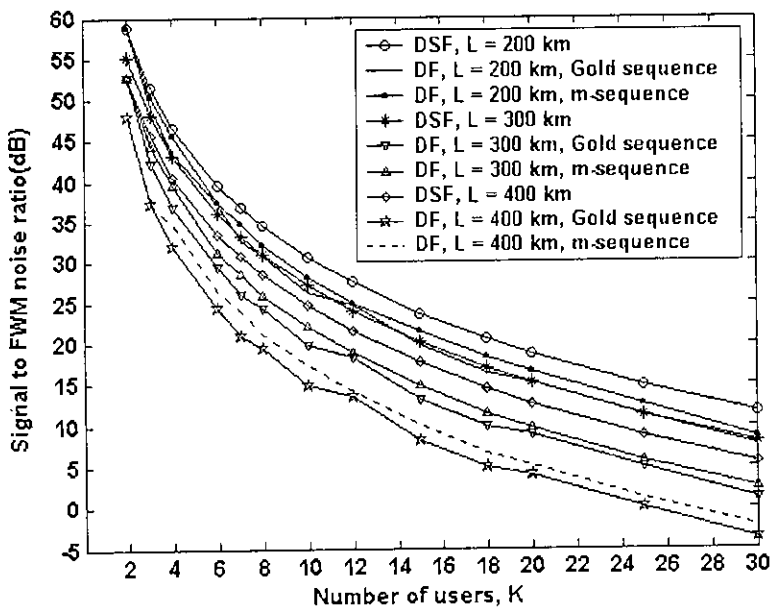

Fig. 6.36 Signal to FWM noise ratio versus number of simultaneous users for different values of transmission distance for a 100 Mb/s OCDMA system. Number of chips per bit is 63 transmitted power per user, P_T = -20 in all cases. Fiber chromatic dispersion coefficient, D_c = 16 ps/km-nm for DF.

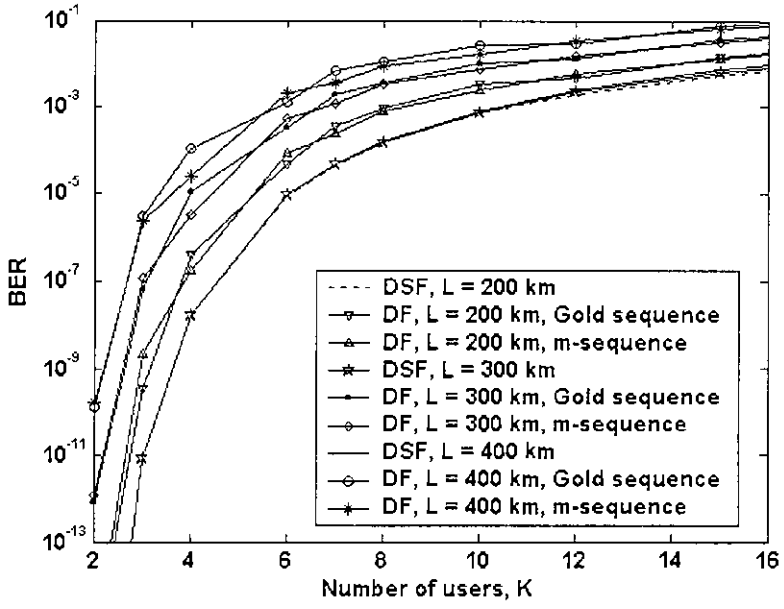

Fig. 6.37 BER versus number of simultaneous users for different values of transmission distance for a 100 Mb/s OCDMA system. Number of chips per bit is 63 transmitted power per user, P_T = -20 in all cases. Fiber chromatic dispersion coefficient, D_c = 16 ps/km-nm for DF.

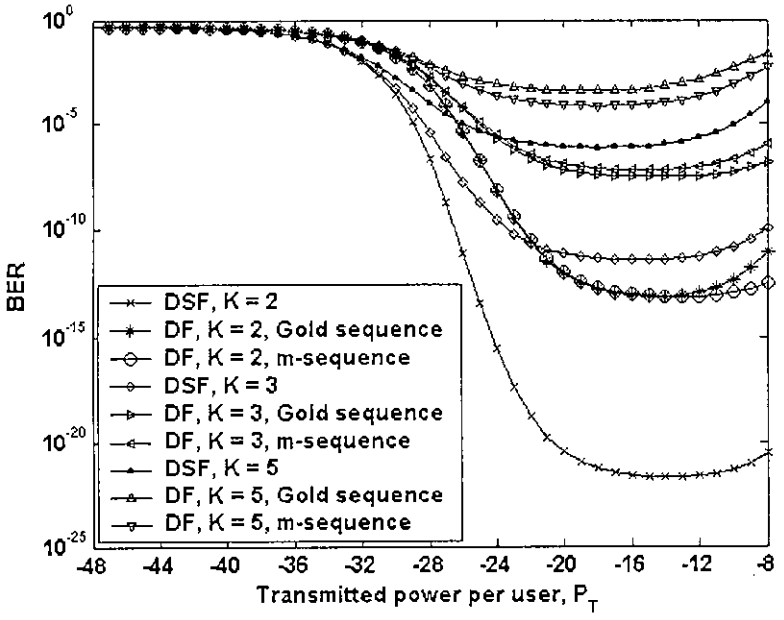

Fig. 6.38 BER versus transmitted power per user for different number of simultaneous users for a 100 Mb/s, 300 km OCDMA system. Number of chips per bit, N = 63 in all cases and fiber chromatic dispersion coefficient, D_c = 16 ps/km-nm for DF.

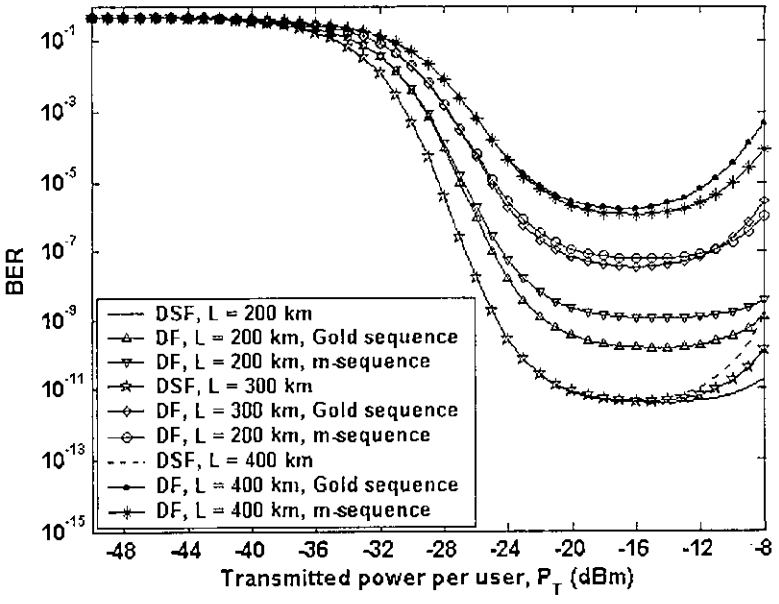

Fig. 6.39 BER versus transmitted power per user for different values of transmission distance for a 100 Mb/s OCDMA system. Number of simultaneous users, K = 3, chips per bit, N = 63 in all cases. Fiber chromatic dispersion coefficient, D_c = 16 ps/km-nm for DF.

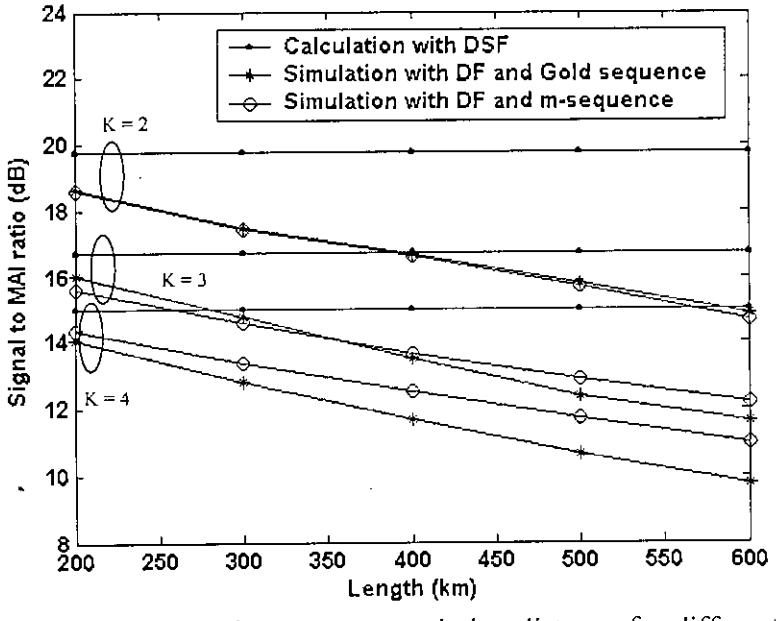

Fig. 6.40 Signal to MAI ratio versus transmission distance for different number of simultaneous users at any value of transmitted power for a 100 Mb/s OCDMA system. Number of chips per bit is 63 and fiber chromatic dispersion coefficient, D_c = 16 ps/km-nm for DF.

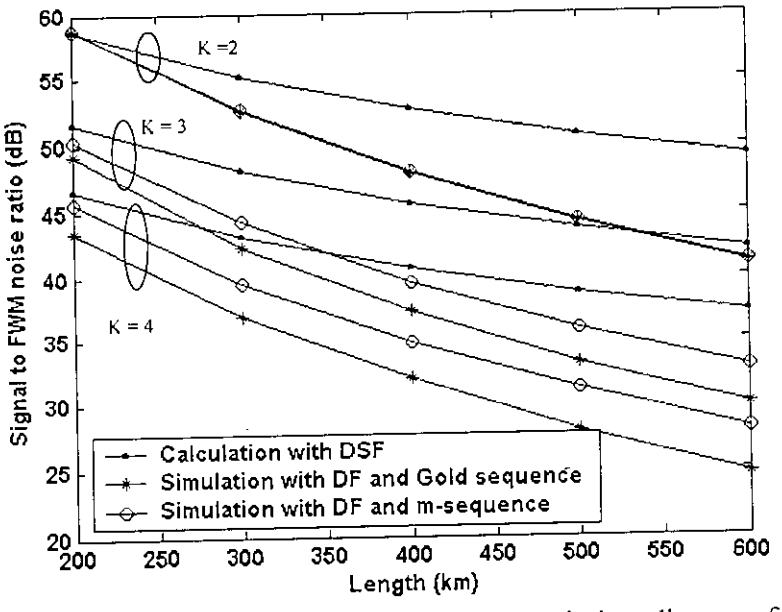

Fig. 6.41 Signal to FWM noise ratio versus transmission distance for different number of simultaneous users at -20dBm transmitted power per user for a 100 Mb/s OCDMA system. Number of chips per bit is 63 and fiber chromatic dispersion coefficient, D_c = 16 ps/km-nm for DF.

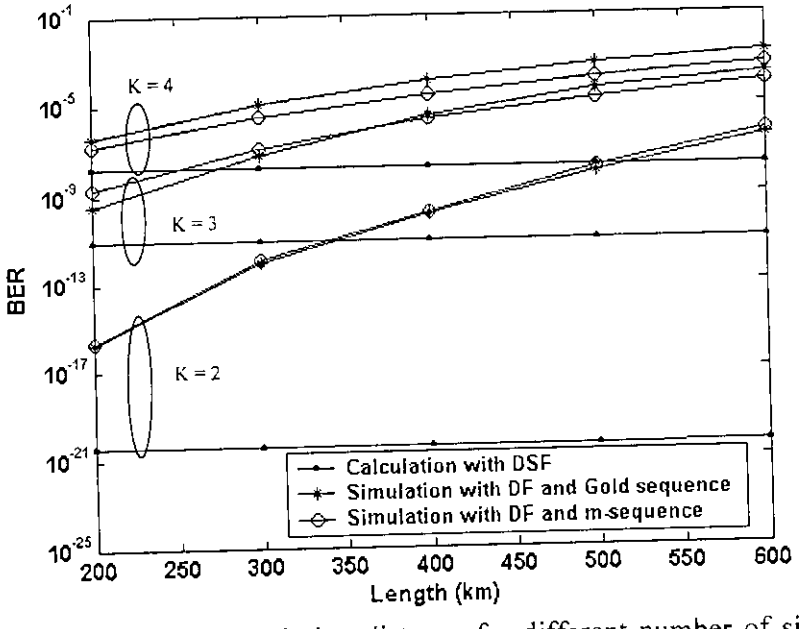

Fig. 6.42 BER versus transmission distance for different number of simultaneous users at -20 dBm transmitted power per user for a 100 Mb/s OCDMA system. Number of chips per bit is 63 and fiber chromatic dispersion coefficient, D_c = 16 ps/km-nm for DF.

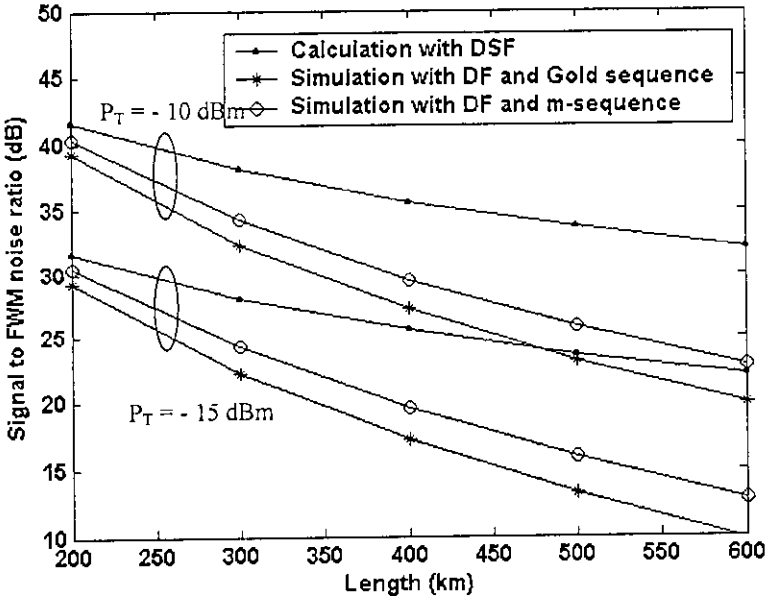

Fig. 6.43 Signal to FWM noise ratio transmission distance for different values of transmitted power per user for a 100 Mb/s OCDMA system. Number of chips per bit, N= 63, number of simultaneous users, K = 3 and fiber chromatic dispersion coefficient, D_c = 16 ps/km-nm for DF.

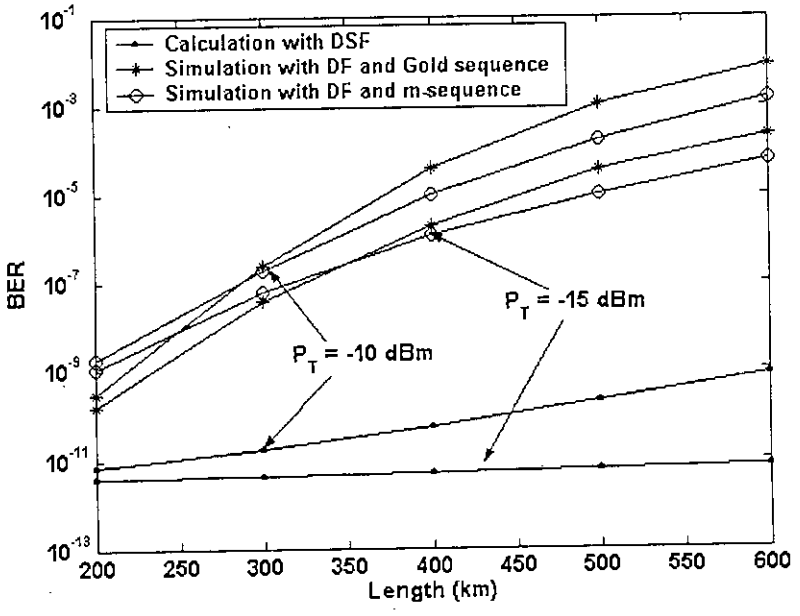

Fig. 6.44 BER as a function of transmission distance for different values of transmitted power per channel for a 100 Mb/s OCDMA system. Number of chips per bit N = 63, number of simultaneous users, K = 3 and fiber chromatic dispersion coefficient, D_c = 16 ps/km-nm for DF.

BER versus transmitted power per user for different number of simultaneous users and different values of transmission distance are shown in Fig. 6.38 and Fig. 6.39, respectively. From Fig. 6.38, it is found that minimum achievable BER with DSF is around 10^{-22} but it degrades to 10^{-14} for dispersive fiber for 2 simultaneous users. From Fig. 6.39, it is seen that minimum achievable BER DSF is around 10^{-9} for 200 km transmission distance but it degrades to 10^{-6} for 400 km transmission distance with dispersive fiber and 2 simultaneous users. Signal to MAI ratio, signal to FWM noise ratio and BER performance varying the of transmission distance for different number of simultaneous users with 63 chips per bit encoding and -20 dBm transmitted power per user are shown in Fig. 6.40, Fig. 6.41, Fig. 6.42, respectively. From Fig. 6.42, it is found that 200 km OCDMA system with DF having a BER of 10^{-16} but it increases to 10^{-7} for 600 km transmission distance for 2 simultaneous users with -20 dBm transmitted power per user. Fig. 6.43 and Fig. 6.44 show the signal to FWM noise ratio and BER performance varying the of transmission distance for different values of transmitted power per user for 3 simultaneous users with 63 chips per bit encoding. It is investigated that BER using DF and DSF differs significantly if the transmission distance is increased.

Chapter 7

Conclusions and Suggestions for future work

7.1 Conclusions

SBS, SRS, FWM, SPM and XPM are the nonlinear effect in fiber optic communications. FWM is one of the most important nonlinear effects in optical communication. But all researchers on optical communication neglect the FWM effect in OCDMA system. They considered that FWM noise power is very less compared to signal power as well as MAI. But the total transmitted power through the fiber is increased significantly if the number of simultaneous users is increased, which causes to increase the FWM noise power. Thus, FWM noise power is not negligible for higher number of simultaneous users and OCDMA should be analyzed considering the FWM effect. In this thesis, a theoretical analysis is provided for a DS-OCDMA system with an IM/DD transmission link using SIK optical correlator receiver. Analysis is carried out to evaluate the MAI, FWM crosstalk and BER performance of the system using DSF as well as normal fiber.

Following the theoretical analysis, BER performance results are evaluated for different values of transmitted power, different number of simultaneous users, different values of transmitted distance and different values of chips per bit. The results show that BER performance is degraded if the number of simultaneous users, transmission distance and transmitted power per user are increased as described before. It is investigated that the BER performance using DSF is better than the BER performance using normal fiber. The BER and power penalty are increased significantly with the transmission distance if the normal dispersive fiber is used. Thus, DSF should be used for long distance optical CDMA system.

It is found that BER performance can be improved significantly by increasing the number of chips per bit. But the effect of chromatic dispersion, polarization mode

dispersion (PMD) and other nonlinearities will be degraded the system performance at higher chip rate of operation.

Number of simultaneous users, transmission distance and transmitted power per channel is limited for a given chip rate at a BER of 10^{-9}. Maximum allowable number of users, maximum allowable transmission distance and maximum allowable transmitted power is determined for DSF for different values of chips per bit at a BER of 10^{-9} which will help to design OCDMA system.

The FWM noise power can be reduced by decreasing transmitted power per but lower transmitted power is not allowable considering the receiver sensitivity. Further, BER performance is poor at very low transmitted power because the received signal power is not much higher than the thermal noise, shot noise and dark noise. Again, BER performance degrades at high transmitted power. Thus, optimum value of power should be transmitted which gives the minimum BER. In this thesis, transmitted power for minimum BER performance is evaluated for different values of transmission distance varying the number of simultaneous users for different number of chip sequence.

7.2 Suggestions for future work

Future research related to this work can be carried out to reduce the effect of FWM using dispersion compensating fiber.

Future research related to this work can be carried out to investigate the influence of fiber FWM in a Frequency hopped (FH) optical CDMA system using FH encoder and decoder.

Further research related work can be carried out to reduce the effect of multiple access interference (MAI) which will increase the number of simultaneous users by placing an optical hard limiter at the front of the SIK receiver of the system.

Further works of importance are to determine the impact of other nonlinear effect such as SPM and XPM on the performance of a direct sequence spread spectrum IM/DD transmission system using SIK correlator receiver.

It will be very good future work if the system performance can be determined by a suitable experiment and compared with the analytical results.

References

[1] A. W. Lam and A. M. Hussin, "Performance of direct detection optical CDMA communication systems with avalanche photodiodes," *IEEE Trans. Commun.*, vol. 40, pp. 810-820, April. 1992.

[2] H. M. H. Shalaby, "Performance analysis of optical synchronous CDMA communication systems with PPM signaling." *IEEE Trans. Commun.*, vol. 43, pp. 624-634, Feb./Mar./Apr. 1995.

[3] H. M. H. Shalaby, "Maximum achievable number of user in optical PPM local area network," *J. Lightwave Technol.*, vol. 18, pp. 1187-1196, Sept. 2000.

[4] K. Kamakura and I. Sasase, "A new modulation scheme using asymmetric error correcting codes embedded in optical orthogonal codes for optical CDMA," *J. Lightwave Technol.*, vol. 19, pp. 1839-1850, Dec. 2001.

[5] H. M. H. Shalaby, "Maximum achievable throughputs for uncoded oppm and mppm in optical direct-detection channels," *J. Lightwave Technol.*, vol. 13, pp. 2121-2128, Nov. 1995.

[6] H. M. H. Shalaby, "Direct detection optical overlapping ppm-cdma communication systems with double optical hardlimiters," *J. Lightwave Technol.*, vol. 17, pp. 1158-1165, July 1999.

[7] H. M. H. Shalaby, "Synchronous fiber-optic cdma systems with interference estimators,"*J. Lightwave Technol.*, vol. 17, pp. 2268-2275, Nov. 1999.

[8] H. M. H. Shalaby, "Effect of thermal noise and apd noise on the performance of oppm-cdma receivers," *J. Lightwave Technol.*, vol. 18, pp. 905-914, July 2000.

[9] S. Zahedi and Jawad A. Salehi, "Analytical comparison of various fiber-optic cdma receiver structures," *J. Lightwave Technol.*, vol. 18, pp. 1718-1727, Dec. 2000.

[10] K. B. Letaief, "The performance of optical fiber direct-sequence spread-spectrum multiple-access communications systems," *IEEE Trans.Commun.*, vol. 43, pp. 2662-2666, Nov. 1995.

[11] J. T. Tang and K. B. Letaief, "Bit-error rate computation of optical cdma communication systems by large deviations theory," *IEEE Trans.Commun.*, vol. 46, pp. 1422-1428, Nov. 1998.

[12] G. C. Yang and Wimg. C. Kwong, "Performance analysis of optical cdma with prime codes," *Electronics Lett.*, vol. 31, pp. 569-570, Mar. 1995.

[13] Wing. C. Kwong, P. A. Perrier, and P. R. Prucnal, "Performance comparison of asynchronous and synchronous code-division multiple-access techniques for fiber-optic local area networks," *IEEE Trans. Commun.*, vol. 39, pp. 1625-1634, Nov. 1991.

[14] Jawad A. Salehi, "Code division multiple-access techniques in optical fiber networks - part i: Fundamental principles," *IEEE Trans. Commun.*, vol. 37, pp. 824-833, Aug. 1989.

[15] Jawad A. Salehi and C. A. Brackett, "Code division multiple-access techniques in optical fiber networks - part ii: Systems performance analysis," *IEEE Trans. Commun.*, vol. 37, pp. 834-842, Aug. 1989.

[16] K. Kamakura and I. Sasase, "A new modulation scheme using asymmetric error correcting codes embedded in optical orthogonal codes for optical CDMA," *J. Lightwave Technol.*, vol. 19, pp. 1839-1850, Dec. 2001.

[17] S. Kim, K. Yu, and N. Park, "A new family of space/wavelength/time spread

three dimensional optical code for OCDMA networks," *J. Lightwave Techol.*, vol. 18, pp. 502-511, Apr. 2000.

[18] H. Fathallah, L. A. Rusch, and S. LaRochelle, "Passive optical fast frequency-hop CDMA Communication System," *J. Lightwave Technol.*, vol. 17, pp. 397-405, Mar. 1999.

[19] S. V. Maric, Z. I. Kostic, and E. L. Titlebaum, "A new family of optical code sequences for use in spread-spectrum fiber-optic local area networks," *IEEE Trans. Commun.*, vol. 41, pp. 1217-1221, Aug. 1993.

[20] S. V. Maric, "New family of algebraically designed optical orthogonal codes for use in cdma fiber-optic networks," *Electronics Lett.*, vol. 29, pp. 538-539, Feb./Mar./Apr. 1993.

[21] Z. Wei and H. Ghafouri-Shiraj, "Proposal of a novel code for spectral amplitude-coding optical CDMA system," *IEEE Photon. Tech. Lett.*, vol. 14, pp. 414-416, Mar. 2002.

[22] C. S. Weng and J. Wu, "Optical orthogonal code for nonideal cross-correlation" *J. Lightwave Technol.*, vol. 19, pp. 1856-1863, Dec. 2001.

[23] Z. Wei and H. Ghafouri-Shiraj, "Unipolar codes with ideal in-phase cross correlation for spectral amplitude-coding optical CDMA Systems," *IEEE Trans. Commun.* vol. 50, pp. 1209-1212, Aug. 2002.

[24] W. C. Kwong and G. C. Yang, "Double weight signature pattern codes for multicore-fiber code division multiple access networks," *IEEE Commun. Lett.* vol. 5, pp. 203-205, May. 2001.

[25] J. G. Zhang, "Flexible optical fiber CDMA networks using strict optical orthogonal codes for multimedia broadcasting and distribution applications," *IEEE*

Trans. Broadcast., vol. 45, pp. 106-115, Mar. 1999.

[26] I. B. Djordjevic, "Design of multiweight unipolar codes for multimedia optical CDMA. applications based on pairwise balanced designs" *J. Lightwave Technol.*, vol. 21, pp. 1850-1856, Sept. 2003.

[27] A. S. Holmes and R. R. Syms, "All-optical cdma using "quasi-prime" codes,'" *J. Lightwave Technol.*, vol. 10, pp. 279-286, Feb. 1992.

[28] G. C. Yang and Wing. C. Kwong, "Performance analysis of optical cdma with prime codes," *Electronics Lett.*, vol. 31, pp. 569-570, Mar. 1995.

[29]Wing. C. Kwong, P. A. Perrier, and P. R. Prucnal, "Performance comparison of asynchronous and synchronous code-division multiple-access techniques for fiber-optic local area networks," *IEEE Trans. Commun.*, vol. 39, pp. 1625-1634, Nov. 1991.

[30] T. Okoshi, "Recent advances in coherent optical fiber communication system," *J. Lightwave Technol.*, vol. 5, no. 1, pp. 44-52, 1987.

[31] M. A. Santaro, "Asynchronous fiber optic local area network using CDMA and optical correlation," *Proc. IEEE,* vol. 75, pp. 1336-1338, 1987.

[32] J. A. Salehi, "Code division multiple access techniques in optical fiber networks-Part I: Fundamental principles," *IEEE Trans. Commun.*, vol. 37, pp. 824-833, August 1989.

[33] T. O'Farrell and S. Lochman, "Performance Analysis of an Optical Correlator Receiver for SIK DS-CDMA Communication System," *Electronics Lett.*, vol.30, no.1, pp. 63-65, Jan. 1994.

[34] T. O'Farrell and S. Lochmann, "Switched Correlator receiver architecture for

optical CDMA networks with Bipolar Capacity", *Electronics Lett.*, vol.31, no.11, pp. 905-906, May. 1995.

[35] M. B. Pursley, "Performance evalution for phase-coded spread spectrum multiple action communication-Part I: System Analysis," *IEEE Trans. Commun.*, vol. 25, pp. 795-799, August 1989.

[36] M. Wehuna, "Performance analysis on phase-encoded OCDMA communication system," *J. Lightwave Technol.*, vol. 20, pp. 798-805, May. 2002.

[37] M. M. R. Dale and R. M. Garliardi, "Channel coding for asynchronous fiber optic CDMA communication," *IEEE Trans. Commun.*, vol. 43, pp. 2485-2492, Sept 1995.

[38] J. Y. Kim and H. V. Poor, "Turbo-coded optical direct detection CDMA system with PPM modulation," *J. Lightwave Techol.*, vol. 19, pp. 312-323, Mar. 2001.

[39] K. Kamakura and I. Sasase, "A new modulation scheme using asymmetric error correcting codes embedded in optical orthogonal codes for optical CDMA," in *Proc. IEEE Int. Symp. Inform. Theory (ISIT' 2001)*, Washington D.C., June 2001, p.274.

[40] K. Kamakura and K. Yashiro, "An embedded transmission scheme using PPM signaling with symmetric error-correcting codes for optical CDMA," *J. Lightwave Technol.*, vol. 21, pp. 1601-1611, Jul. 2001.

[41] C. Argon and S. W. McLaughlin, "Optical OOK-CDMA and PPM-CDMA systems with turbo product codes," *J. Lightwave Technol.*, vol. 20, pp. 1653-1663, Sept. 2002.

[42] T. Ohtsuki, "BER performance of turbo-coded ppm cdma systems on optical fiber," *J. Lightwave Technol.*, vol. 18, pp. 1776-1784, Dec. 2000.

[43] J. Y. Kim and H. V. Poor, "Turbo-coded packet transmission for an optical cdma network," *J. Lightwave Technol.*, vol. 18, pp. 1905-1917, Dec. 2000.

[44] K. Kiasaleh, "Turbo-coded optical ppm communication systems," *J. Lightwave Technol.*, vol. 16, pp. 18-26, Jan. 1998.

[45] T. M. Duman, "New performance bounds for turbo codes," *IEEE Trans. Commun.*, vol. 46, pp. 717-723, June 1998.

[46] P. C. Teh, P. Petropoulos, M. Ibsen, and D. J. Richardson, "A comparative study of the performance of seven and 63-chip optical code division multiple access encoders and decoders based on superstructured fiber Bragg gratings," *J. Lightwave Technol.*, vol. 19, pp. 1352-1365, Sept. 2001.

[47] P. Petropoulos, M. Ibsen, M. N. Zervas, and D. J. Richardson, "Generation of a 40-Ghz pulse stream by pulse multiplication with a sampled fiber Bragg grating," *Opt. Lett.*, vol. 25, no. 8, pp. 521-523, 2000.

[48] P. Petropoulos, M. Ibsen, A. D. Ellis, and D. J. Richardson, "Rectangular pulse generation based on pulse reshaping using a superstructured fiber Bragg grating," *J. Lightwave Technol.*, vol. 19, pp. 746-752, May 2001.

[49] C. H. Chua, F. M. Abbou, H. T. Chuah and S. P. Majumder, "Performance analysis on phase-encoded OCDMA communication system in dispersive fiber medium," *IEEE Photon. Tech. Lett.*, vol. 16, pp. 668-670, Mar. 2002.

[50] Afreen Azhari, "Performance analysis for an optical CDMA system in presence of fiber chromatic dispersion," *M.Sc. Thesis*, Bangladesh University of Engineering and Technology, Bangladesh, 2004

[51] G. P. Agrawal, *Nonlinear Fiber Optics,* 2nd ed. New York: Academic, 1995.

[52] A. R. Chraplyvy, "Limitations on lightwave communications imposed by optical-fiber nonlinearities," *J. Lightwave Technol.*, vol. 8, no. 10, pp. 1548-1557, 1990.

[53] K. Inoue and H. Toba "Four-wave mixing in multi-amplifier system with nonlinear chromatic dispersion," *J. Light wave Technol.*, vol.13, no.1, January 1995, 88-93.

[54] M. Forkan Uddin, A. B. M. Nasirud Doulah, Abul Bashar Mohammad Ishteak Hossain, Muhammad Zulfiker Alam and Mohammed Nazrul Islam, "Reduction of four wave mixing effect in an optical WDM system by controlling channel spacing and chromatic dispersion," *Optical Engineering*, 42(9) September 2003, 2761-2767.

[55] K. O. Hill, D. C Johnson, B. S. Kawasaki and R. I. Macdonald, "CW three wave mixing in single mode fibers," *J. Appl. Phys.*, vol. 49, pp. 5098-5106, 1978.

[56] K. Inoue, "Fiber four-wave mixing in the zero dispersion wavelength region," *J. Lightwave Technol.*, vol. 10, pp 1553-1561, 1992.

[57] K. Inoue, K. Nakanishi, K. Oda, and H. Toba, "Crosstalk and power penalty due to fiber four wave mixing in multichannel transmission," *J. Lightwave Technol.*, vol. 12, no. 8, pp. 1423-1439, 1994.

[58] J. M. Senior, Optical Fiber Communication, 2nd edition, Prentice-Hall, India, 2000.

[59] A. F. Elrefaic and R. E. Wagner, "Chromatic dispersion limitation for FSK and DPFSK systems with direct detection receivers," *IEEE Photon. Tech. Lett.*, vol. 8, no. 1, January 1991.

[60] D. Cotter, "Stimulated Brillouin scattering in mono mode optical fiber," *J. Opt. commun.*, vol. 4, pp. 10-19, 1983.

[61] D. Marcuse, A. R. Chraplyvy, and R. W. Tkach "Effect of fiber nonlinearity on long distance transmission," *J. Lightwave Technol.*, vol. 9, no. 1, pp. 121-128, Jan 1991.

[62] A. R. Chraplyvy, " Limitation of lightwave communication imposed by optical fiber non linearities," *J. Lightwave Technol.*, vol. 8, no. 10, pp. 1548-1557, March 1991.

[63] H. Zheng, S. Xie, Z. Zhou, and B. Zhou, "A simple formula on allowable fiber input power for unequal channel spaced WDM transmission system," *J. Optical Commun.*, vol 20, no. 4, pp. 153-155, 1999.

[64] Enrico Forestieri and Giacarlo Prati, "Novel optical line codes tolerant to fiber chromatic dispersion," *J. of lightwave Technol.* vol. 19, pp. 1675-1684, Nov. 2001.